Wisconsin Electric POWER COMPANY
231 W. MICHIGAN, P.O. BOX 2046, MILWAUKEE, WI 53201

May 2, 1980

Mr. H. R. Denton, Director
Office of Nuclear Reactor Regulation
U. S. NUCLEAR REGULATORY COMMISSION
Washington, D. C. 20555

Attention: Mr. Robert A. Clark, Chief
Operating Reactors Branch #3

Gentlemen:

DOCKET NO. 50-266
FINAL REPORT OF STEAM GENERATOR TUBE INSPECTION
POINT BEACH NUCLEAR PLANT UNIT 1

On March 28, 1980 we transmitted the results of the March 1980 eddy current inspection of the Point Beach Nuclear Plant Unit 1 steam generators. As a result of the eddy current inspection, we had agreed to remove three tubes from the "B" steam generator to perform additional metallurgical examinations of the defects identified in those tubes. The preliminary results of the evaluation of these tube samples were provided to members of your staff during a meeting in Pittsburgh at the Westinghouse Forest Hills Laboratory on March 28. A detailed report on the metallographic and laboratory examinations performed on the removed tubes to date is provided herewith as Attachment 1. The results of the tube examinations performed in October 1979 confirmed that corrosion of the steam generator tubing is confined to the tube sheet crevice region. The present examinations also verify that this corrosion attack is similarly restricted to the tube sheet crevice area.

In addition to this detailed report, we committed in our March 28 letter to provide two items of additional information. The first of these is a detailed re-evaluation of all previous eddy current tapes for tubes R19C37, R30C41, R26C53, R30C44, R28C38, R32C42, R22C46, and R30C57. This re-evaluation is provided as Attachment 2. The second item was a discussion of the capability of re-evaluating 400 KHZ single frequency eddy current signals by mixing with a pseudo tube sheet or tube support plate signal. This discussion is provided in Attachment 3. We have concluded that this mixing technique produces unreliable results and is not an effective re-evaluation method.

A001
S
1/1

We have also committed to provide the NRC, or your independent consultant, a section or sections of the removed tubes if requested. It is our understanding from our March 28 meeting that you presently have no need for any tube sections. Should you require a tube section or sections in the future, please notify us.

We believe this letter and the attached material satisfy our commitments to you regarding the Point Beach Unit 1 steam generator inspections. If you have any questions regarding this material, please contact us.

Very truly yours,

C. W. Fay

C. W. Fay, Director
Nuclear Power Department

Attachments

Copies to C. F. Riederer - PSCW
Peter Anderson - WED
Joan Estes - LSCFSE

ATTACHMENT 1

APRIL 25, 1980

MICROSCOPIC AND OTHER EXAMINATIONS OF NUCLEAR STEAM GENERATOR TUBING REMOVED FROM POINT BEACH NO. 1 IN MARCH 1980

F. W. Pement
Materials Science Division
Westinghouse R & D Center
Pittsburgh, PA 15235

E. P. Morgan
Nuclear Technology Division
Westinghouse Nuclear Energy Systems
Pittsburgh, PA 15230

ABSTRACT

Tubes B(26-53), B(30-41), and B(19-37) from the hot leg regions of the Point Beach 1 steam generators were removed in March 1980 and were examined by NDE and microscopy. General intergranular corrosion was absent above the tube sheet on the tube OD surfaces. Shallow intergranular involvement was absent or was limited to 0.002 in maximum depth on cross sections at or above the top of the tube sheet. Deeper intergranular corrosion within the tube sheet region was observed to depths of 40% of the wall thickness on B(19-37), 65% on B(30-41) and 80% on B(26-53). The results were based on extensive optical metallography and SEM fractography, and they confirm that the corrosion-producing environment was confined to within the tube sheet crevice region.

SUMMARY

Three hot leg tubing sections from the "B" nuclear steam generator of Point Beach 1 were examined in detail by optical metallography and scanning election microscope fractography. Intergranular corrosion was shown to exist within the tube sheet region with maximum depths of 40% on Tube B(19-37), 65% on Tube B(30-41) and 80% on Tube B(26-53). At the top of the tube sheet and immediately above the tube sheet, general intergranular corrosion tended to be absent or, if present, was microscopic, of the order of one or two grains in depth not exceeding 0.002 in. The examinations therefore confirm earlier examinations on tubes removed in October 1979, that the corrosion of the Inconel 600 tubing developed in the confines of the annulus between the tubes and the tube holes within the tube sheet. Corrosion above the tube sheet was shown in the present examination to be absent or superficial. The presence of 0.002 in. of grain boundary involvement such as observed at the top of the tube sheet in the present examination, is not considered atypical.

INTRODUCTION

Three tube samples were removed from the "B" nuclear steam generator of Point Beach Unit 1 in March, 1980. The samples were hot-leg sections of (1) Row 26 - Column 53 [B(26-53)], (2) B(30-41), and (3) B(19-37). Tube B(26-53) had a reported in-plant eddy current (EC) indication of 86% wall thickness at an elevation of 18 in. above the primary face of the 22 1/4 - in. - thick tube sheet. Tube B(30-41) had a reported EC indication of 47% at 21 in. above the primary face, and Tube B(19-37) had an EC indication of 58% at 22 3/4 in. above the primary face.

The lengths of the cuts made at the Point Beach site and the forces used to extract the tubes from the generator were reported to be as follows:

	Cut Length above primary Face of tube sheet (in.)	Extraction Forces (lb.)
B(26-53)	70	21,000 Break away 8000-9000 Pulling
B(30-41)	65	24,000 Break away 21,000 Pulling
B(19-37)	70	22,000 Breakaway 4000-8000 Pulling

The tube sections were examined by techniques of nondestructive evaluation (NDE) and by microscopy on selected, inlet-end sections. Both optical metallography and scanning electron microscope (SEM) fractography were used for the microscopic examinations. This report summarizes the results of the NDE and presents the details of the microscopic examinations.

NON DESTRUCTIVE EVALUATION (NDE)

The NDE work was conducted at Westinghouse Forest Hills. All as-received tube sections were photographed, measured, radiographed, and re-tested by eddy current. Measurements included overall lengths and salient features on the outer diameter (OD) surfaces. Figures 1 - 4 are photographs of the inlet-end sections of the as-received tubes. Figures 4A, B and C provide in plant comparison of E.C. signals and E.C. findings in the laboratory. Dimensions appear on drawings in figures associated with the microscopic examinations of the individual tubes and are described later.

All sections were double-wall radiographed using a Siemens X-ray machine and the following parameters:

Type M Film, Double Pack
200 KV - 5 mA Exposure
60-in. Film-to-Sample Distance
110-sec. Exposure

Four rotations (0°, 45°, 90°, and 135°) were used for each tube section. The 0° mark was made at the plant site on the area of each tube section which faced the divider plate in the steam generator. Reference to the orientation of all tube sections over the entire removed length was based on these 0° marks. The rotations to 45°, 90°, etc. were counterclockwise when the tube was viewed axially in the direction of the internal primary flow. Selected prints of inlet-end areas of Tube B(26-53) are given in Figure 5 and are representative of the observations from radiography in the tube sheet region of all tubes.

MICROSCOPIC EXAMINATIONS

Tube B(26-53)

The as-received tube lengths, the locations of sections for microscopic examinations, and a conspectus of the metallography and fractography appear schematically in Figure 6. Two axial cross sections, numbered 1 and 2 in Figure 6, were made through a circumferential, OD "ring" mark which appeared at an elevation on the tube which corresponded with the top of the tube sheet. This ring and adjacent tubing surfaces are shown at 4 rotations in Figure 7.

Sectioning of one of the axial sections at the tubesheet ring is depicted in Figure 8, together with a photomacrograph of the resultant section and photomicrographs of the OD edge at an elevation immediately below the ring. Similar photomicrographs at elevations of the ring and immediately above it appear in Figure 9. Very shallow grain boundary involvement ($\leq$ 0.002 in. long) was detected below the ring over the entire 0.08 in. axial length shown in Figure 8. Isolated 0.002 in. max. indications were found in a short zone (0.02 in. long) above the ring, as shown in Area 3 of Figure 9. Figures 10 and 11 correspond to Figures 8 and 9 for the second axial cross section through the ring at 180° from the preceding section. Photomicrographs show the same shallow ($\sim$0.002 in.) grain boundary involvement (Figure 10), except that a deeper, opened network of intergranular corrosion 1/2 to 5/8 in. below the ring was also present (Figure 11).

The remaining four samples for micrographic examination are shown as-cut in Figure 12. Two of these (numbered 3 and 6 in Figure 6) contained fractures that occurred on tube removal. These were studied with the SEM to map the depth of intergranular corrosion and the width of unaffected metal as evidenced by ductile shear. The other samples were examined metallographically. Sample 4 (of Figure 6) was first bent to open the intergranular networks to their maximum depth. Sample 5 was a transverse cross section at a region of distortion by the tube pulling. The results of these examinations appear as SEM fractographs in Figures 13 - 15 for the

higher elevation (Sample 3), optical photomicrographs for the next, lower samples in Figures 16 and 17 (Samples 4 and 5), and as SEM fractographs for the lower fracture (Sample 6) in Figures 18 - 20.

Study of the 24 fractographs (taken every 30 degrees) from the sum of both fractures reveals a shear lip at every point examined, indicating that the intergranular corrosion was not through wall and confirming that the fractures were the result of pulling the tube apart in the removal operations. The depth of intergranular corrosion as determined by the fractography, varied with circumferential location but was usually 50 to 80% through-wall at both elevations. The bent cross sections shown in Figure 16 contained about 0.010 in. of deformed metal near the inside surface after the intergrunular corrosion was opened up. This value, ~20% of the tube wall thickness, was consistent with the fractography with respect to the depth of intergranular corrosion in this area of the tube.

TUBE B(30-41)

This tube contained a ring, located at an elevation which was consistent with the top of the tube sheet and through which an axial cross section was prepared and examined metallographically. Above the ring, there was a bright-appearing, relatively deposit-free zone about 2 in. long. Figure 21 locates the ring, the axial cross section, and the bright zone. This figure also contains the as-received length measurements and the locations and orientations of two additional metallographic cross sections from within the tube sheet region. Sectioning of the region containing the ring and 4 views of ring at 4 rotations are shown in Figure 22.

The results of the metallography through the tube sheet ring appear in Figures 23 and 24. Very shallow grain boundary involvement to a maximum of 2 grains (0.002 in.) was detected below the ring (Figure 23), and even more shallow involvement, less than 1 grain deep ($\leq$ 0.001 in.), was observed at and above the ring (Figure 24). The axial cross section taken 1-1/4 to 2-1/4 in. below the ring and shown in Figures 25 and 26 contained intergranular corrosion to 65% of the wall thickness,

and the transverse cross section just below this axial section had intergranular corrosion to 55 - 60% of the wall (Figures 27 and 28).

TUBE B(19-37)

A clear visual indication of the top of the tube sheet was not present in the tube sections. Therefore, a special, (oversized) 2-in. long axial cross section was prepared to span an elevation which, from tube dimensions and reconstruction of site dimensions, corresponded to the top of the tube sheet. This section was examined and then ground and polished 0.006 in. for a second examination. It was then broken out of its mount and shortened into 3 sections which were subsequently bent to open up any weakened grain boundaries. The bends were examined with the SEM. These operations, and the location of this and 3 other metallographic sections are summarized, together with the as-received tube section dimensions, in Figure 29. Figure 30 shows 4 views of the zone from which the 2-in.-long micro was cut, and Figure 31 provides higher magnification views of the area, the location of the sample and the resultant section.

The results of the metallographic examination of the special 2-in.-long micro are collected in Figures 32 through 36. A maximum depth of 0.0185 in. of intergranular involvement was detected at the mid-elevation of this section (Figures 33 and 36). Above this point, two areas studied had only extremely shallow ($\leq$0.0008 in.), isolated indications (Figure 34). The cut and bent sections from 3 elevations on this section are shown in Figures 37 and 38. The uppermost bend sample (Figure 37) contained the shallowest, opened intergranular involvement which, from the scanning electron micrographs, were superficial.

A number of photomicrographs from 3 additional samples within the tube sheet are collected in Figures 39-42. These show intergranular corrosion of up to 40% through the wall ($\leq$0.020 in. depth).

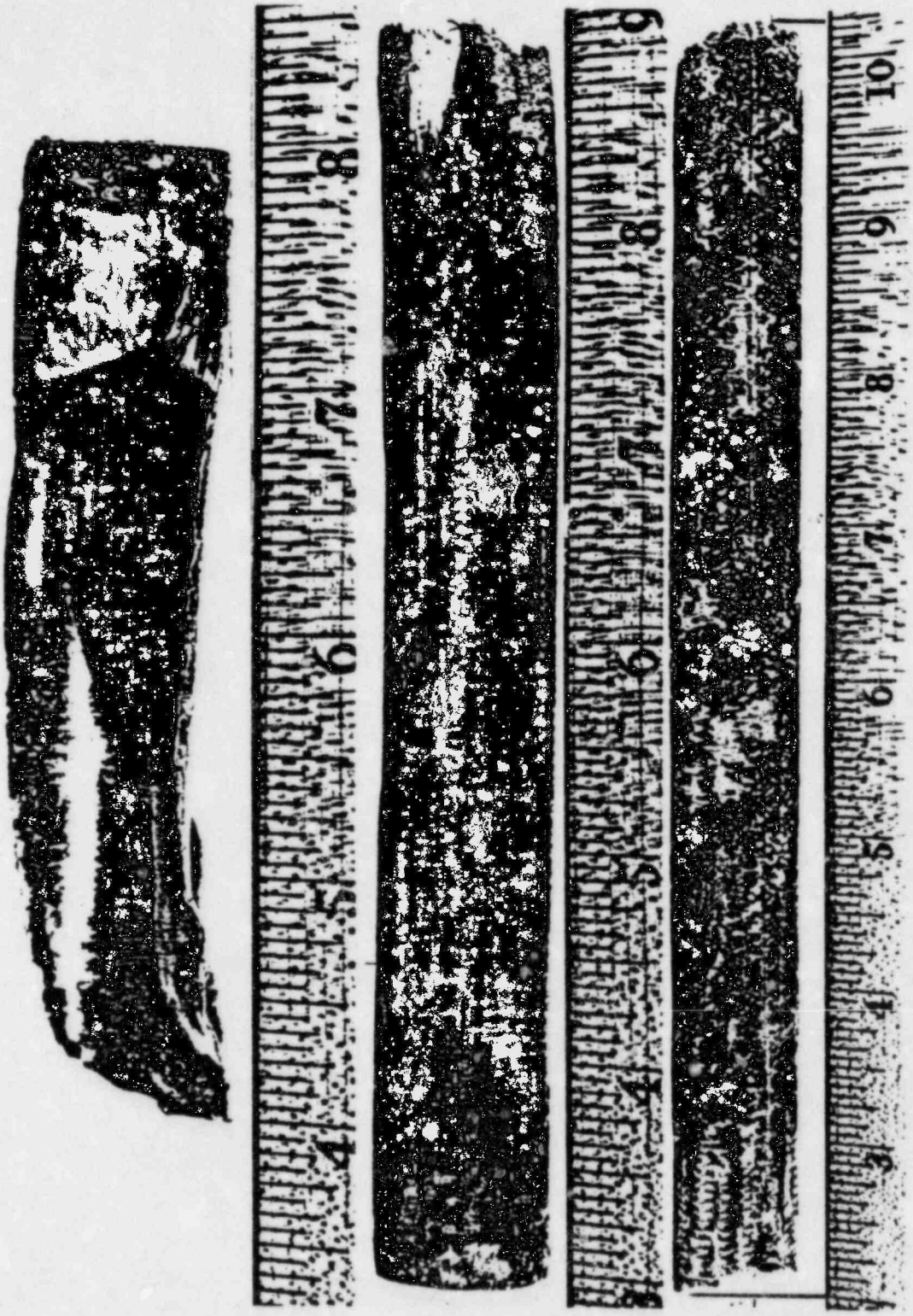

FIGURE 1. Tube B(26-53), Hot leg Inlet Sections, As-Received. Left-to-right = increasing elevation from piece nearest primary face of tube sheet (far left). Ruler insets, used in bench-top photographing, are of slightly different magnifications than accompanying tube sections and provide only relative guides to the individual magnification. Primary flow direction is upward.

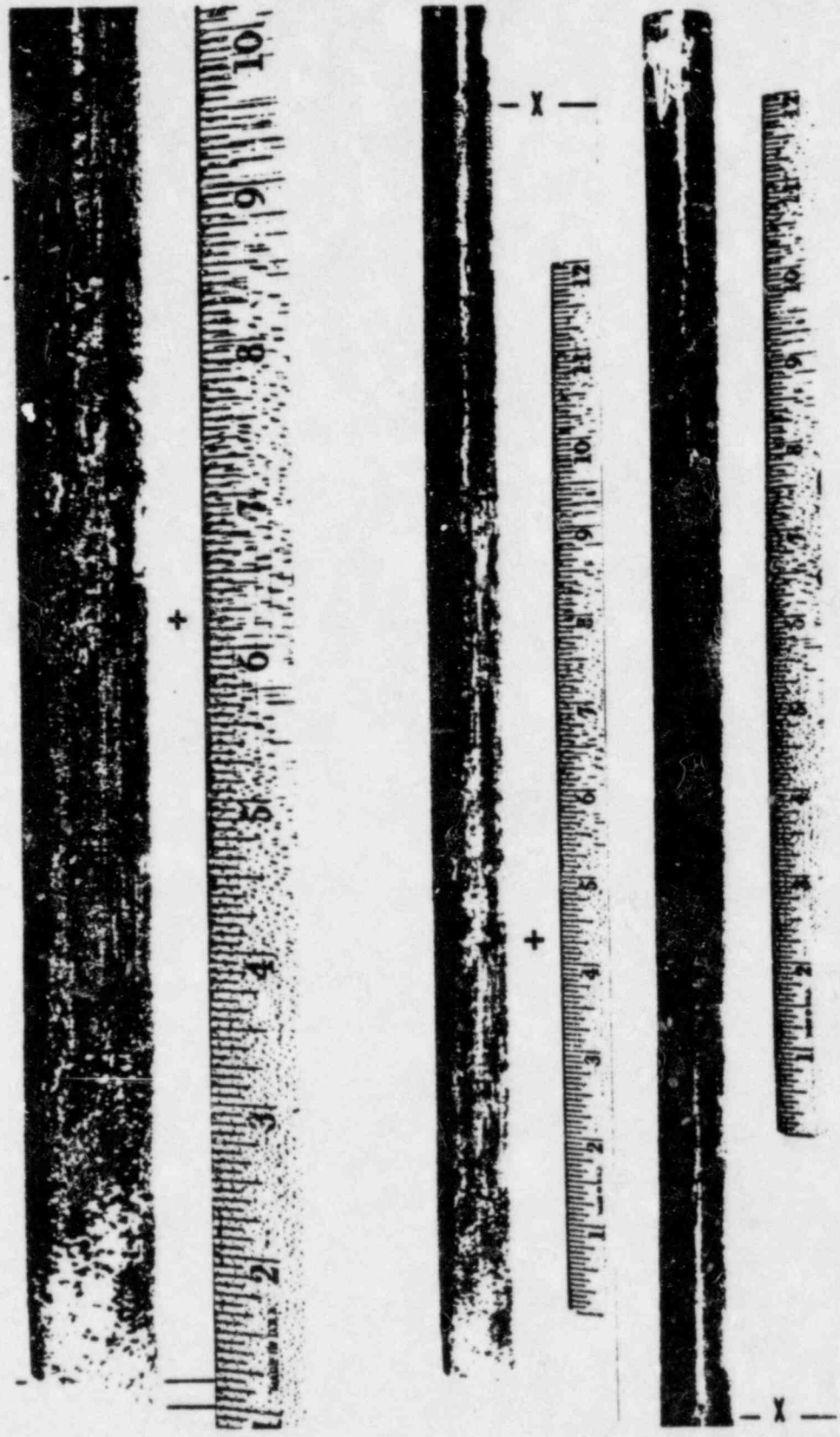

FIGURE 2. Tube B(26-53), Additional As-Received Section adjoining and above the topmost section of Figure 1. The + denotes the tube sheet ring, (shown at 2 magnifications). X-X are match lines of the montage of the pair at right. Primary flow is upward. (A higher section of this tube was also received and photographed but is not shown.)

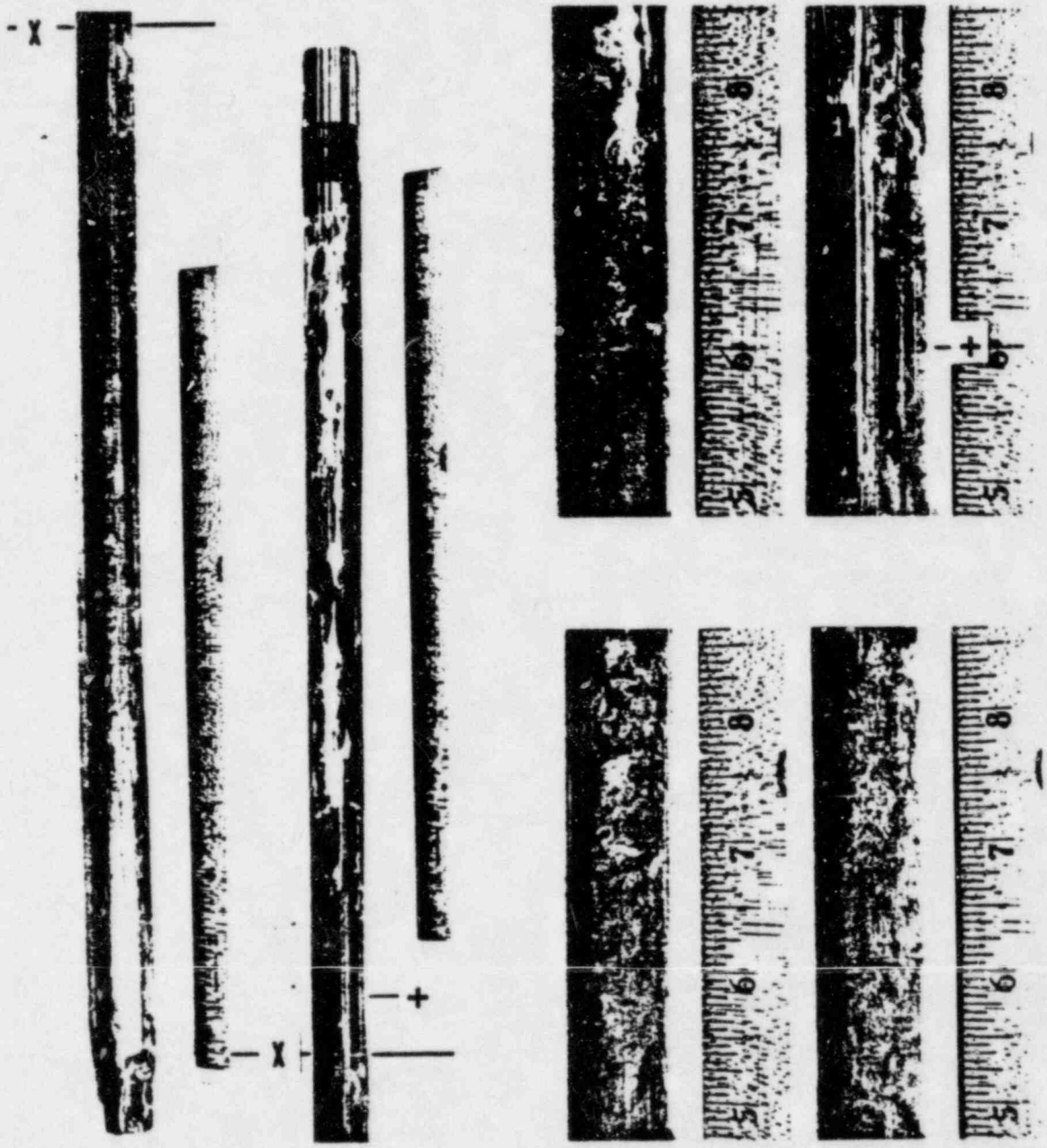

FIGURE 3. Tube B(30-41), As-received Inlet-End Section. X-X denotes match lines in the pair at left, and the + mark locates the tube sheet ring, shown in 2 magnifications and 4 rotations at the right. Primary flow is upward and the 4 pictures are arranged with 0° = top left, 90° = top right, 180° = lower left, and 270° = lower right. Ruler insets provide only relative magnifications. (A second section above this section was also photographed and is not shown.)

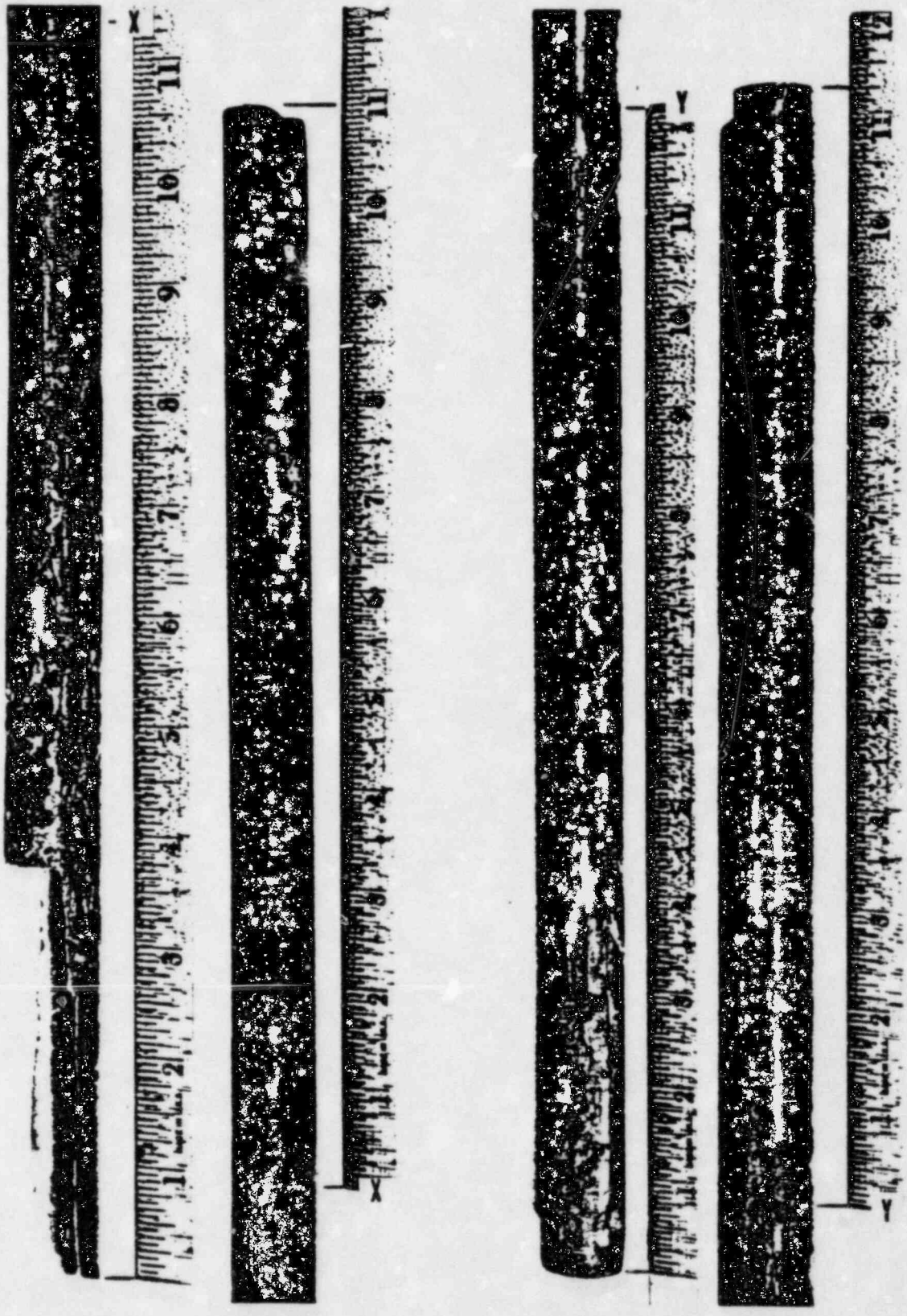

FIGURE 4. Tube B(19-37), As-received Inlet-End Sections. Section nearer the primary face of tube sheet is left, with X-X denoting match lines. Adjoining higher section is at right, with match lines at Y-Y. Primary flow is upward.

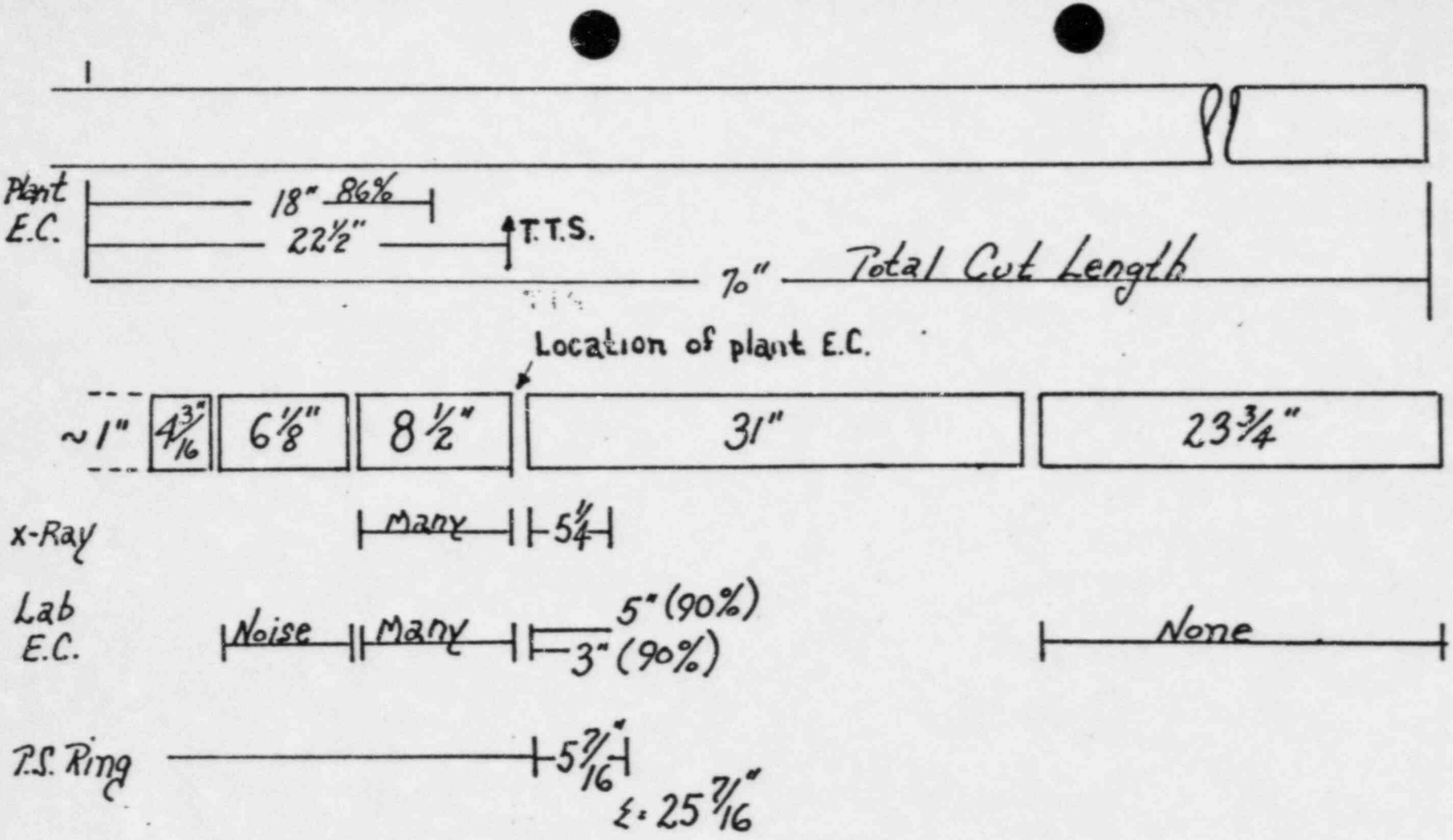

FIGURE 4A. Comparison of plant E.C. signal locations and E.C. findings in the laboratory.

Tube 26-53
Total Lab Length : 74 9/16"
Less : 70
Total Stretch : 4 9/16"
Stretch Above T.S. : 3.7%
Stretch Inside Crevice : 25%

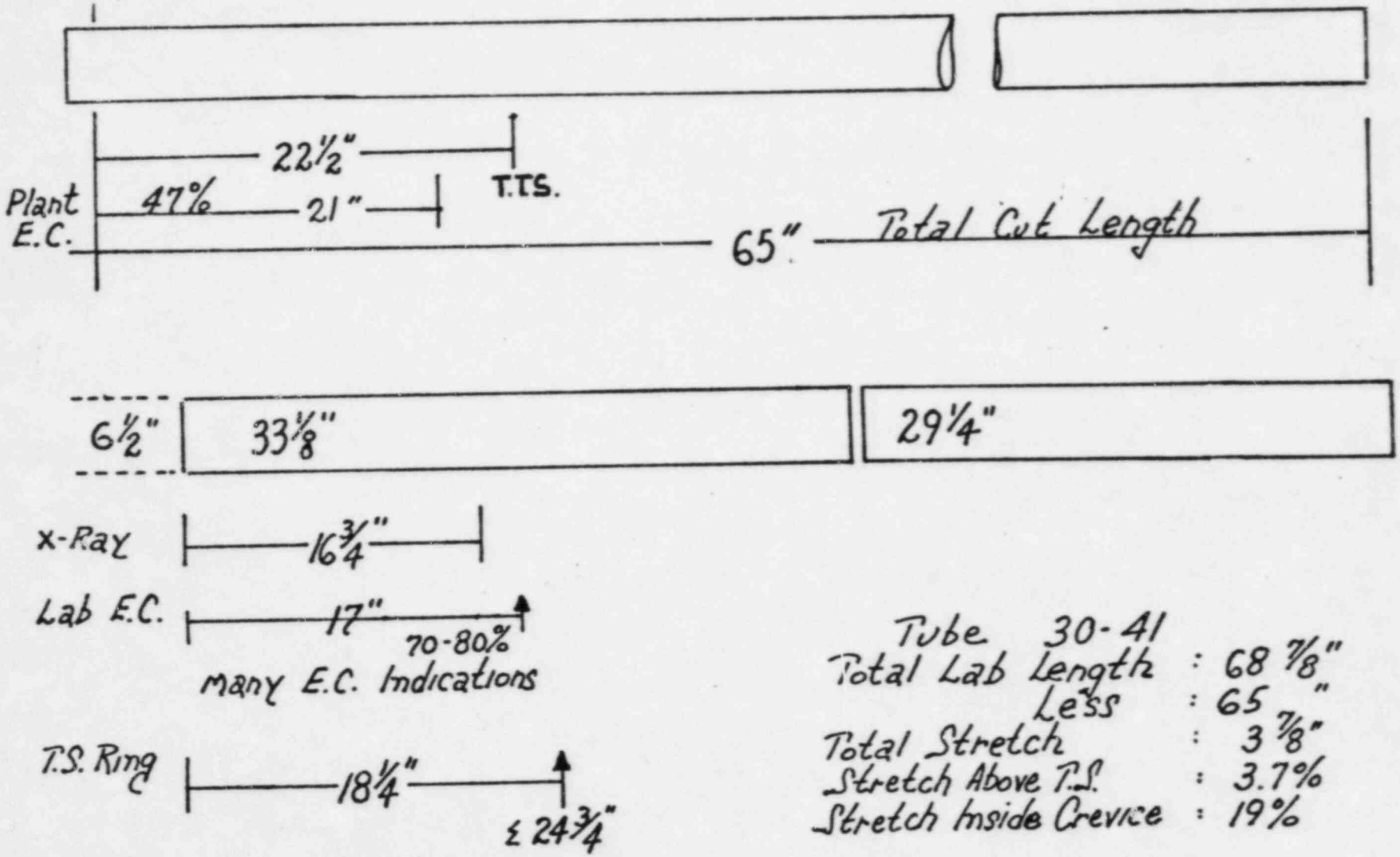

FIGURE 4B. Comparison of plant E.C. signal locations and E.C. findings in the laboratory.

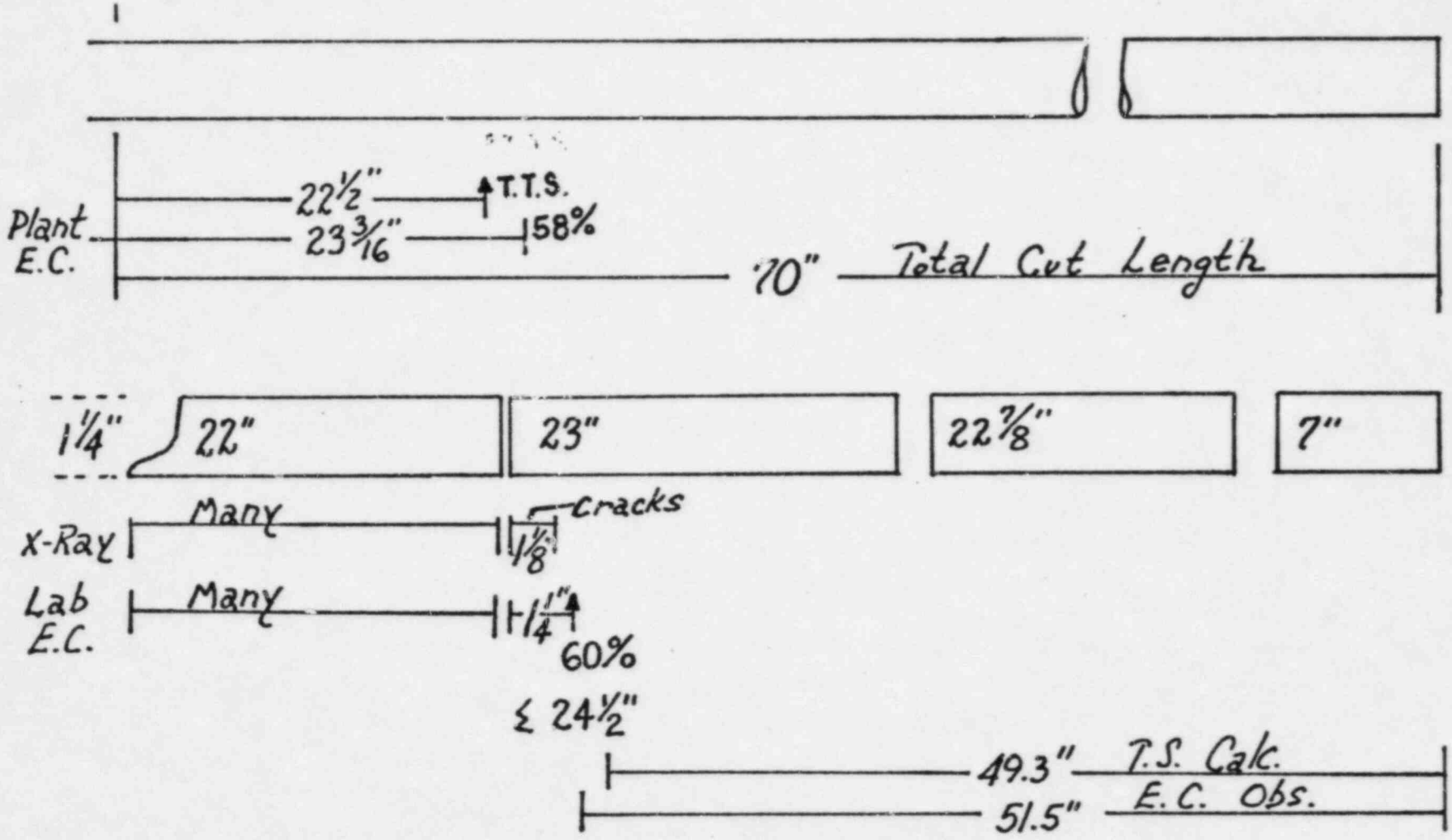

Tube 19-37

Total Tube Length	76⅛"
Less	70"
Total Stretch	6⅛"
Stretch Above T.S.	3.7%
Stretch Inside Device	12.5%

FIGURE 4C. Comparison of plant E.C. signal locations and E.C. findings in the laboratory.

FIGURE 5. Tube B(26-53), Radiograph Prints of Selected Areas. Left = Tube sheet region with breaks at each end due to pulling, 0° view. Right pair = Lower end of next higher piece, exiting tube sheet. Left = 0°, Right = 45°.

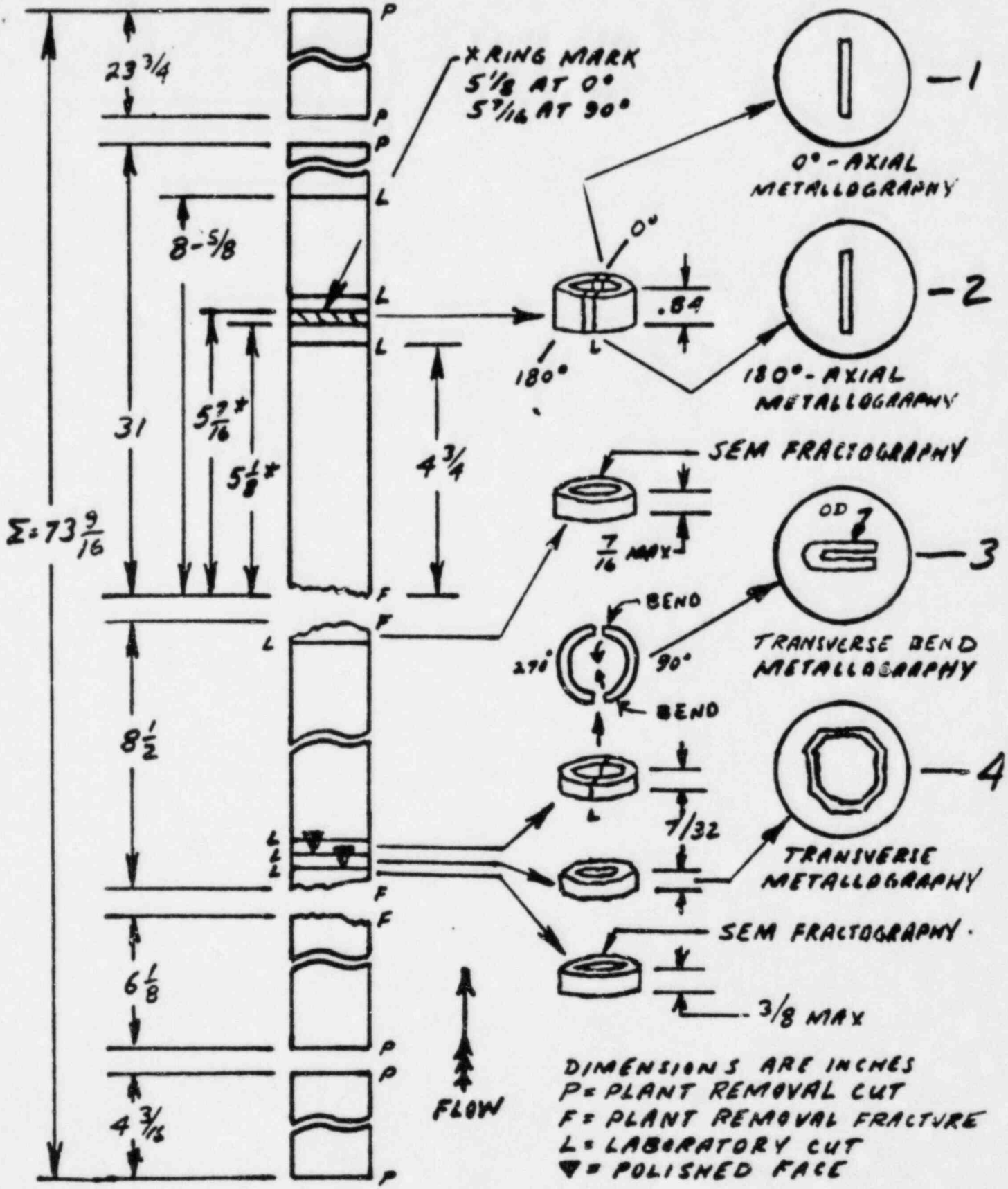

FIGURE 6. WEP B(26-53) - Laboratory Samples for Microscopic Examinations.

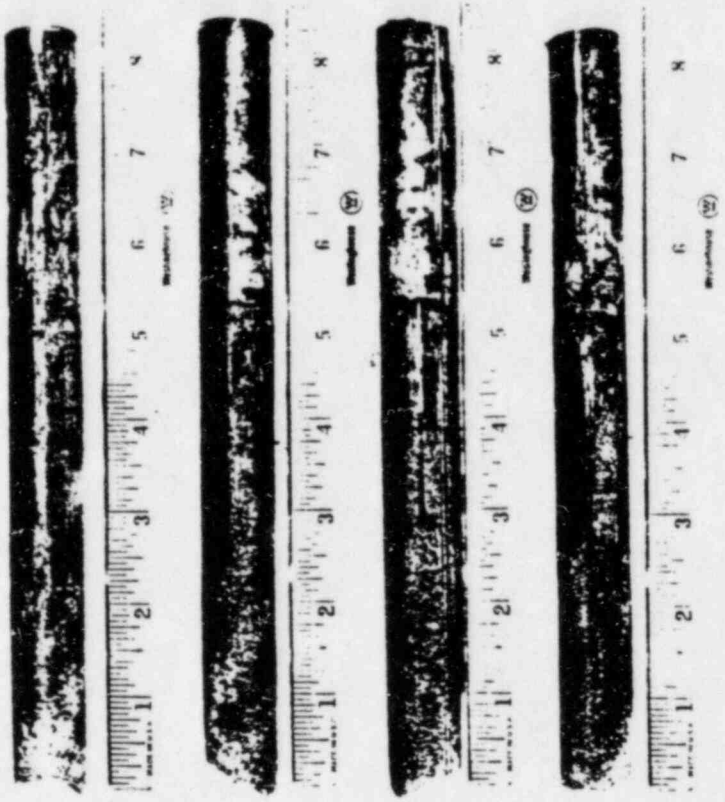

FIGURE 7. Tube B(26-53). Additional views of area containing ring at top of tube sheet, after preliminary sectioning prior to metallographic sampling. Left-to-right: 0°, 90°, 180°, 270°. Primary flow is upward.

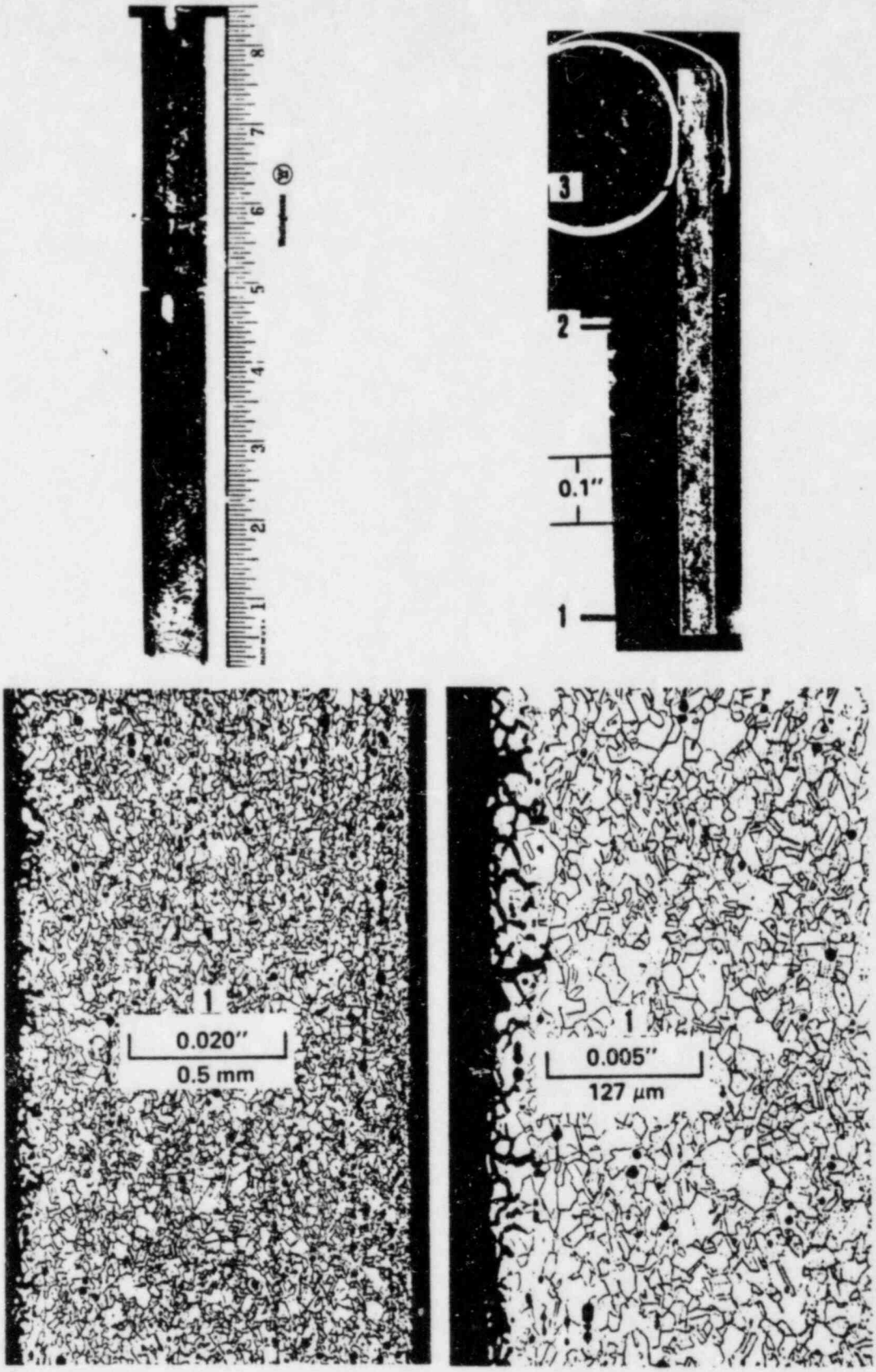

FIGURE 8. B(26-53), Metallography through Ring at Top of Tubesheet. Upper left = sectioning. Upper right = photomacrograph of polished and etched longitudinal cross section with OD on left. Lower pair = photomicrographs of OD area 1 below ring. Etchant = bromine in methanol. (Primary flow is upward.)

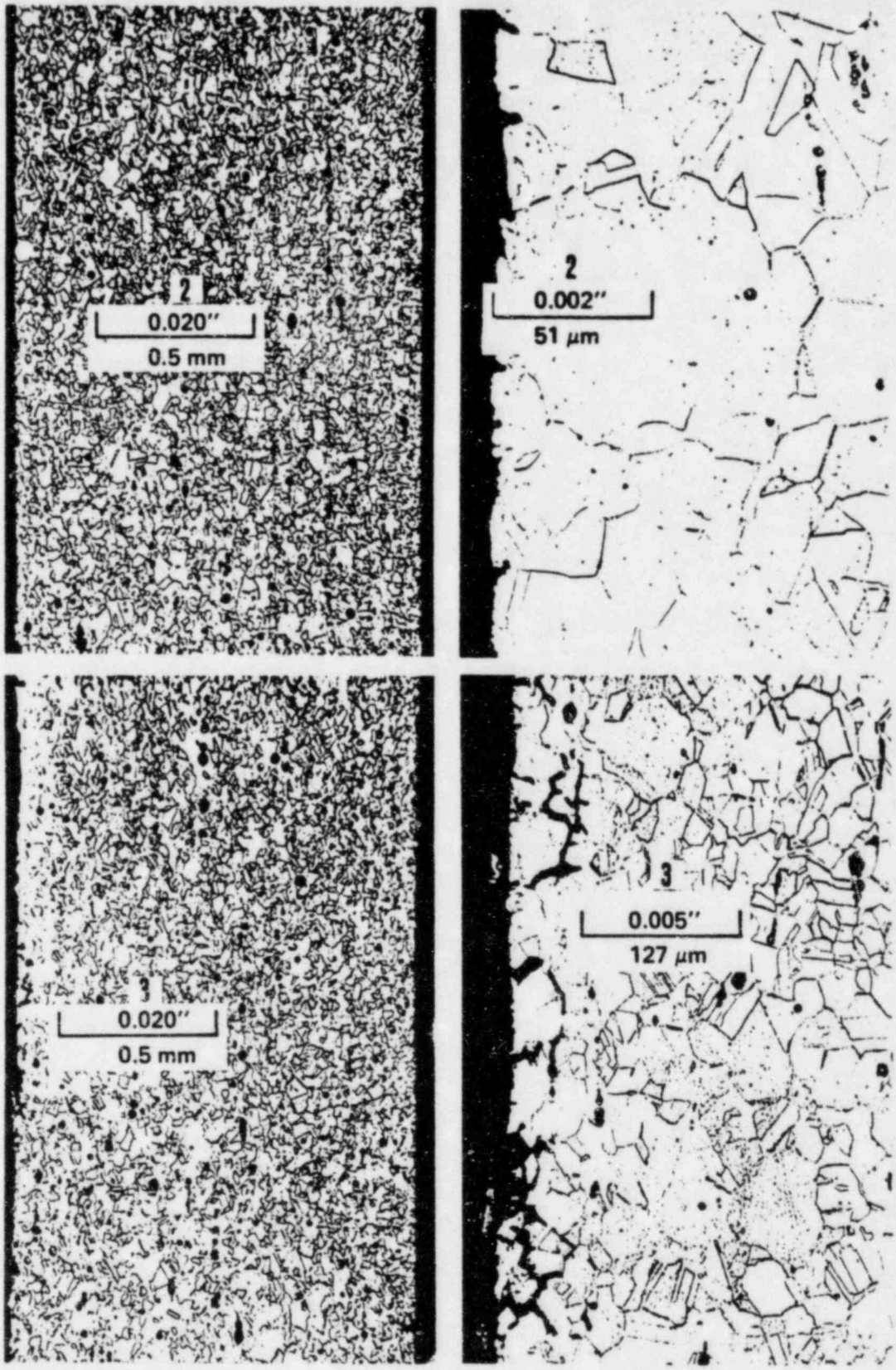

FIGURE 9. R(26-53), Etched Photomicrographs of Longitudinal Section through Tube Sheet Ring. Area 2 = near ring; Area 3 = above ring. Areas are located in Figure 7. OD is at left; primary flow is upward.

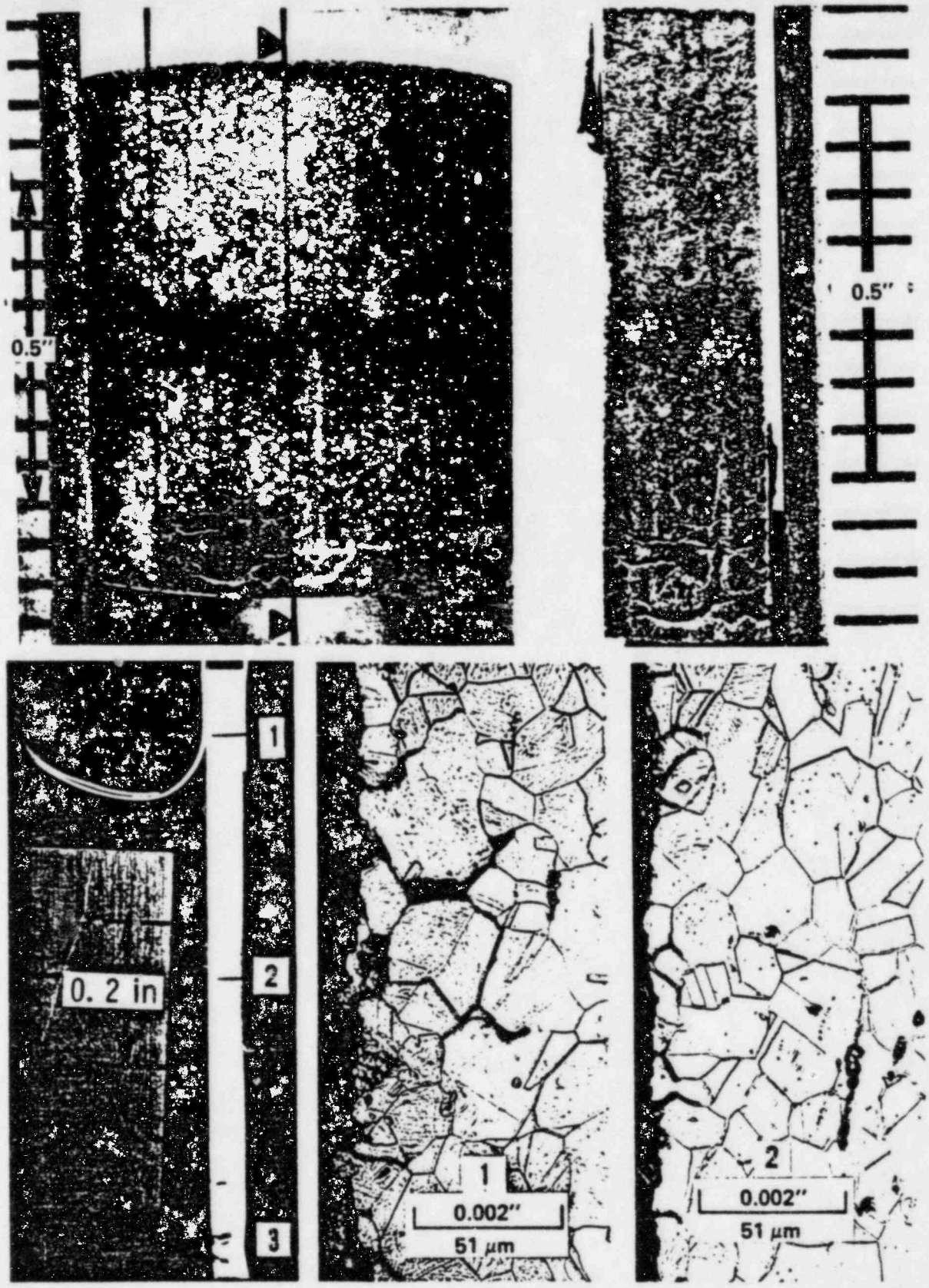

FIGURE 10. B(26-53), Longitudinal Cross Section No. 2 through Tube Sheet Ring. Opposite side of tube from section shown in Figures 8 and 9. Upper pair shows sectioning and resultant section. Lower left is a photomacrograph of as-polished cross section. OD areas 1 and 2 are shown in high-magnification etched photomicrographs at bottom. Primary flow is up.

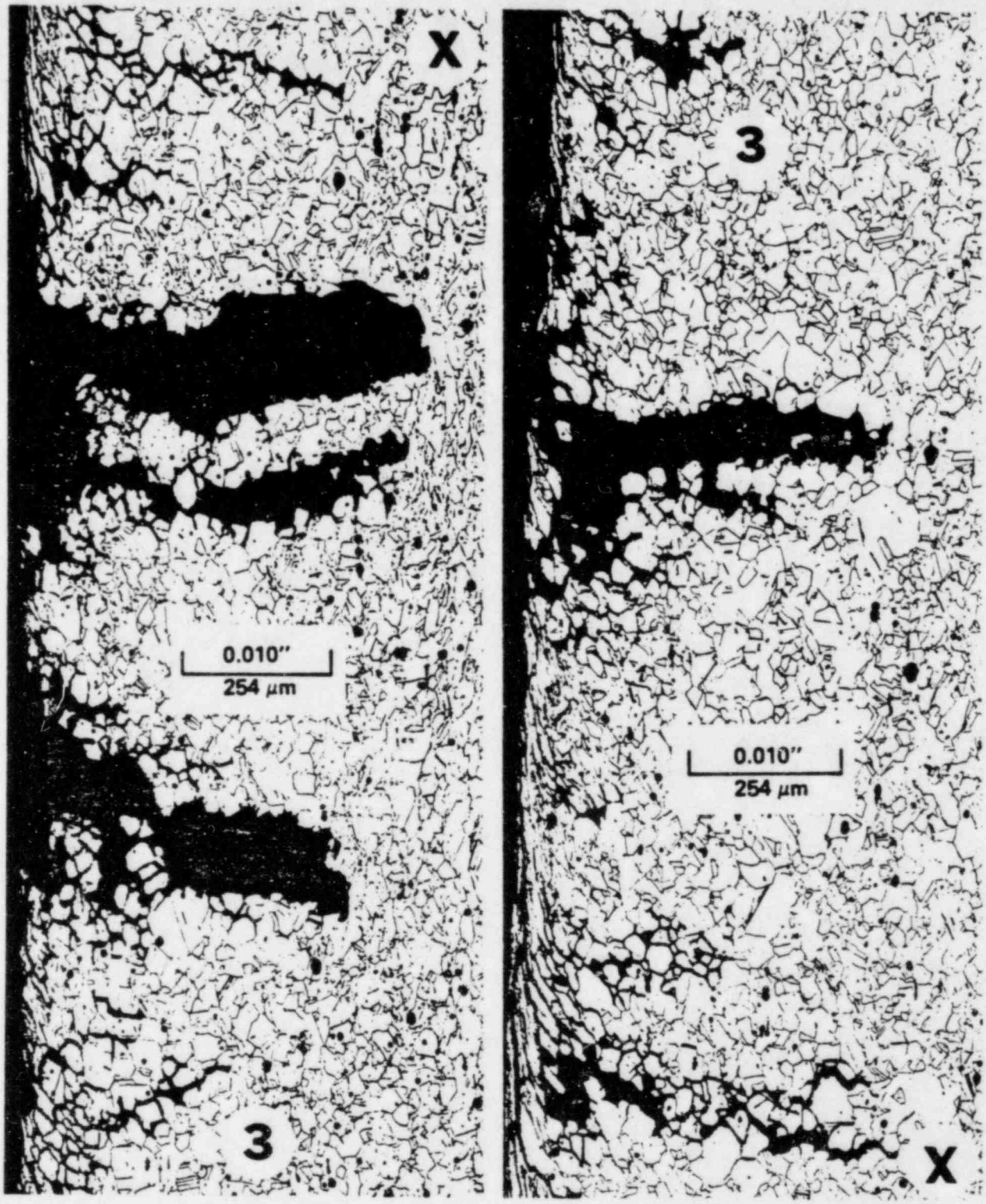

FIGURE 11. B(26-53), Longitudinal Cross Section No. 2, below Tube Sheet Ring, Area 3 of Figure 10. OD is left; primary flow is up.

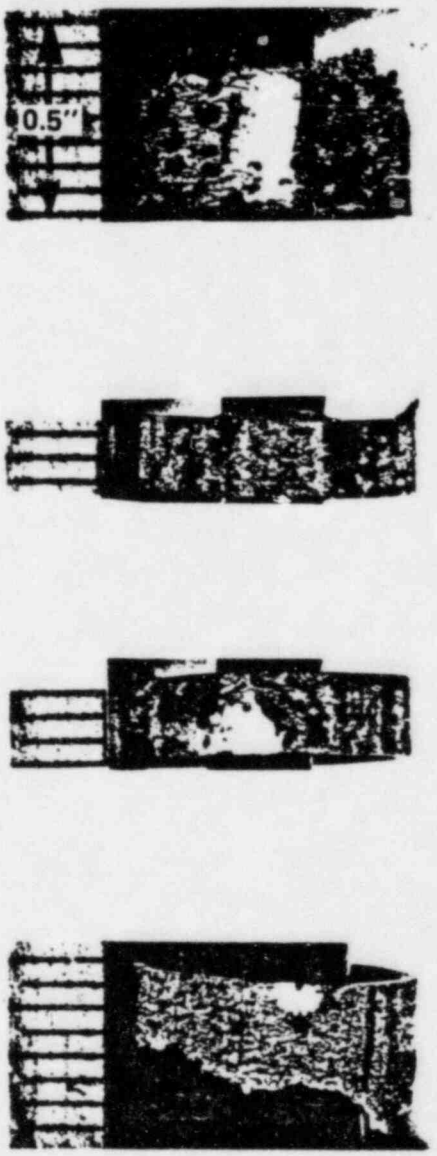

FIGURE 12. B(26-53), Additional Microscopic Samples from within Tube Sheet.
Top = Sample 3 (Figure 6): SEM fractography
Top Middle = Sample 4: Bend transverse metallography
Lower Middle = Sample 5: Transverse metallography
Bottom = Sample 6: SEM fractography.

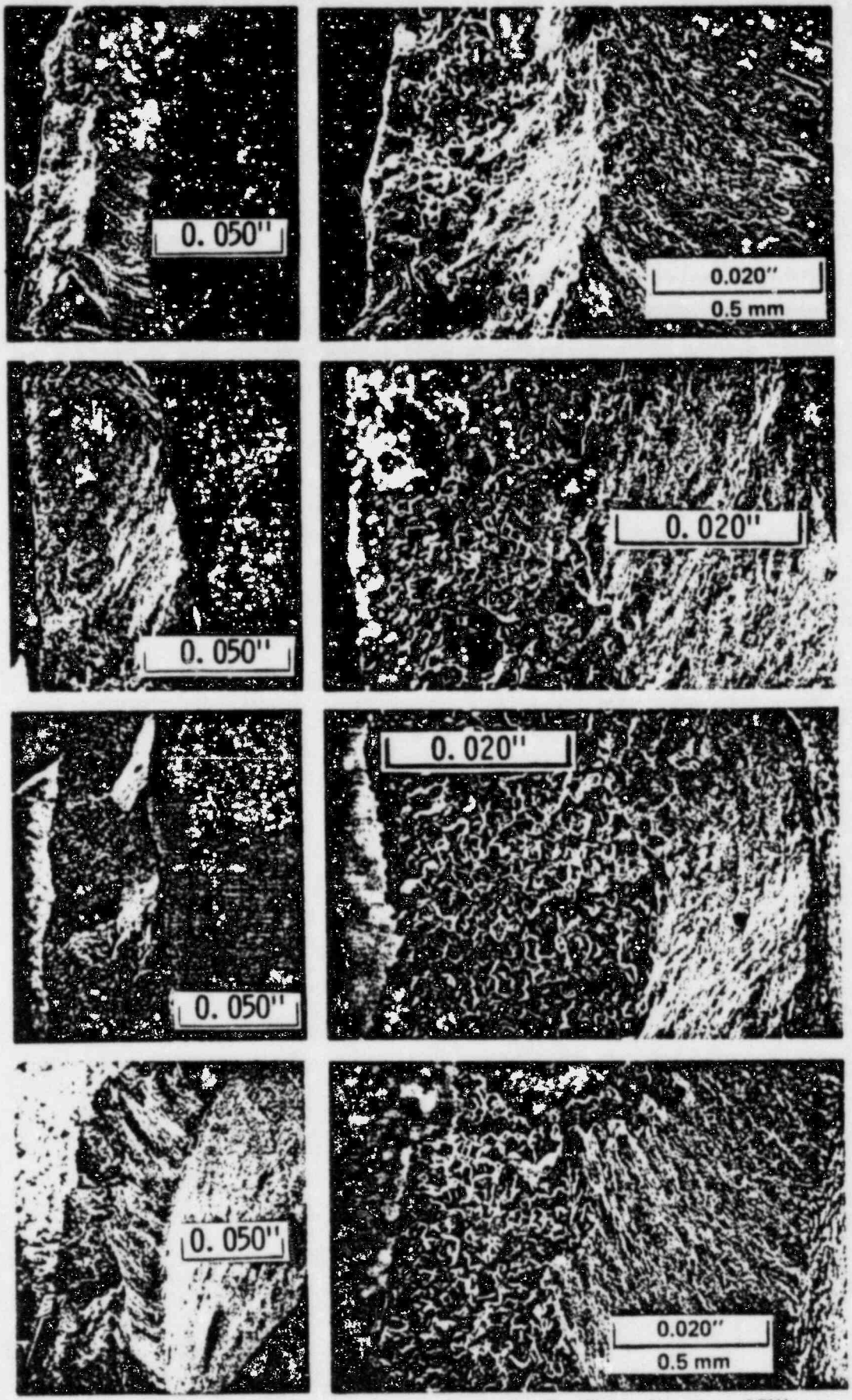

FIGURE 13. B(26-53), Sample 3, Fracture Face within Tube Sheet. SEM's taken at 30° intervals beginning at 0° (top) to 90° (bottom). Magnifications vary from point to point within each SEM because of specimen tilt.

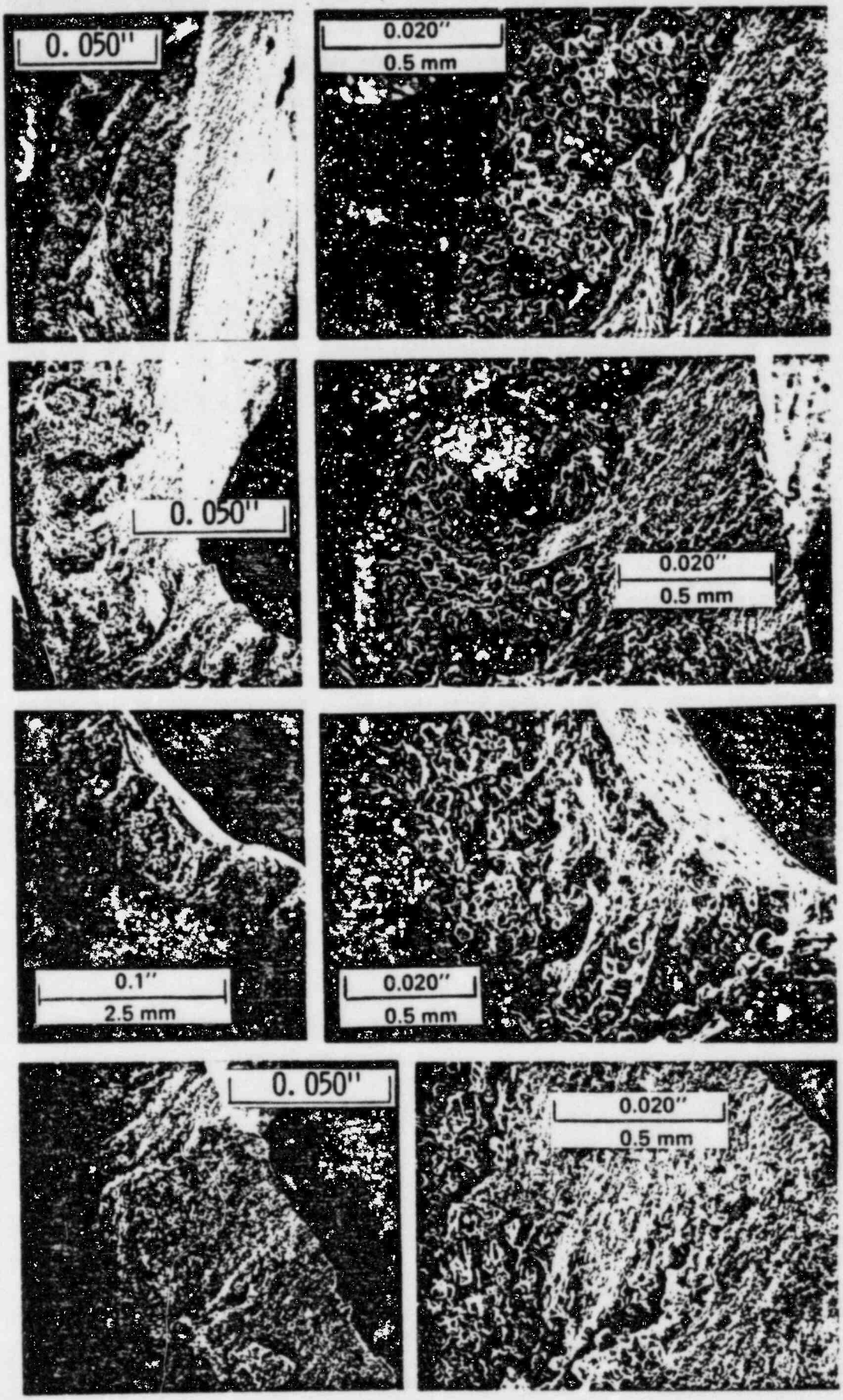

FIGURE 14. B(26-53), Sample 3. SEM fractographs of preceding series. Top = 120°, Bottom = 200°, sequentially arranged in 30° intervals. Magnifications vary because of sample tilt.

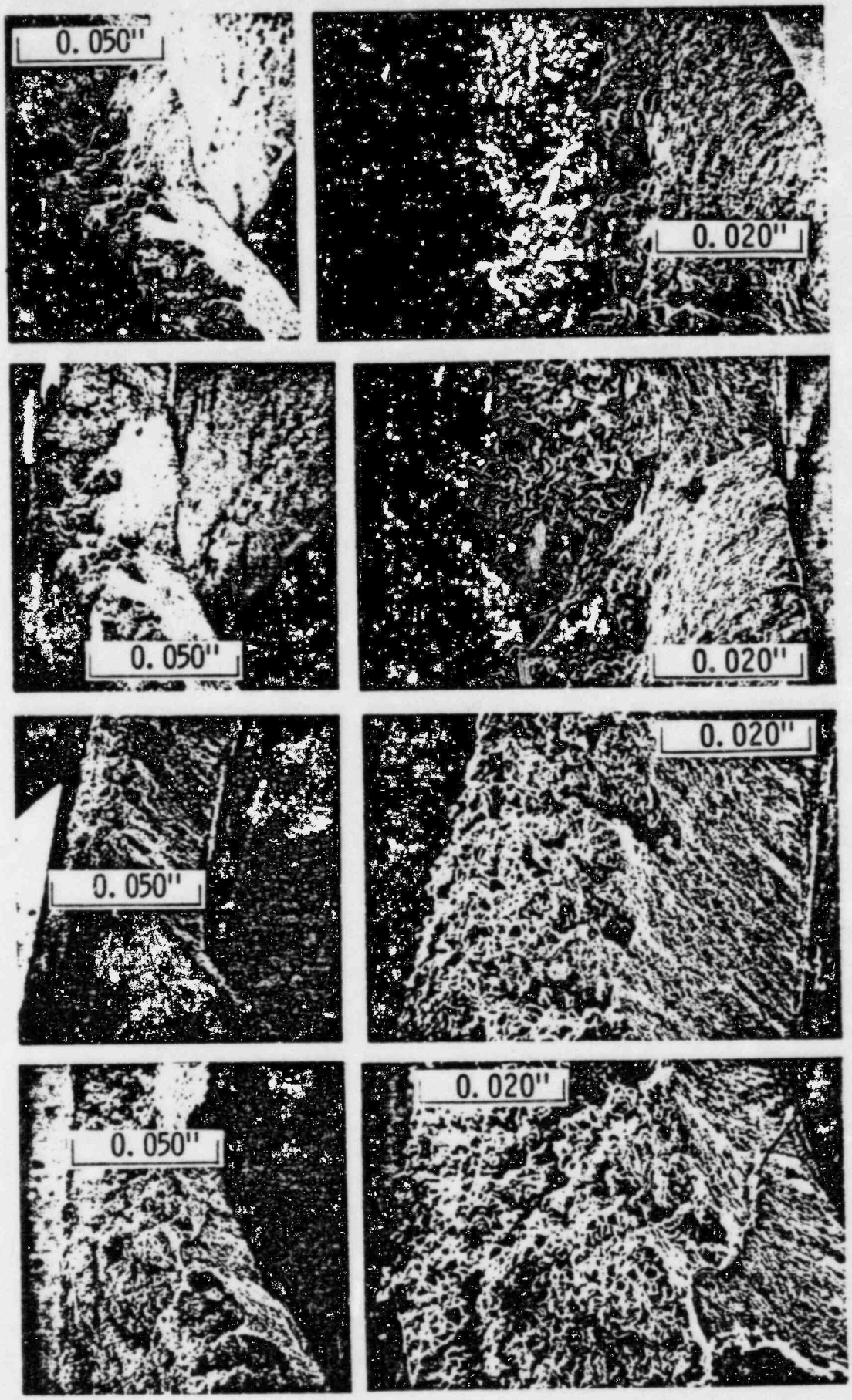

FIGURE 15. B(25-53), Sample 3. Conclusion of SEM fractography of Figures 13 and 14. Top = 240°, Bottom = 330°, with 30° intervals in order. Variable magnifications due to tilt of sample.

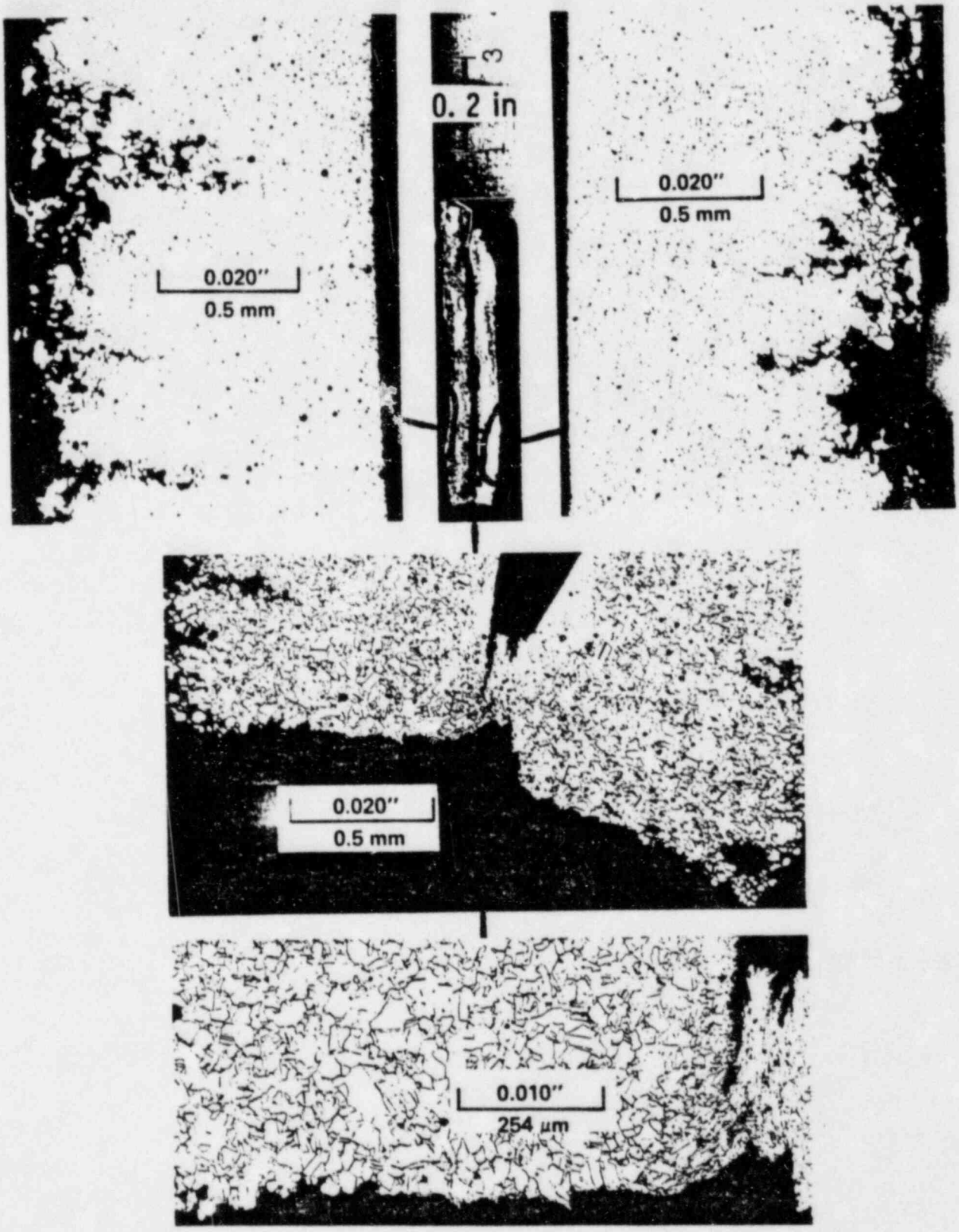

FIGURE 16. B(26-53), Transverse Half-Ring Cross Section within Tube Sheet (Sample 4 of Figure 5). Sample was first bent on itself to open up OD intergranular involvement. Inset at top shows OD at outer edges, ID surfaces touching in middle, and remaining ligament at bottom. Lower 2 photomicrographs show the intergranular involvement edge-on (horizontal orientation) and ligament area.

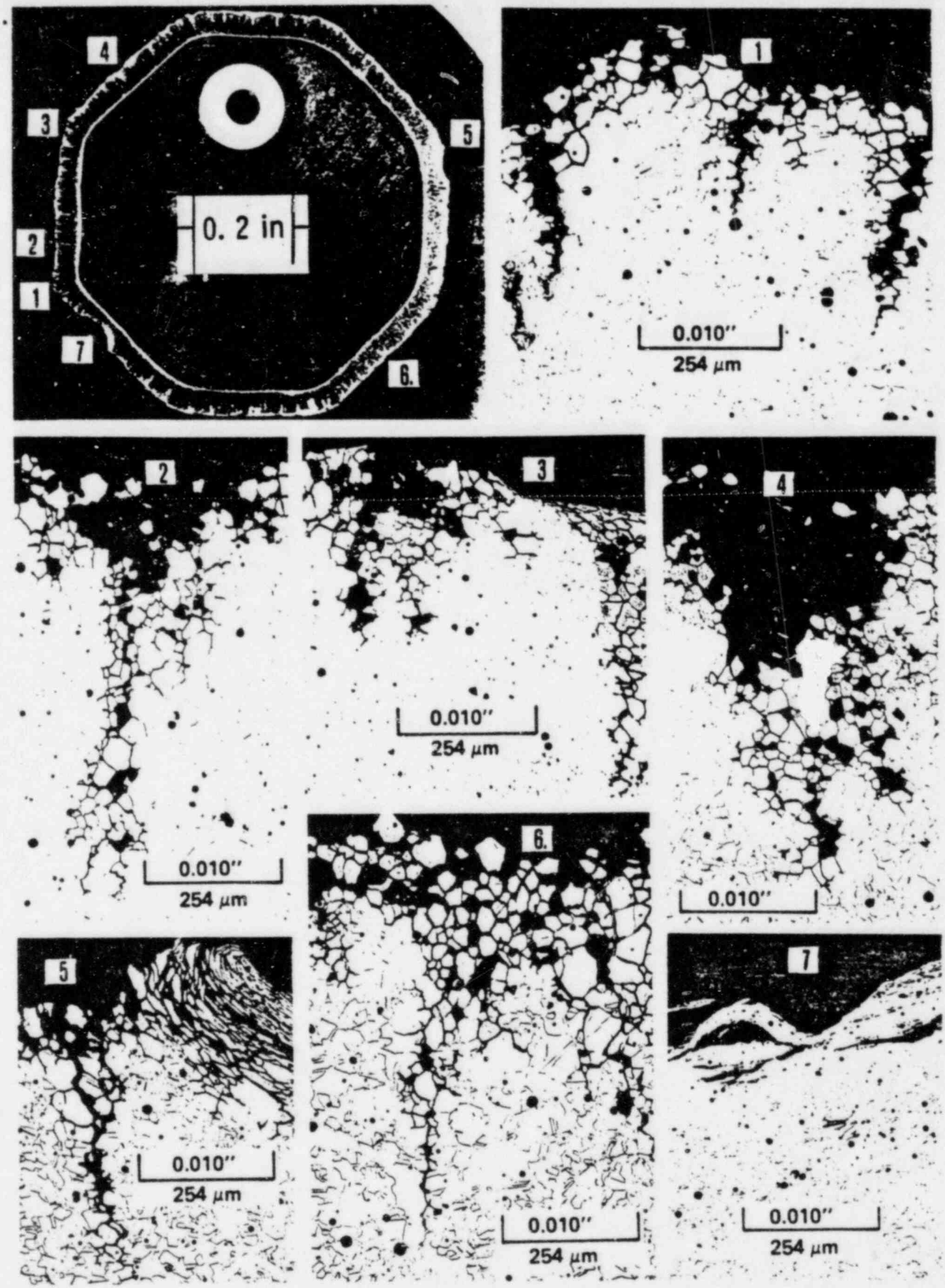

FIGURE 17. B(26-53), Transverse Full-Ring Cross Section within Tube Sheet at Point of Distortion due to Tube Pulling. Upper left = photomacrograph of etched octagonal-shaped (distorted) transverse sample (No. 5 of Figure 6). Photomicrographs are of OD areas.

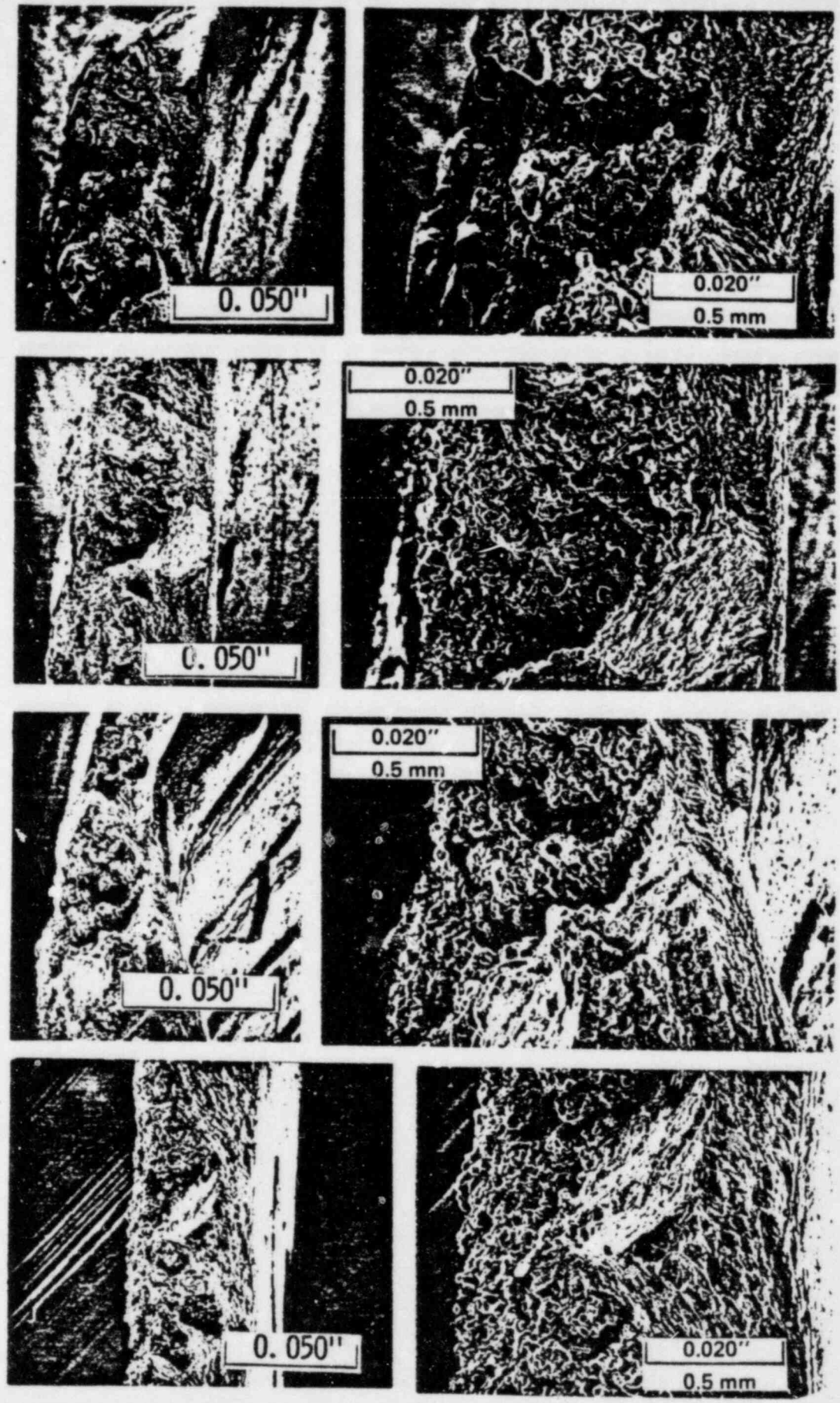

FIGURE 18. B(26-53), Sample 6 of Figure 7. Fracture surface nearer to primary face of tube sheet than similar sample of Figures 13 - 15. SEM's at 30° intervals from 0° (top) to 90° (bottom). Magnifications vary with location within each SEM due to specimen tilt.

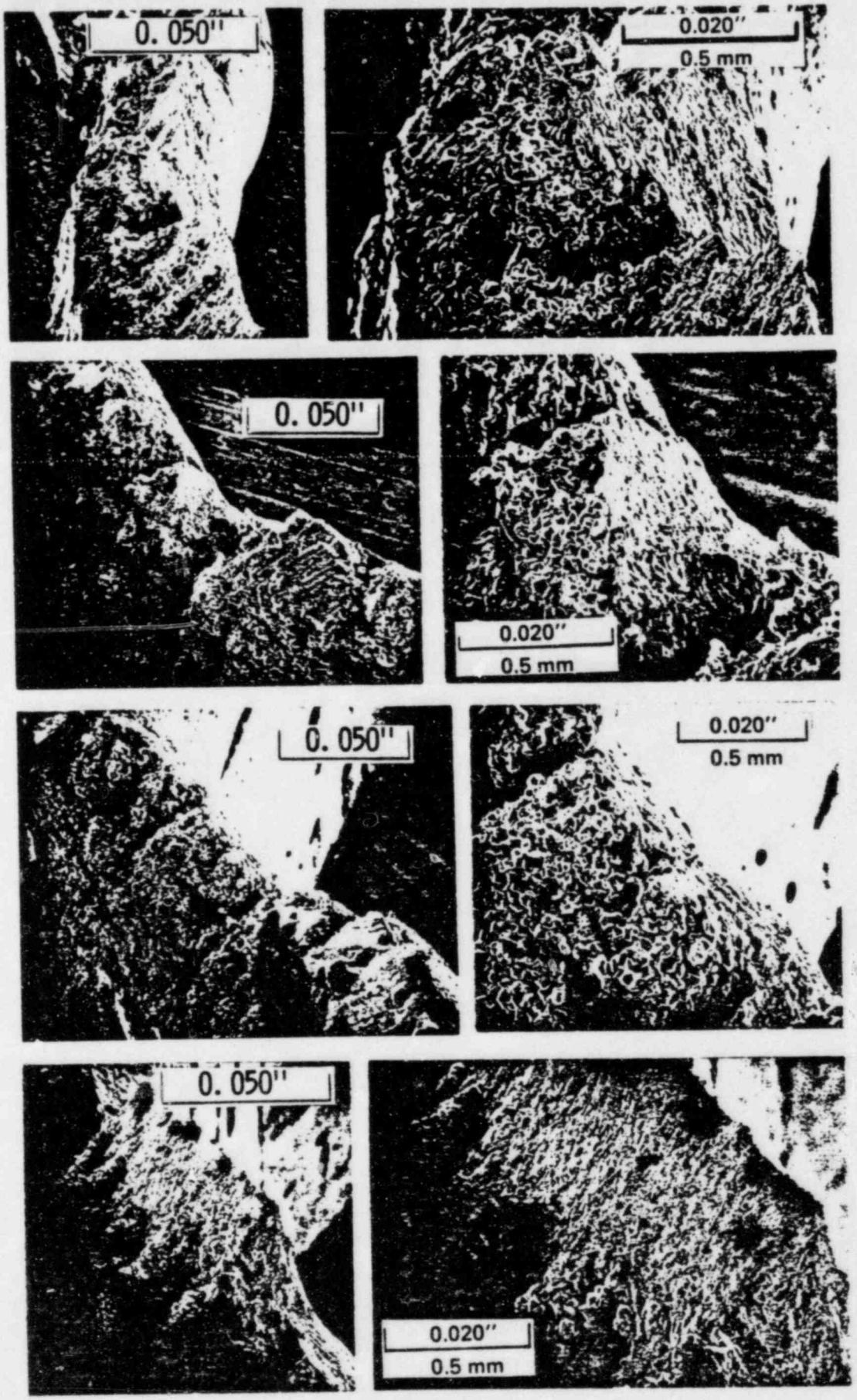

FIGURE 19. B(26-53), Sample 6. Additional SEM fractographs at 30° intervals from 120° (top) to 200° (bottom). Variable magnifications due to specimen tilt.

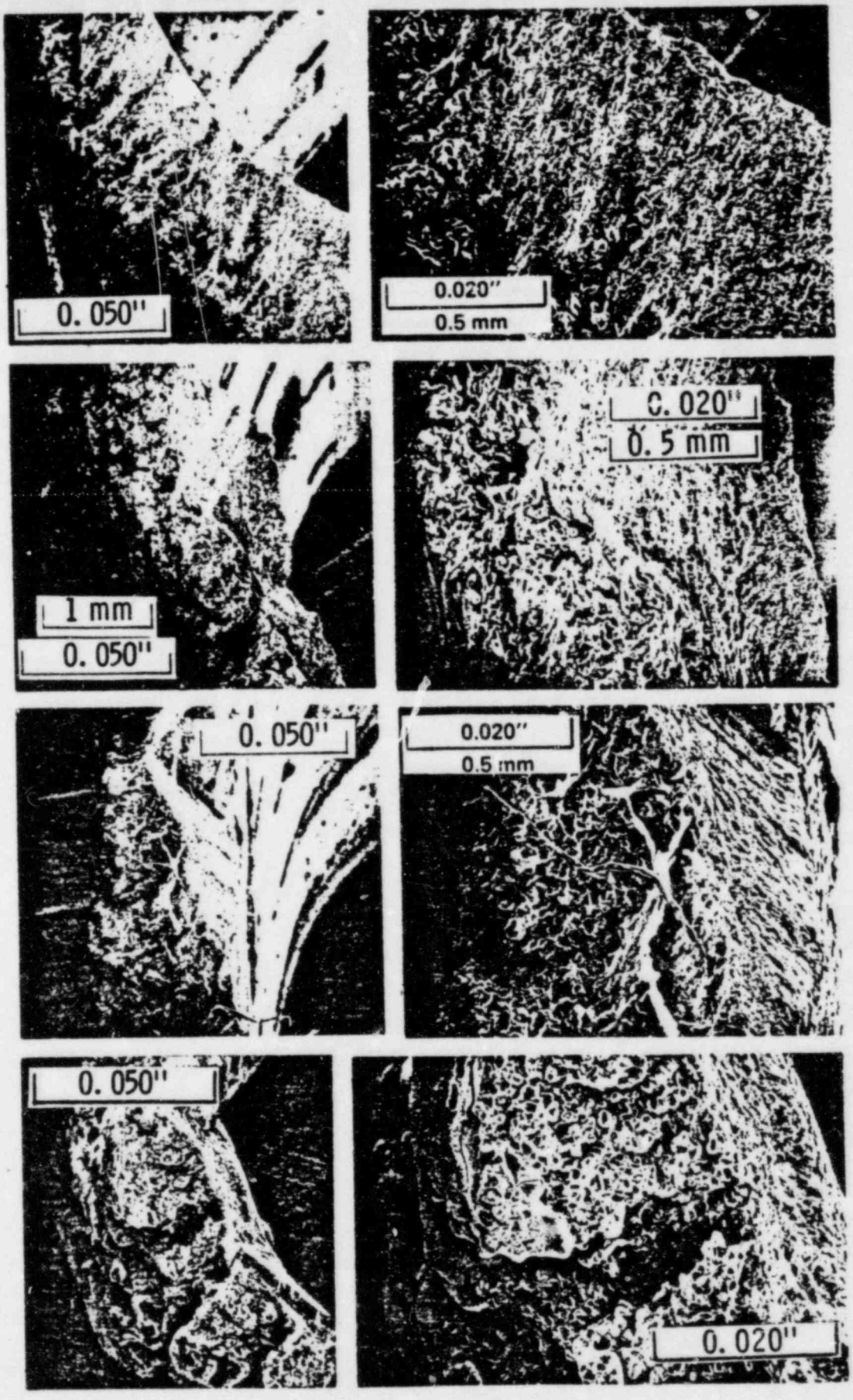

FIGURE 20. B(26-53), Sample 6. Concluding SEM fractographs at 30° intervals from 240° (top) to 330° (bottom). Magnifications vary within each photomicrograph due to specimen tilt on the stage of the SEM.

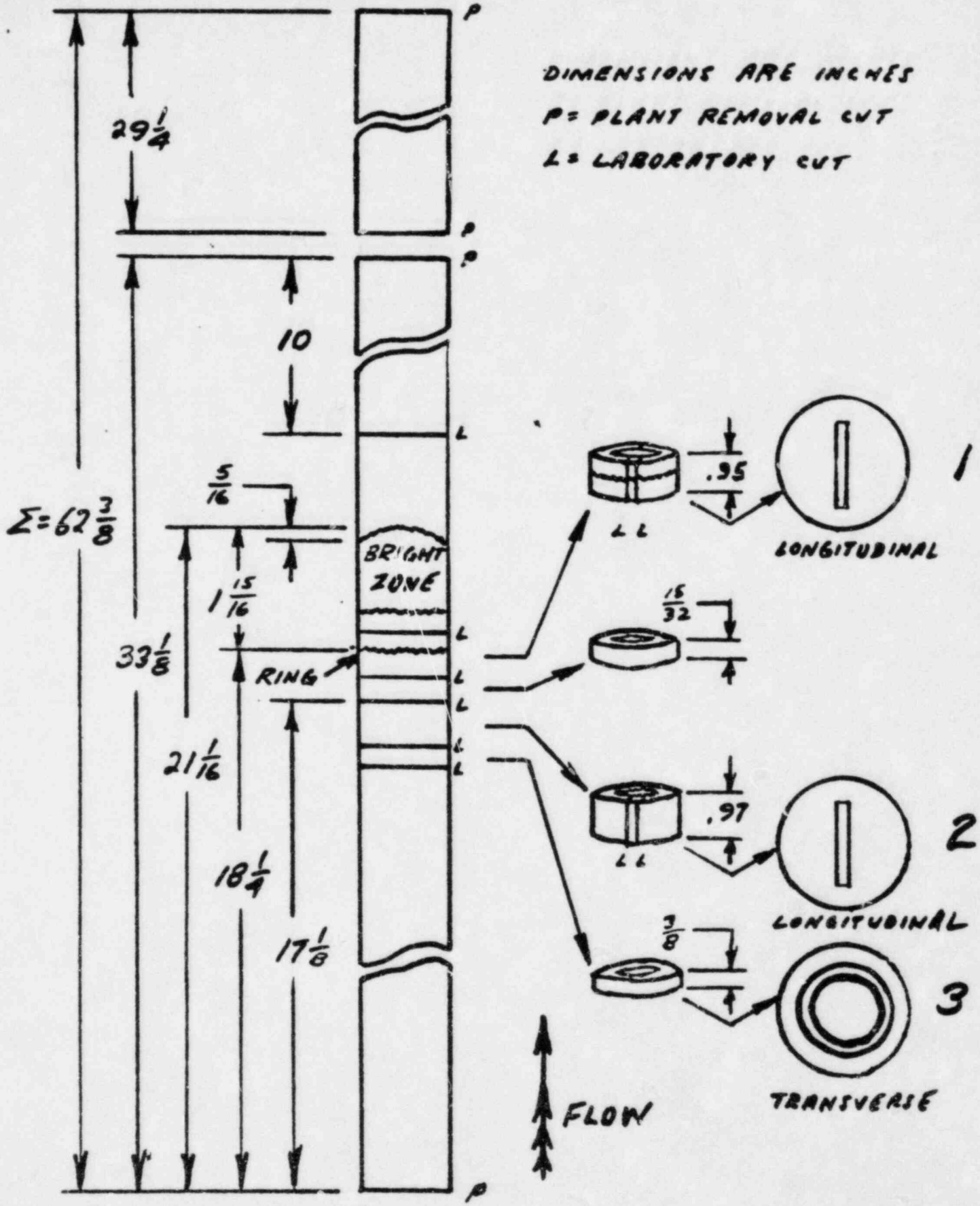

FIGURE 21. WEP B(30-41) - Laboratory Samples for Microscopic Examinations.

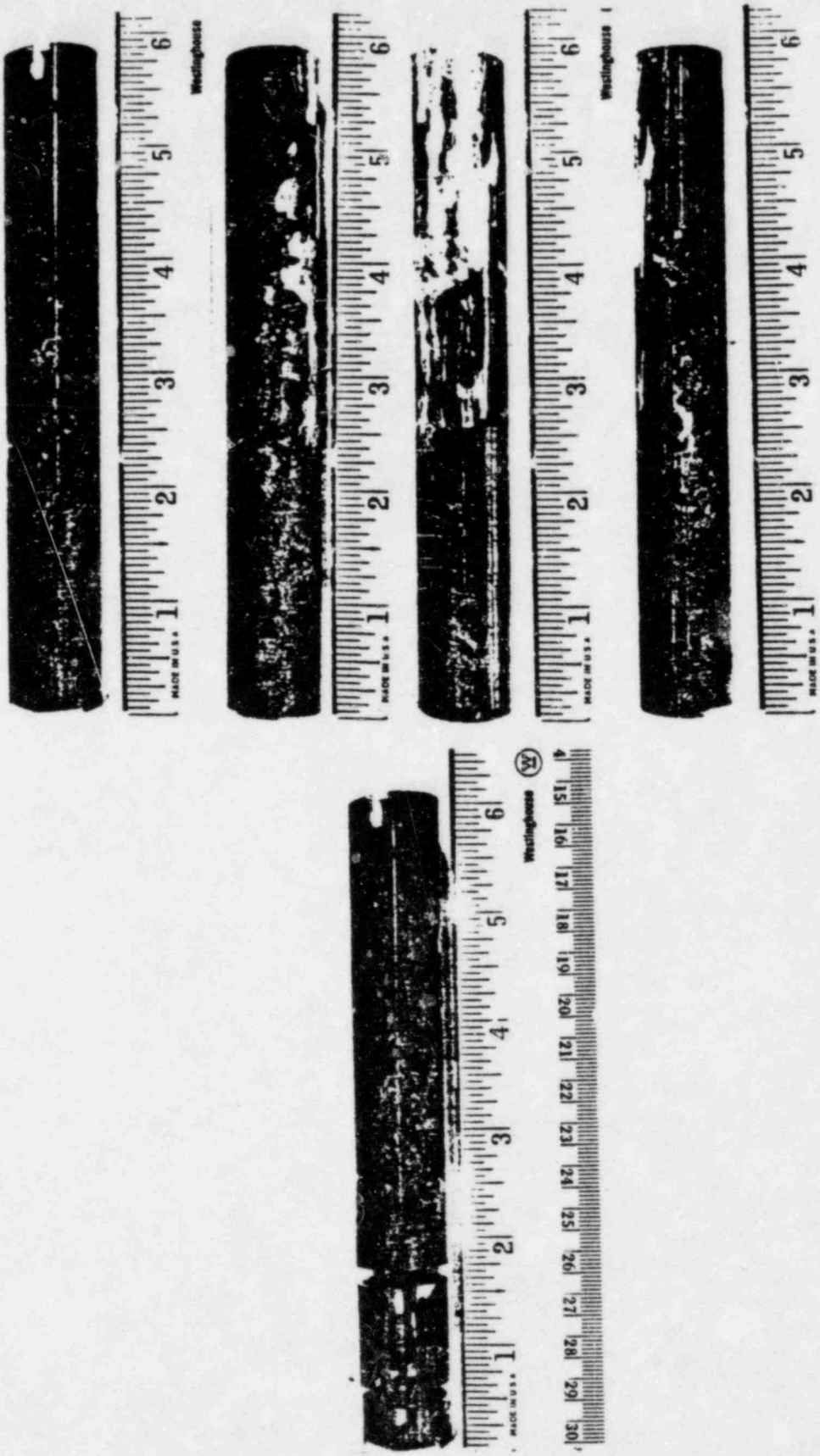

FIGURE 22. B(30-41), Zone near the Top of the Tube Sheet Containing the Ring (located at the 1-in. Mark in the Upper pictures arranged, left-to right: 0°, 90°, 180°, 270°). Lower picture shows sectioning for a longitudinal micro through the ring. Primary flow is upward.

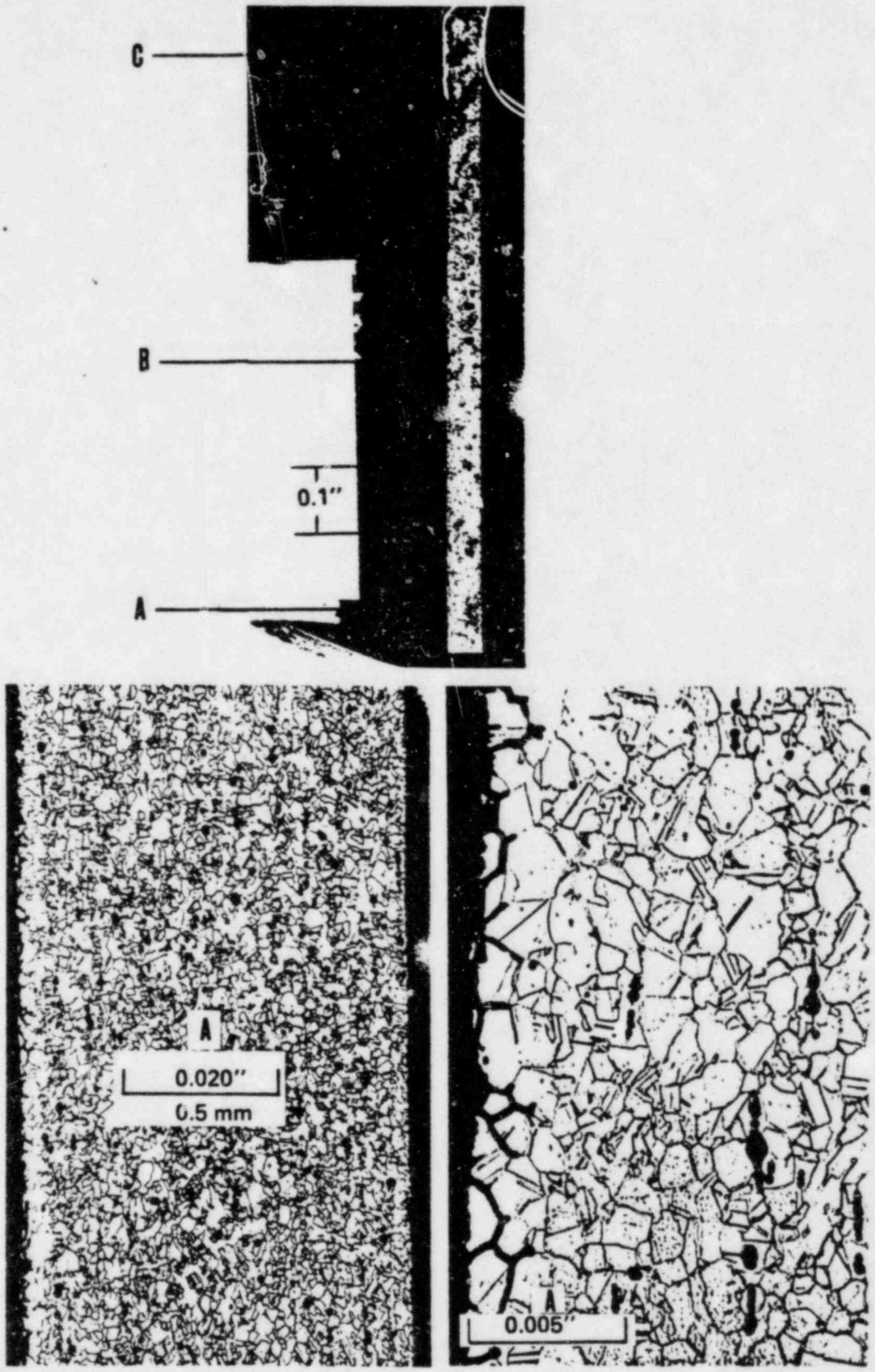

FIGURE 23. B(30-41), Longitudinal Section through Tube Sheet Ring. Upper picture: etched photomacrograph of mounted section with OD at left and primary flow upward. Lower pair of photomicrographs: Area A below the ring, OD on left. (Bromine - methanol etchant.) Sample 1 of Figure 21.

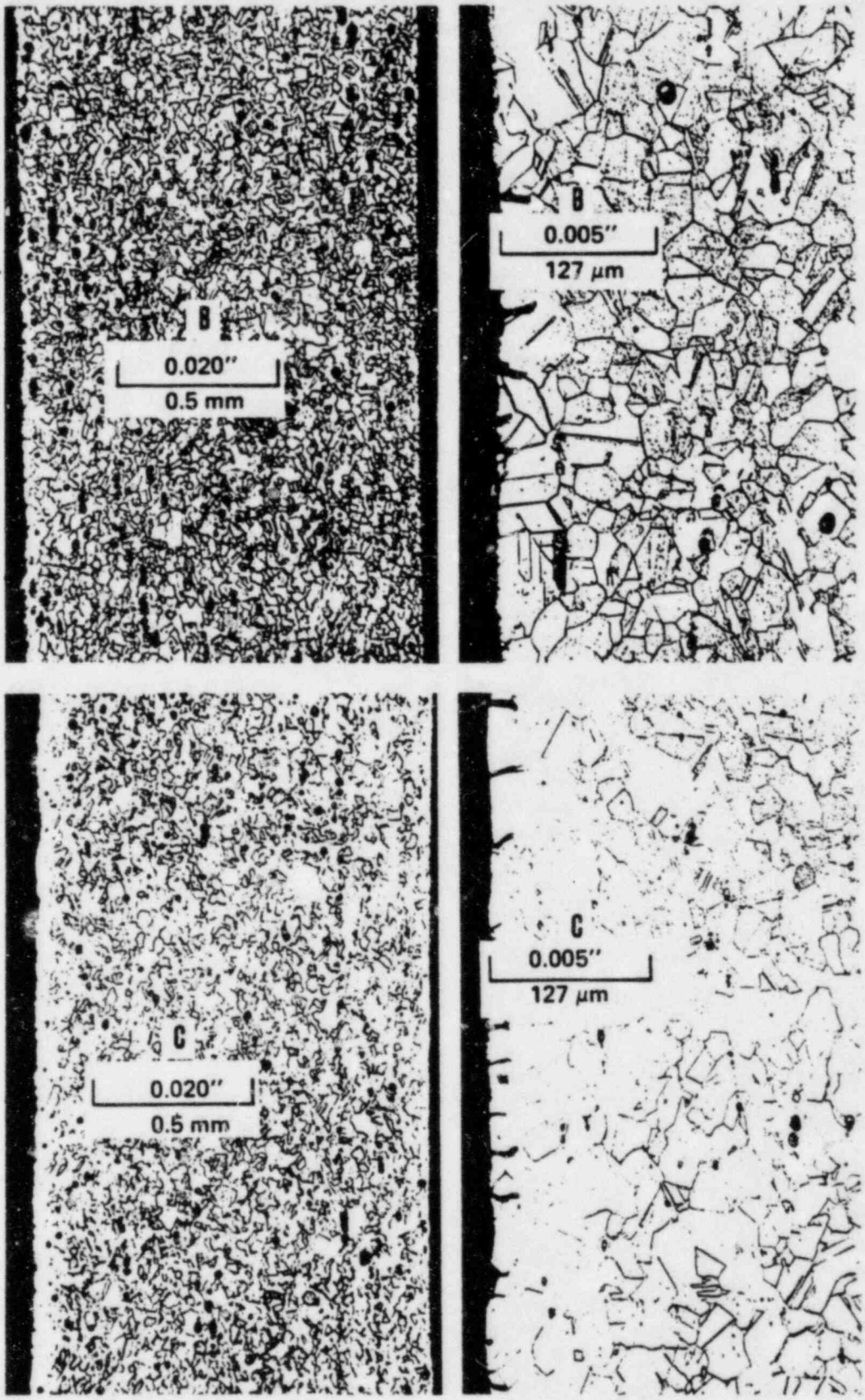

FIGURE 24. B(30-41), Longitudinal Cross Section through Tube Sheet Ring. Area B (near ring) and Area C (above ring) of Figure 23. The OD is at the left.

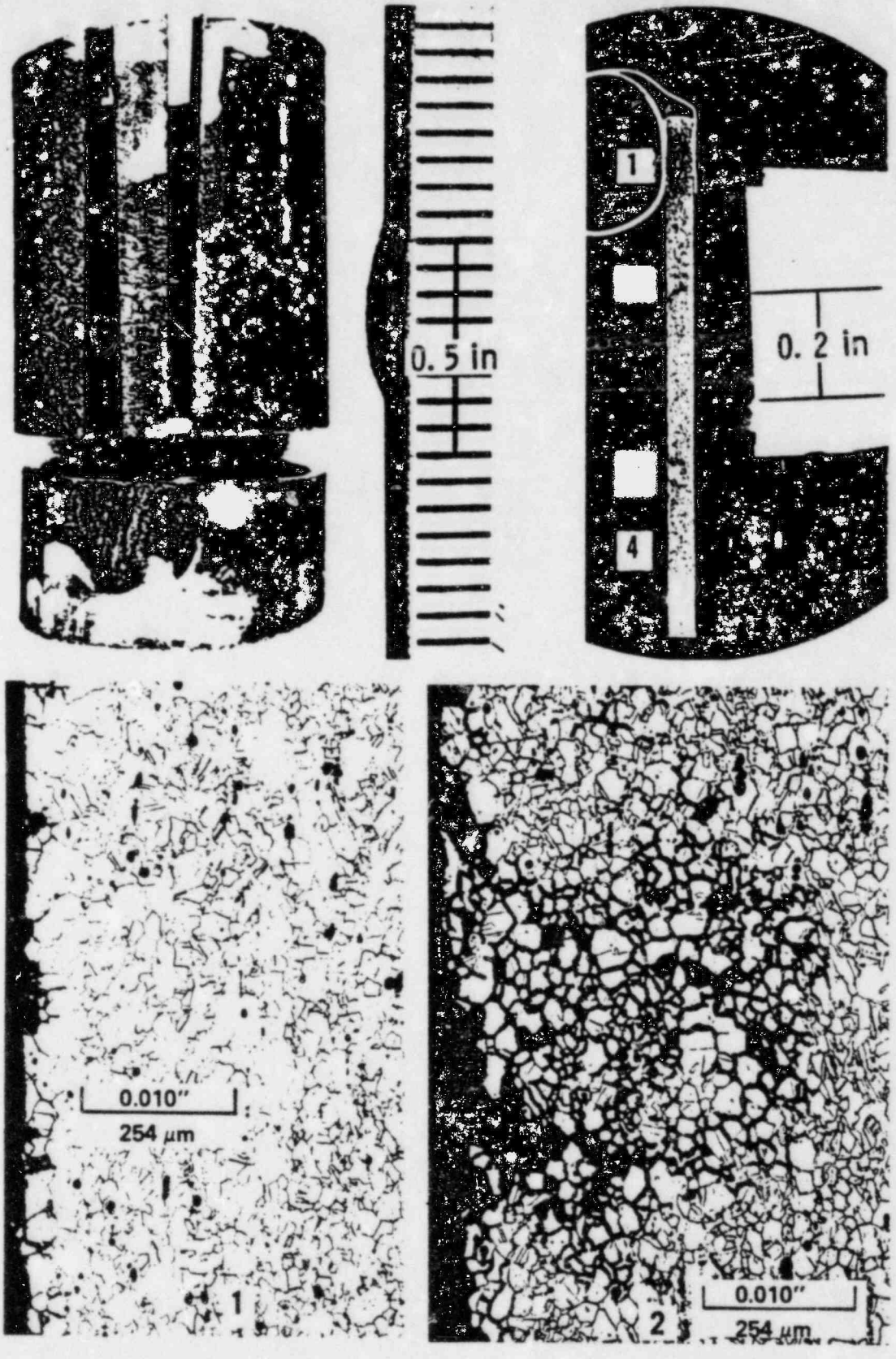

FIGURE 25. B(30-41). Microscopic samples from within the tube. Upper left shows longitudinal sample (No. 2 of Figure 21) and lower ring transverse section (No. 3 of Figure 21). Upper right = photomacrograph of mounted longitudinal section, OD at left. Lower 2 = Longitudinal Areas 1 and 2, with OD at left. Primary flow = upward.

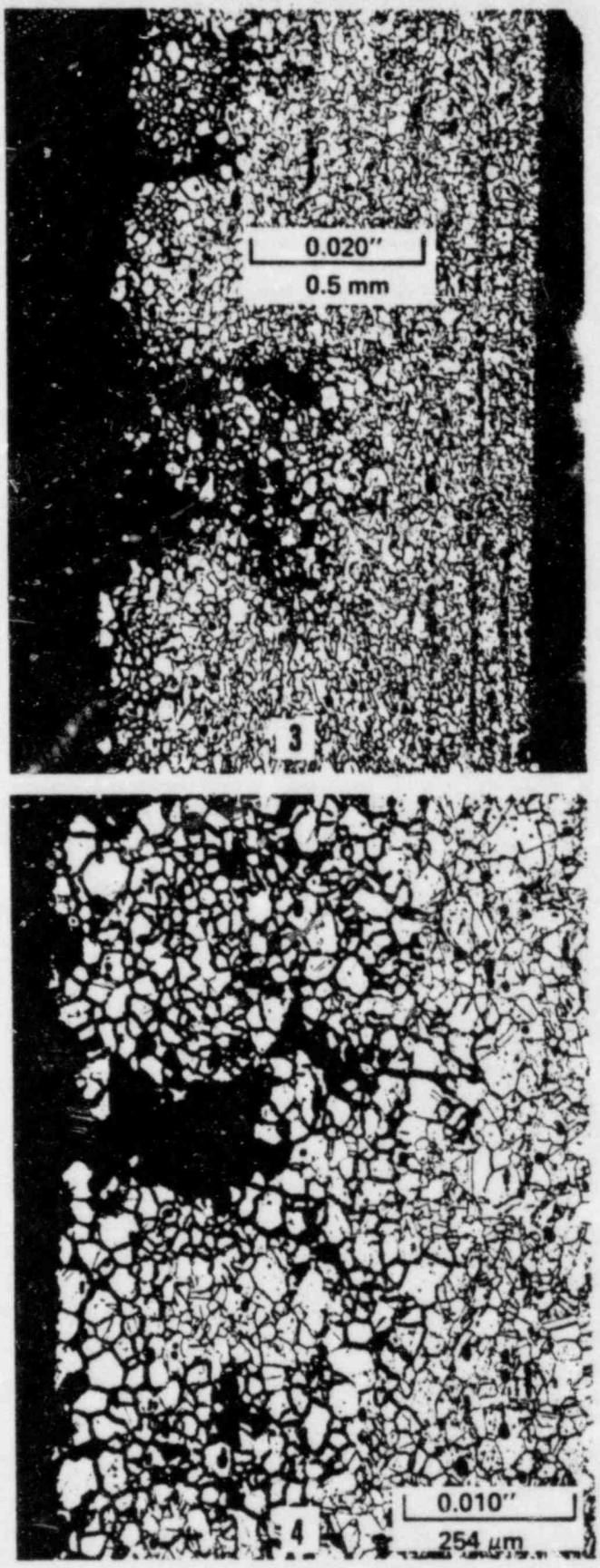

FIGURE 26. B(30-41), Longitudinal Cross Section within Tube Sheet (Sample 2 of Figure 21). Areas 3 and 4 of Figure 25. OD is at left.

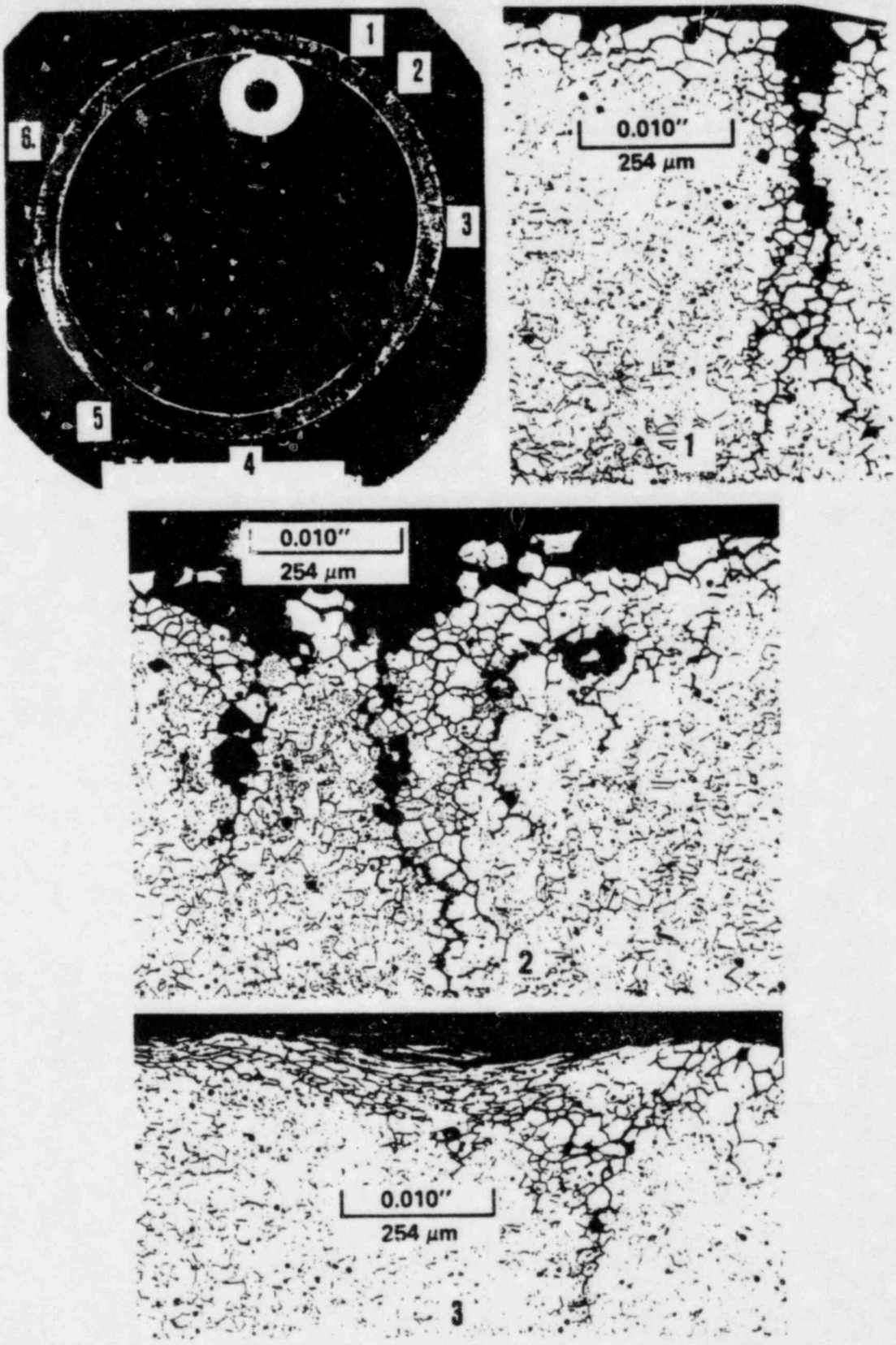

FIGURE 27. B(30-41), Transverse Cross Section within Tube Sheet, Sample 3 of Figure 21. Photomicrographs are of OD edges at identified locations.

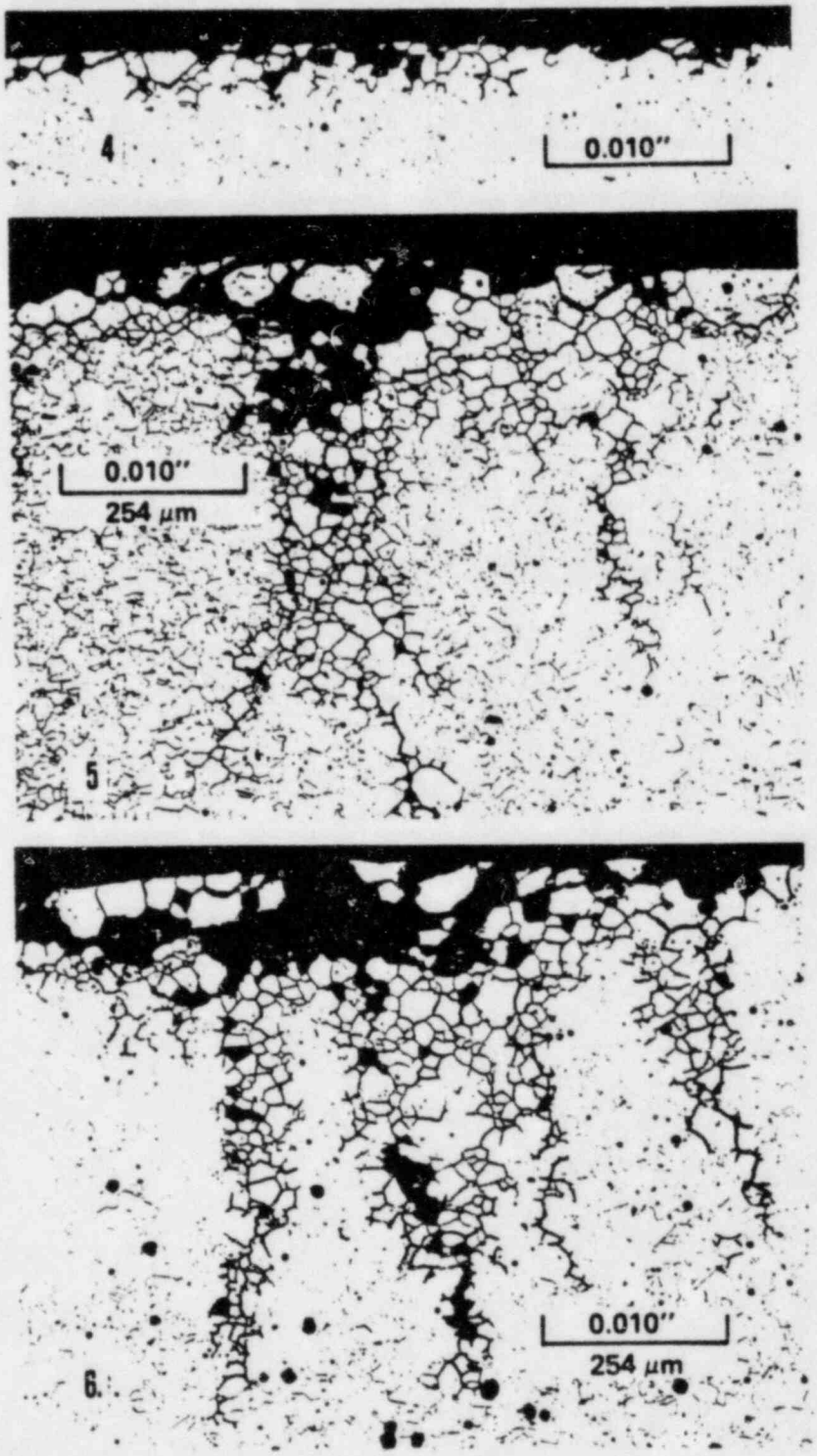

FIGURE 28 B(30-41), Transverse Cross Section with Tube Sheet. Continuation of OD photomicrographs at location shown in Figure 27.

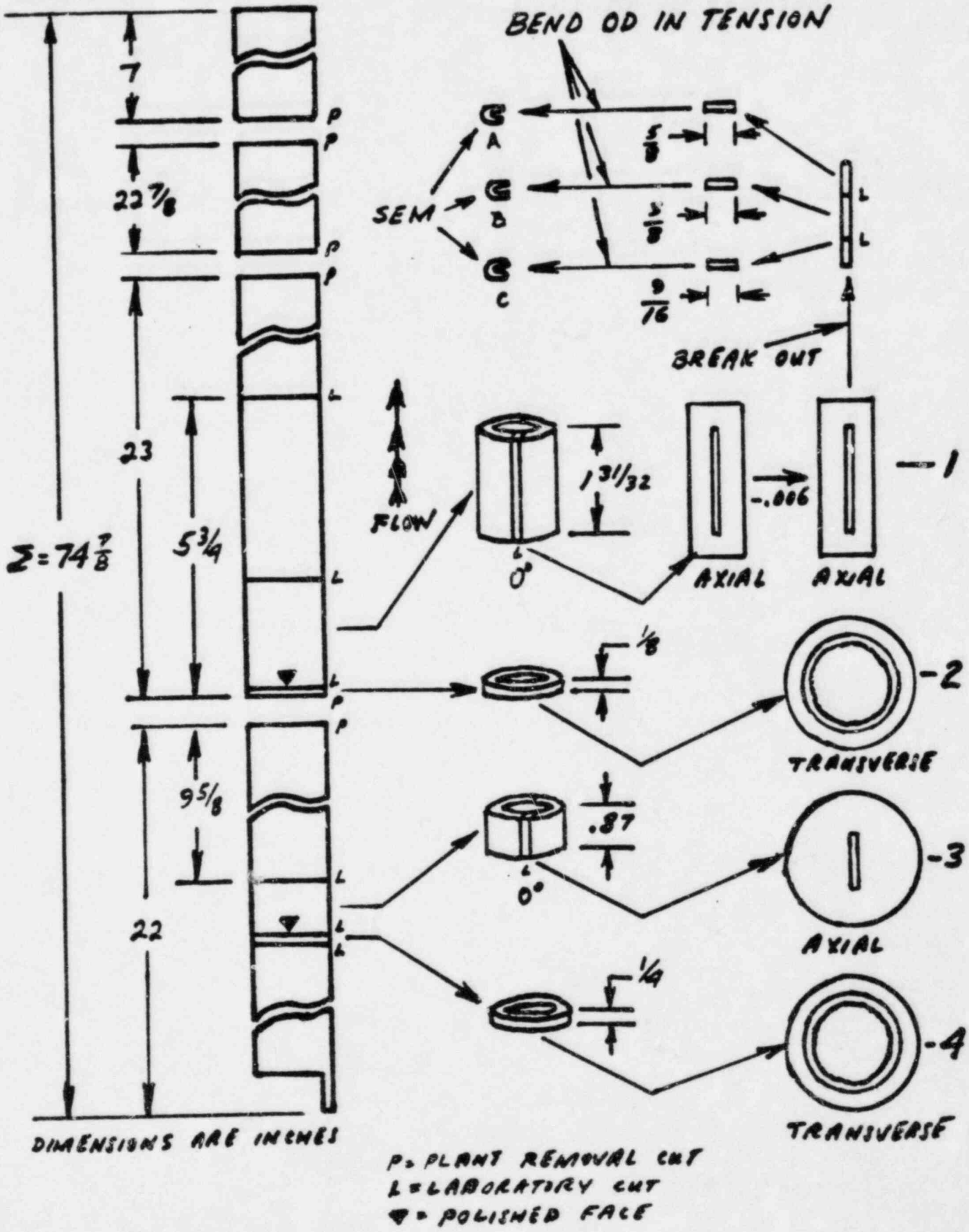

FIGURE 29. WEP B(19-37) - Laboratory Samples for Microscopic Examinations.

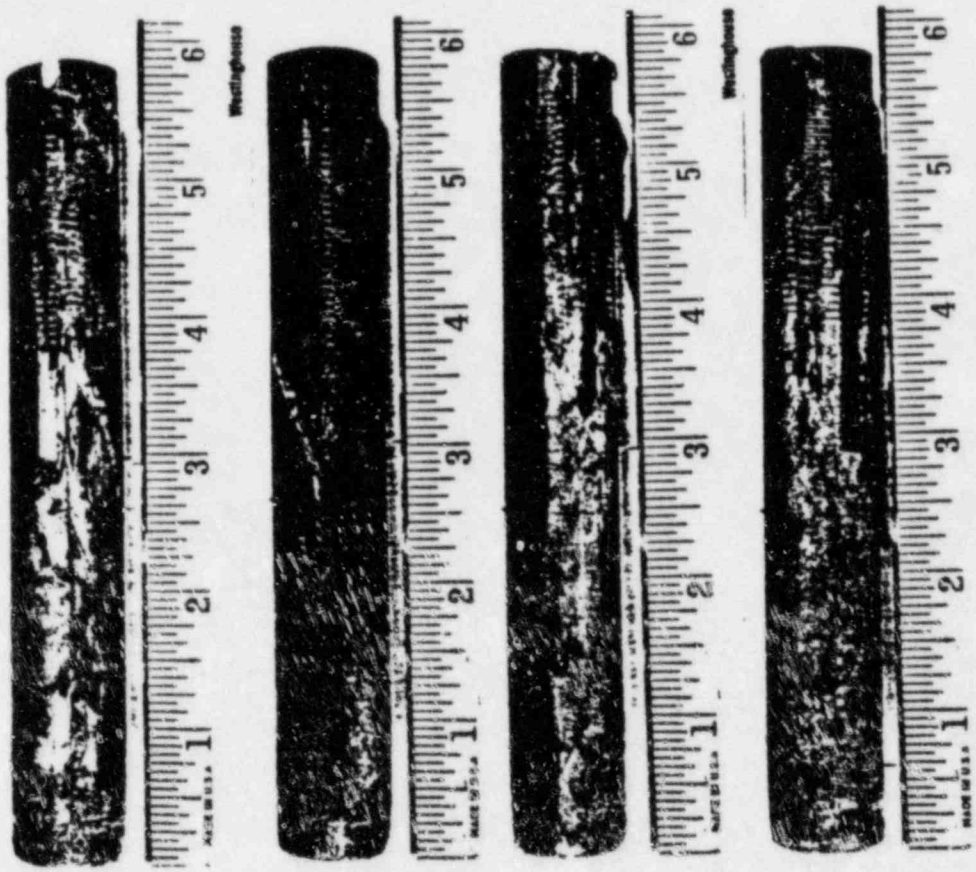

FIGURE 30. B(19-37) - Sectioned piece containing the elevation corresponding to the top of the tube sheet. This is the 5-3/4-in.-long piece, shown in Figure 29, from which a 2-in.-long longitudinal micro (Figure 31) was prepared.

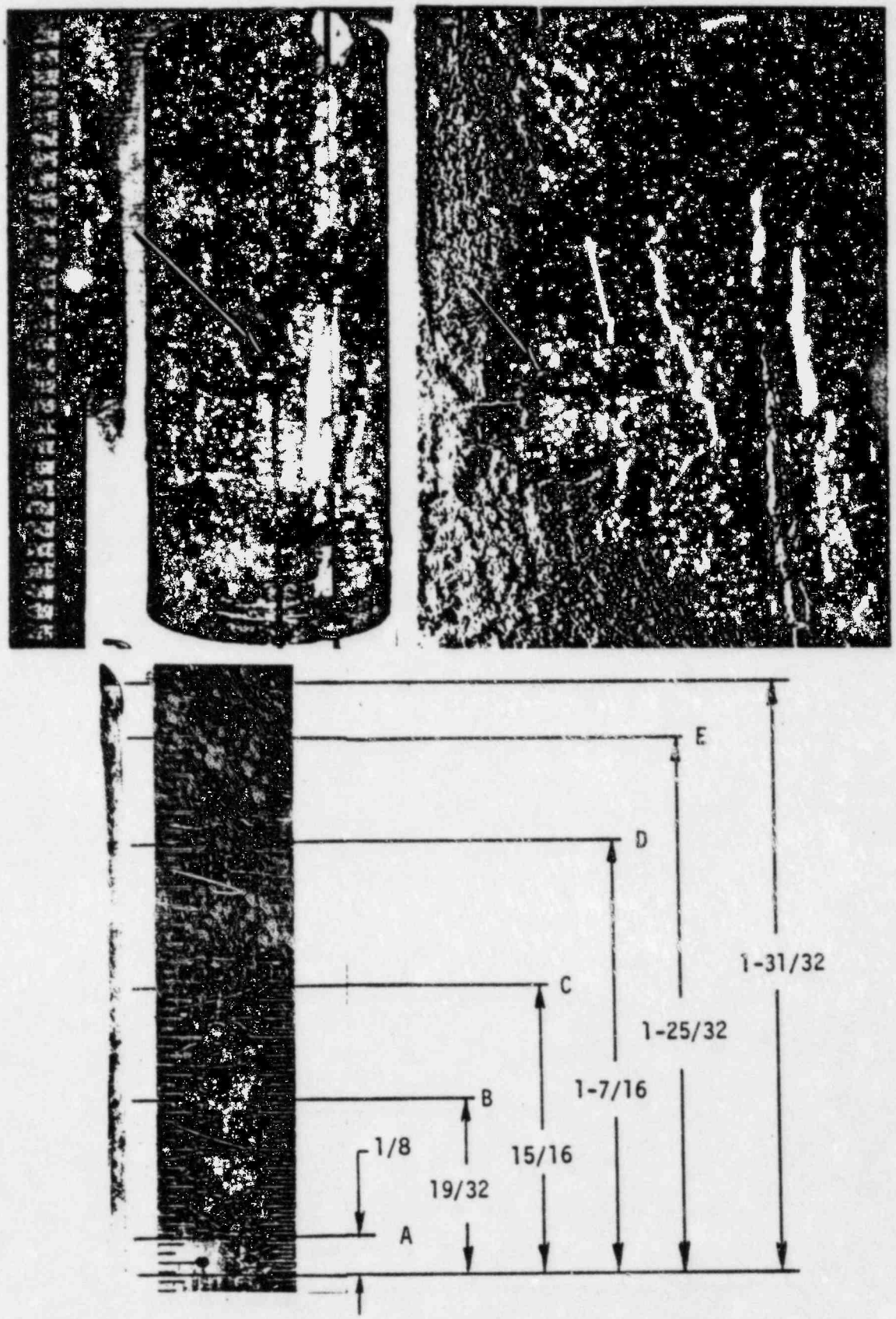

FIGURE 31. B(19-37). Top of Tube sheet Region. Sectioning for special 2-in.-long longitudinal micro. Upper pair shows cut lines and zone through which micro was made (arrows). The symbol ▶ denotes the polished face. Lower picture is a photomacrograph of the resultant cross section (OD on left) with locations (A-E) of high-magnification photomicrographs (Figures 32-35). Primary flow is upward. (Sample 1 of Figure 29.)

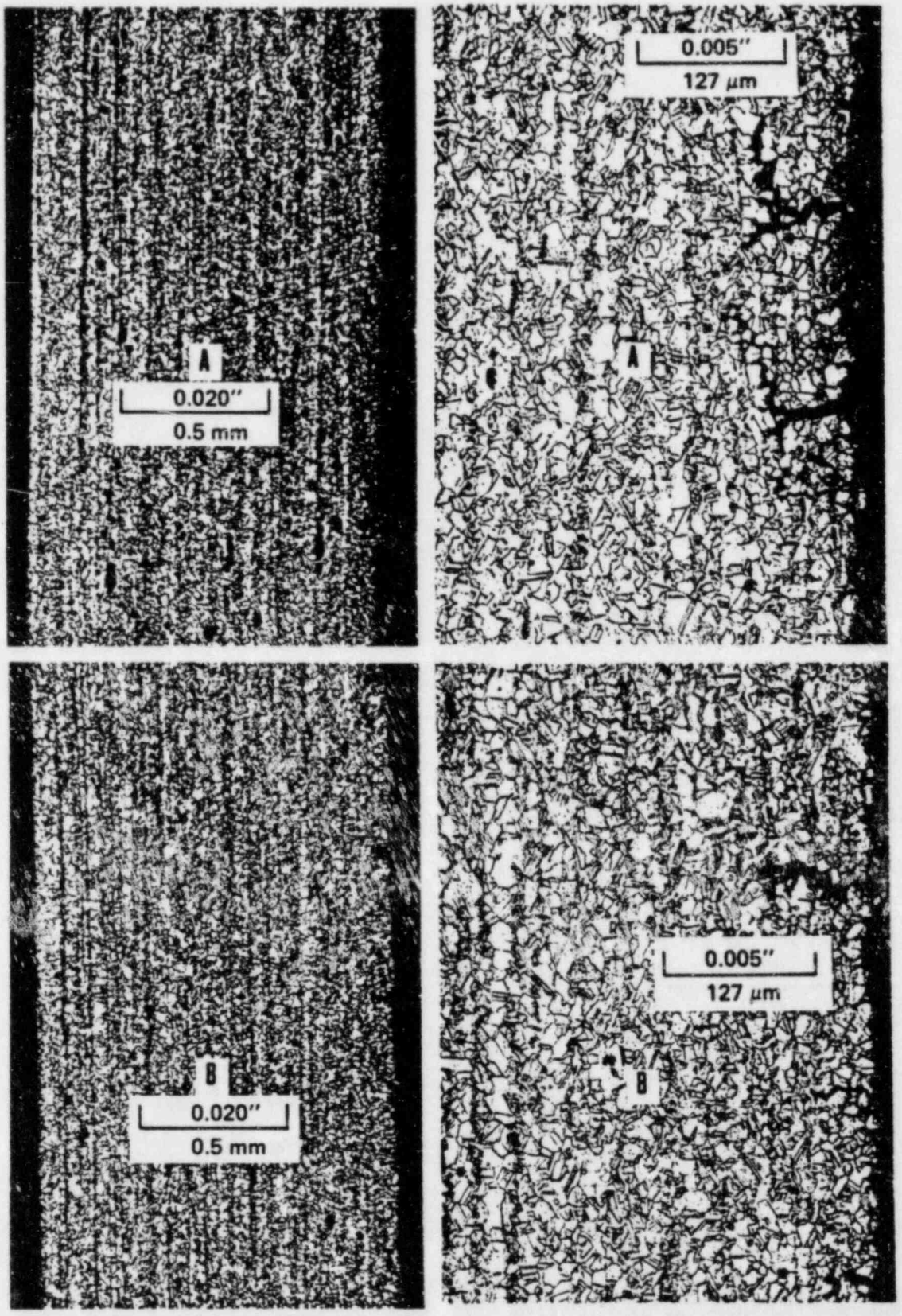

FIGURE 32. B(19-37), Top of Tube Sheet, 2-in.-long Axial Micro. Areas A and B of Figure 31, lower. OD edges are at right; primary flow is upward. Etched with bromine in methanol.

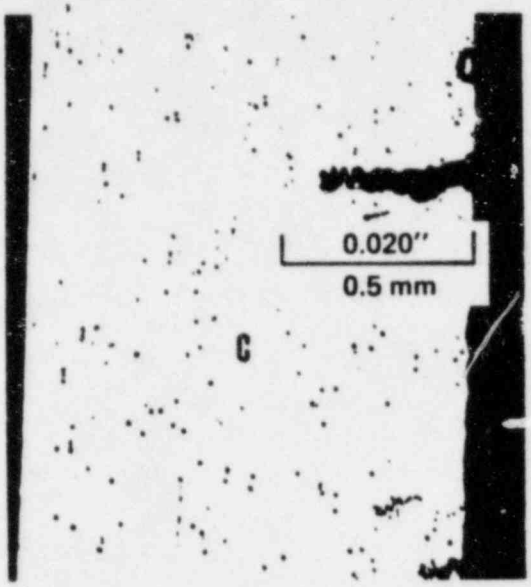

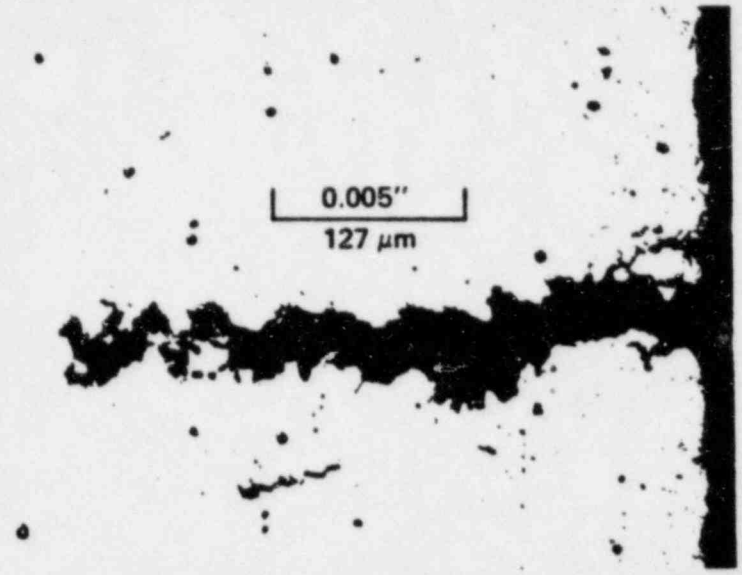

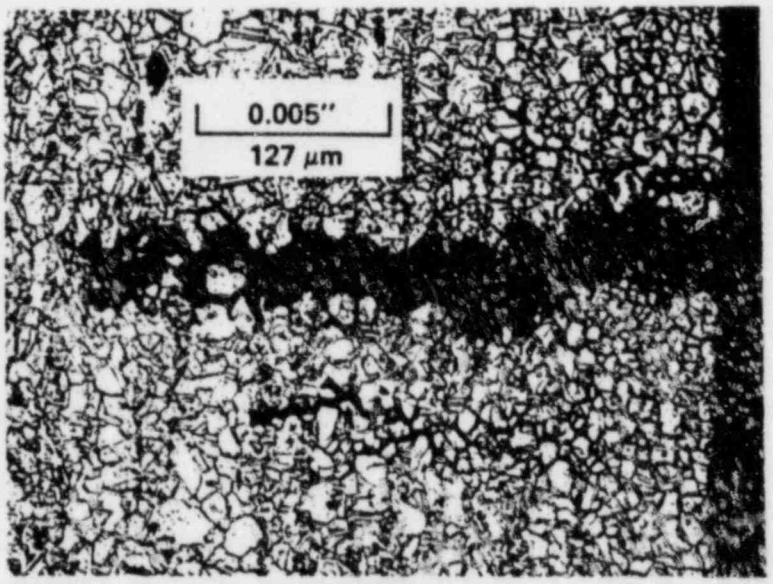

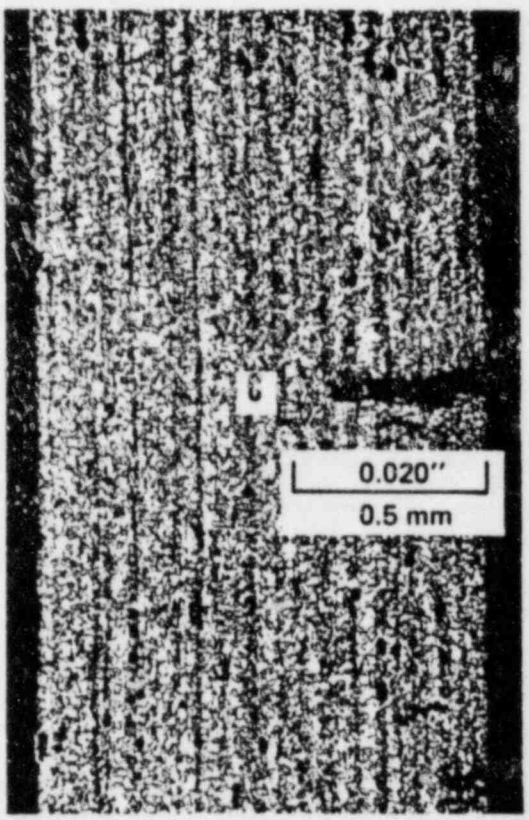

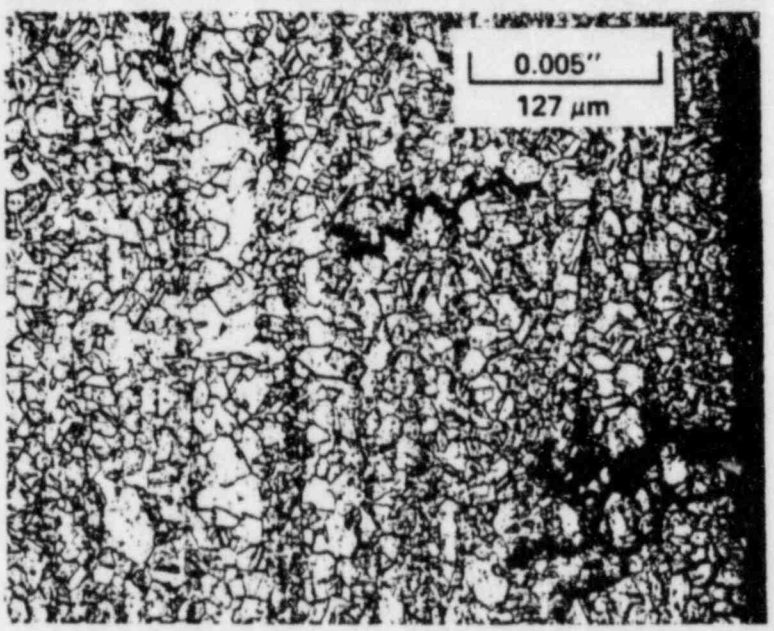

FIGURE 33. B(19-37), Axial Section at Top of Tube Sheet, Area C of Figure 21. OD is at left; primary flow is upward.

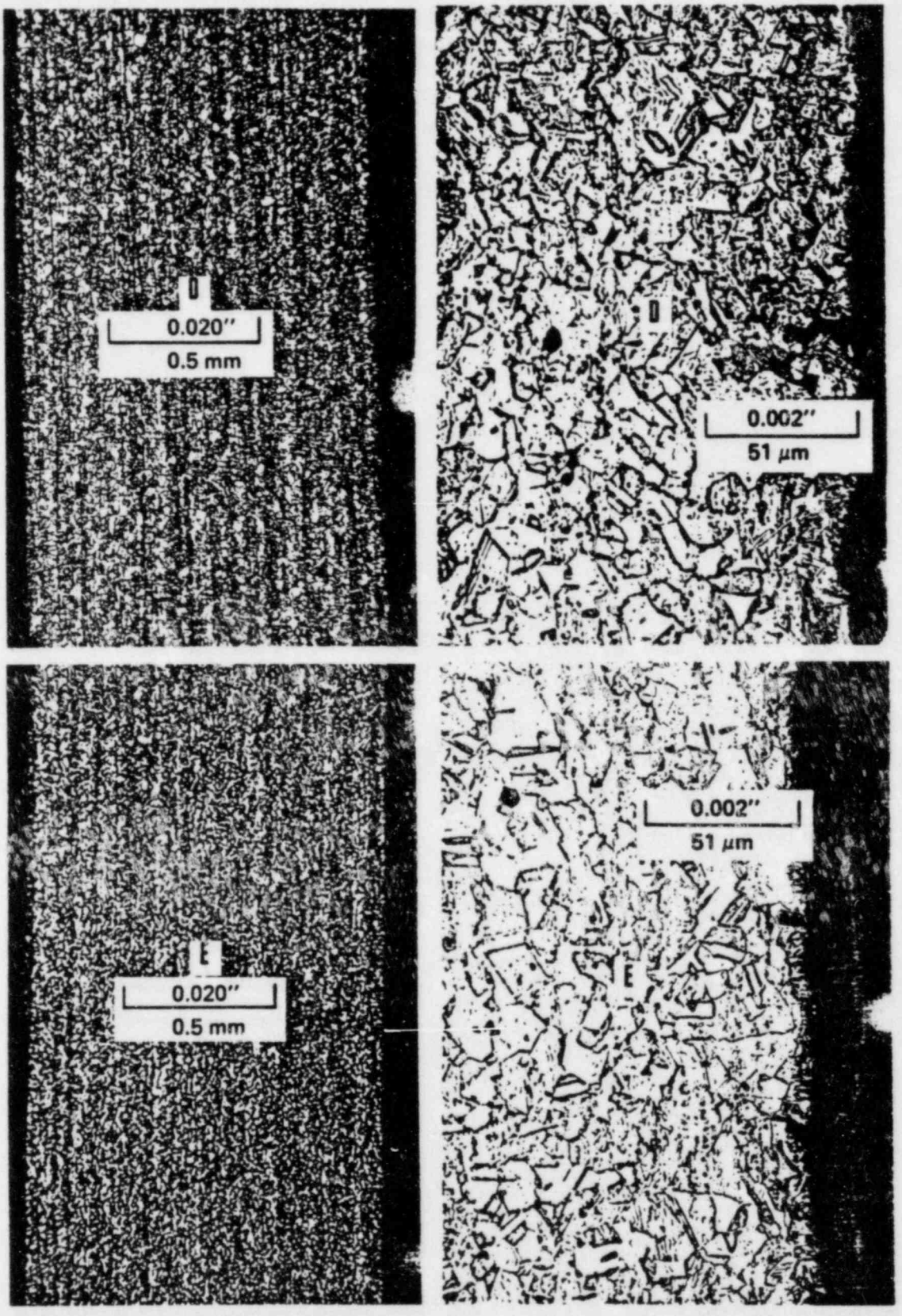

FIGURE 34. B(19-37,, Axial Section at Top of Tube Sheet, Areas D and E of Figure 31. OD edges are to the right and primary flow is upward.

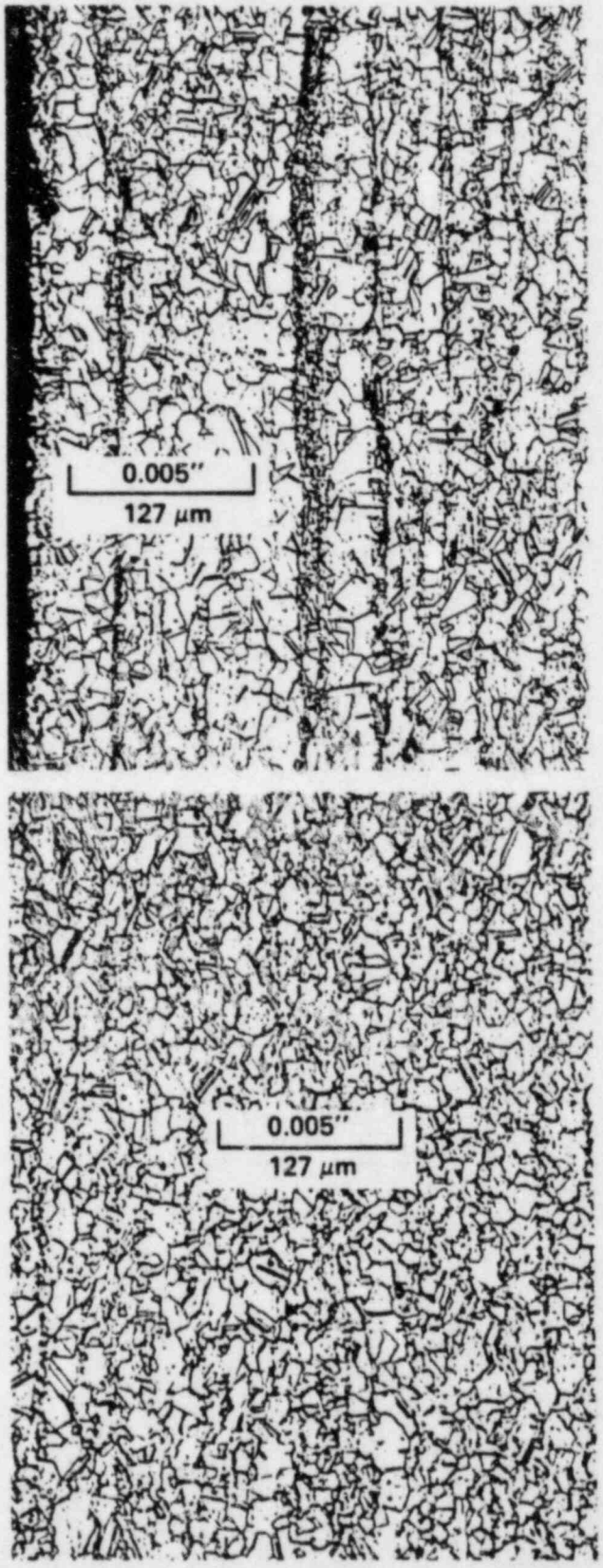

FIGURE 35. B(19-37), Axial Section at Top of Tube Sheet, Area A of Figure 31. Photomicrographs of ID edge (upper) and midwall region (lower).

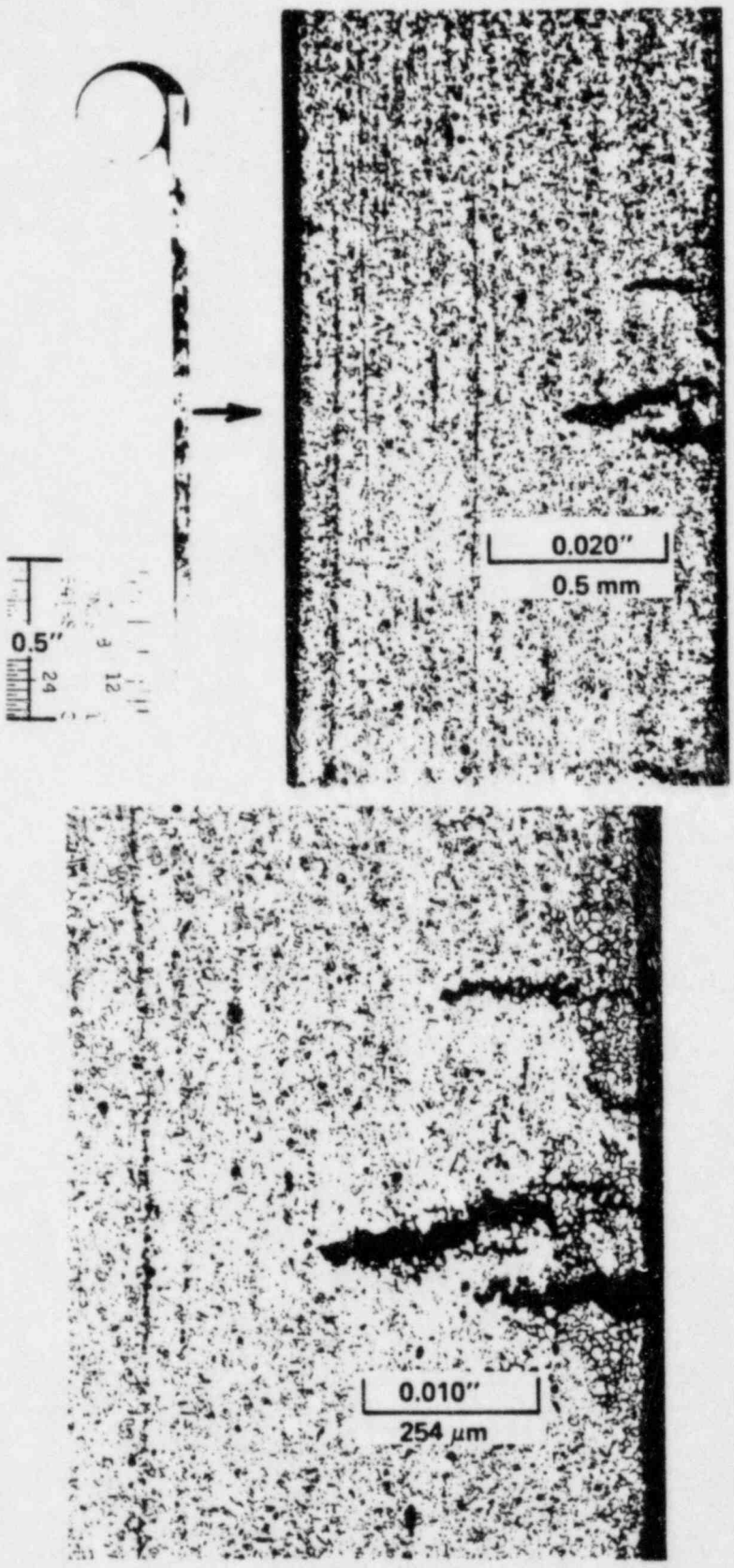

FIGURE 36. B(19-37). Axial Cross Section at Top of Tube Sheet (Sample 1 of Figure 29), Reground 0.006 in. deeper than plane of Figures 31 - 35. Upper left = photomacrograph of repolished sample. Photomicrographs are at Area C of Figures 31 and 33. The OD is at right and primary flow is upward.

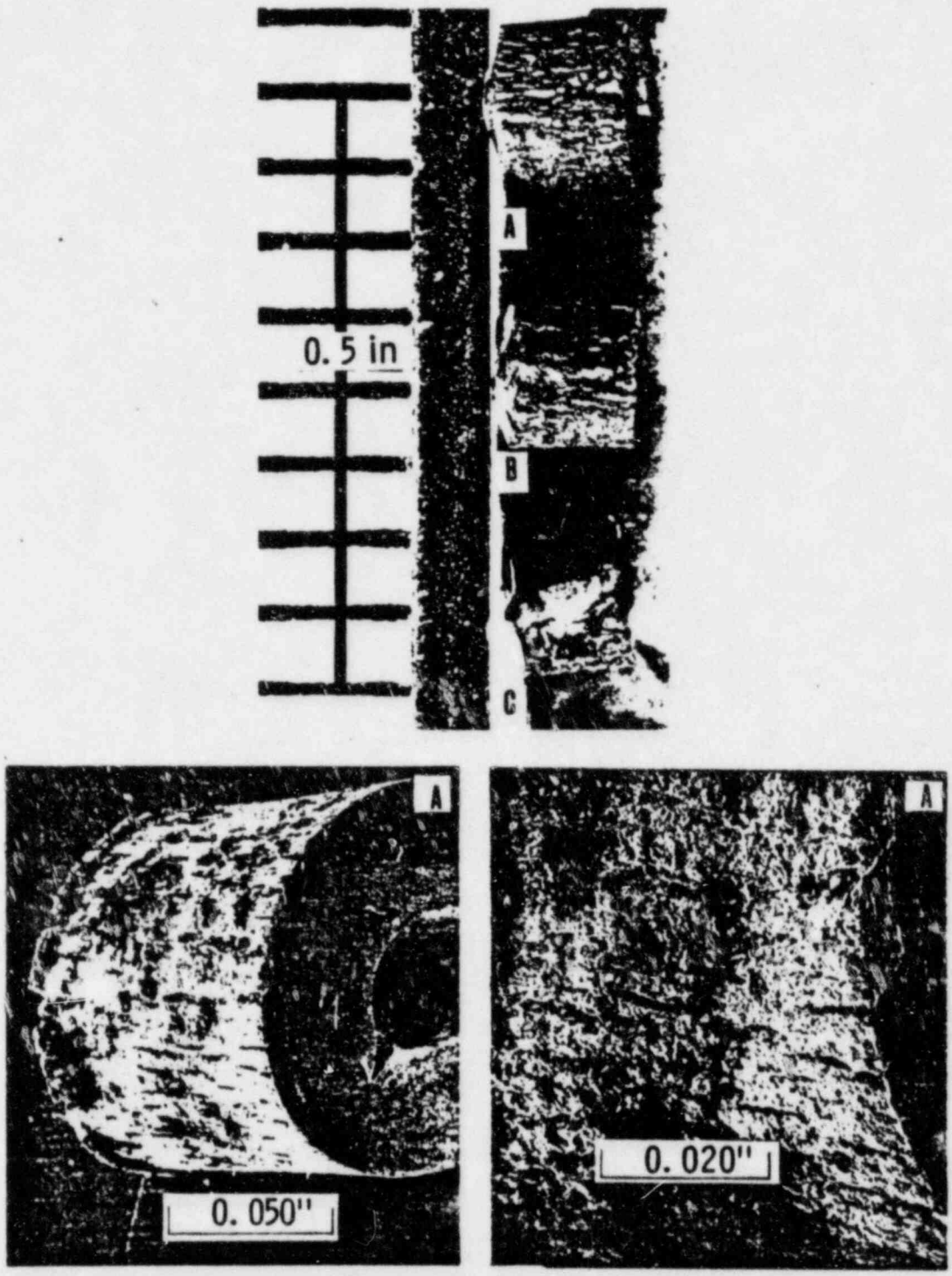

FIGURE 37. B(19-37), Axial Cross Section at Top of Tube Sheet. Broken out of mount, cut in thirds, and bent to expose OD and open the intergranular involvement. Upper photograph shows samples A, B, C (Keyed to Figure 29). Lower pair of SEM's is of topmost sample, A.

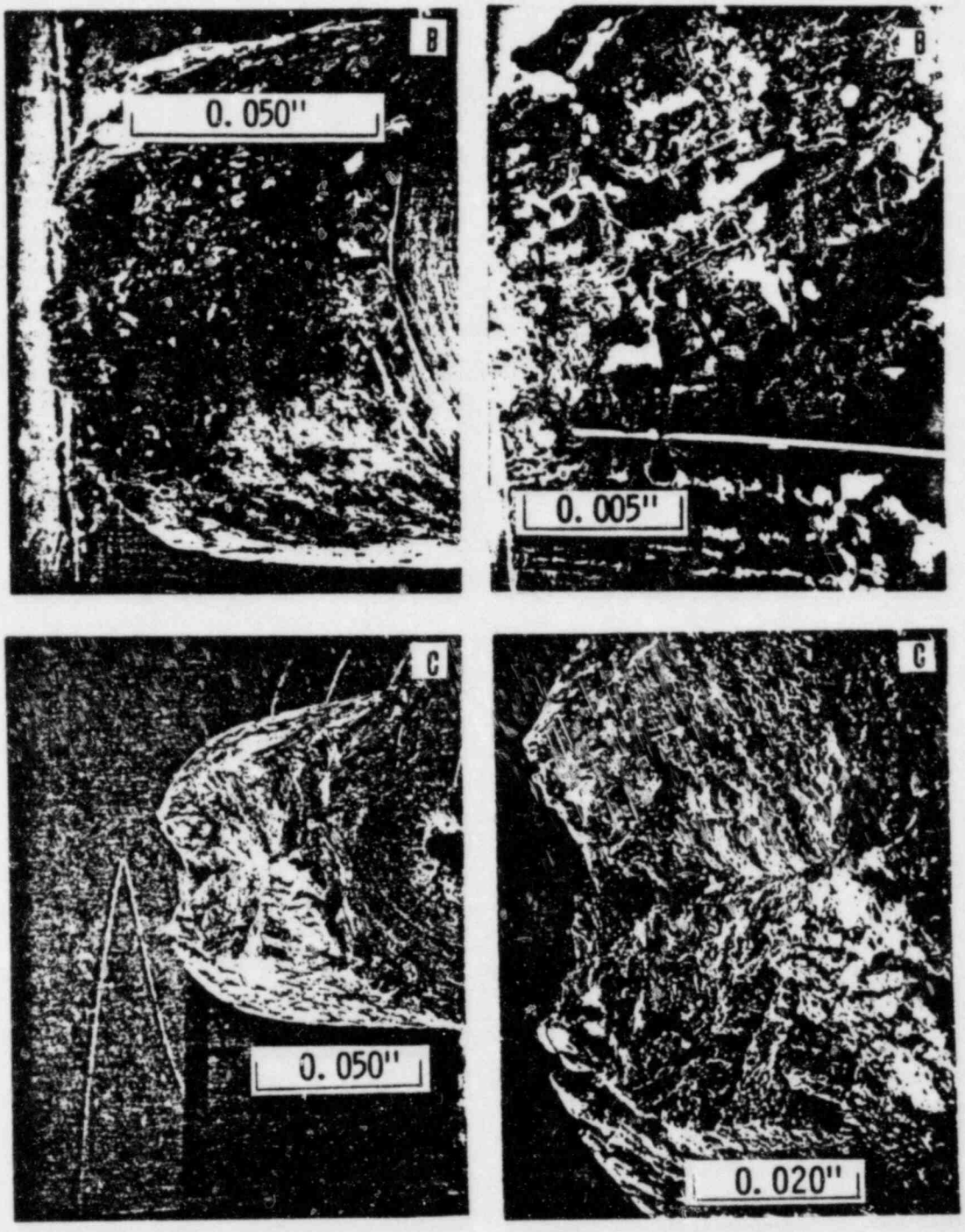

FIGURE 38. B(19-37), Axial Section at Top of Tube Sheet. Bent sections B and C of Figures 29 and 37, SEM's.

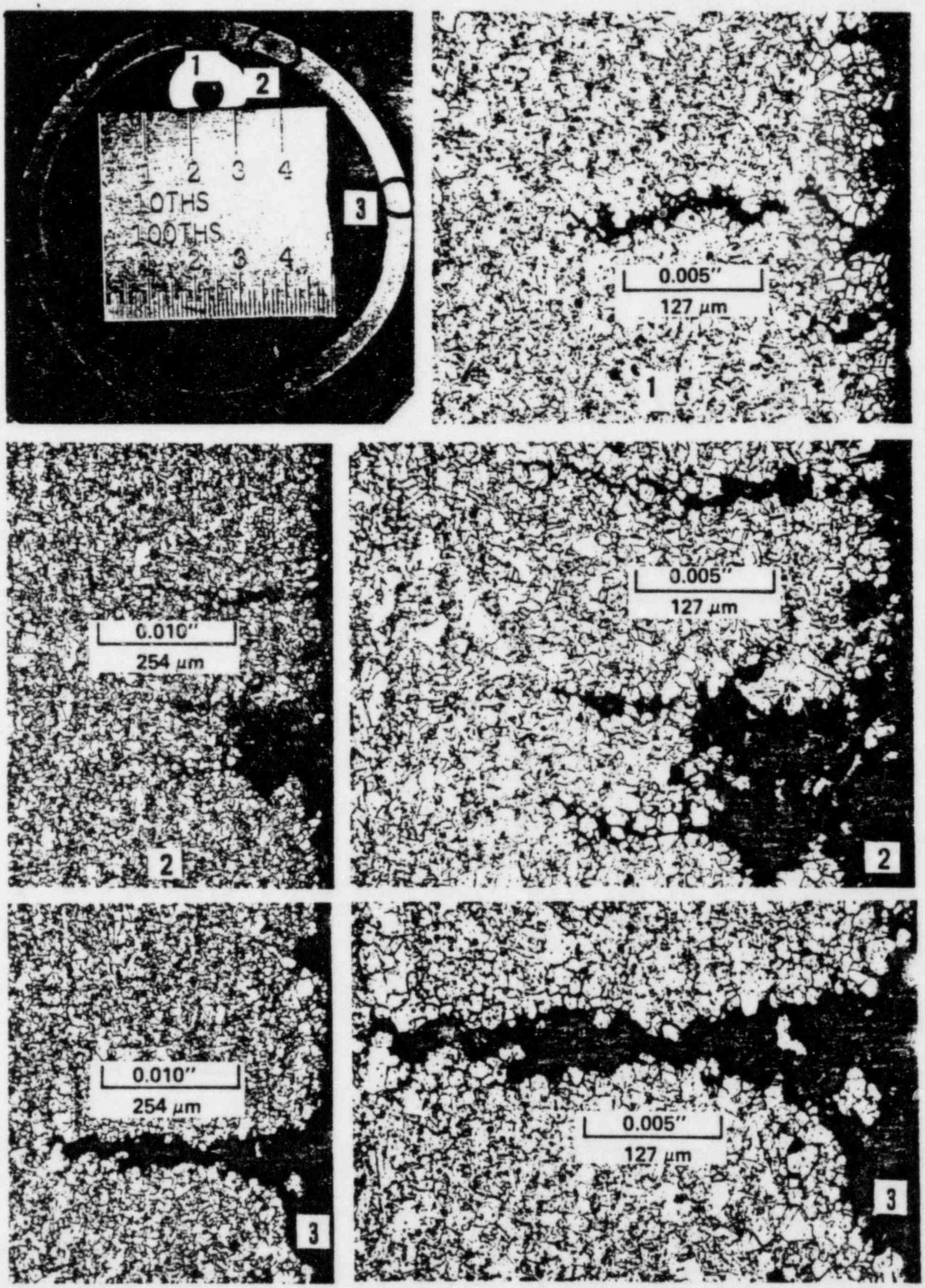

FIGURE 39. B(19-37), Transverse Cross Section below and adjacent to the 2-in.-long micro at top of tube sheet. This is sample 2 of Figure 29. Photomicrographs are of OD edges.

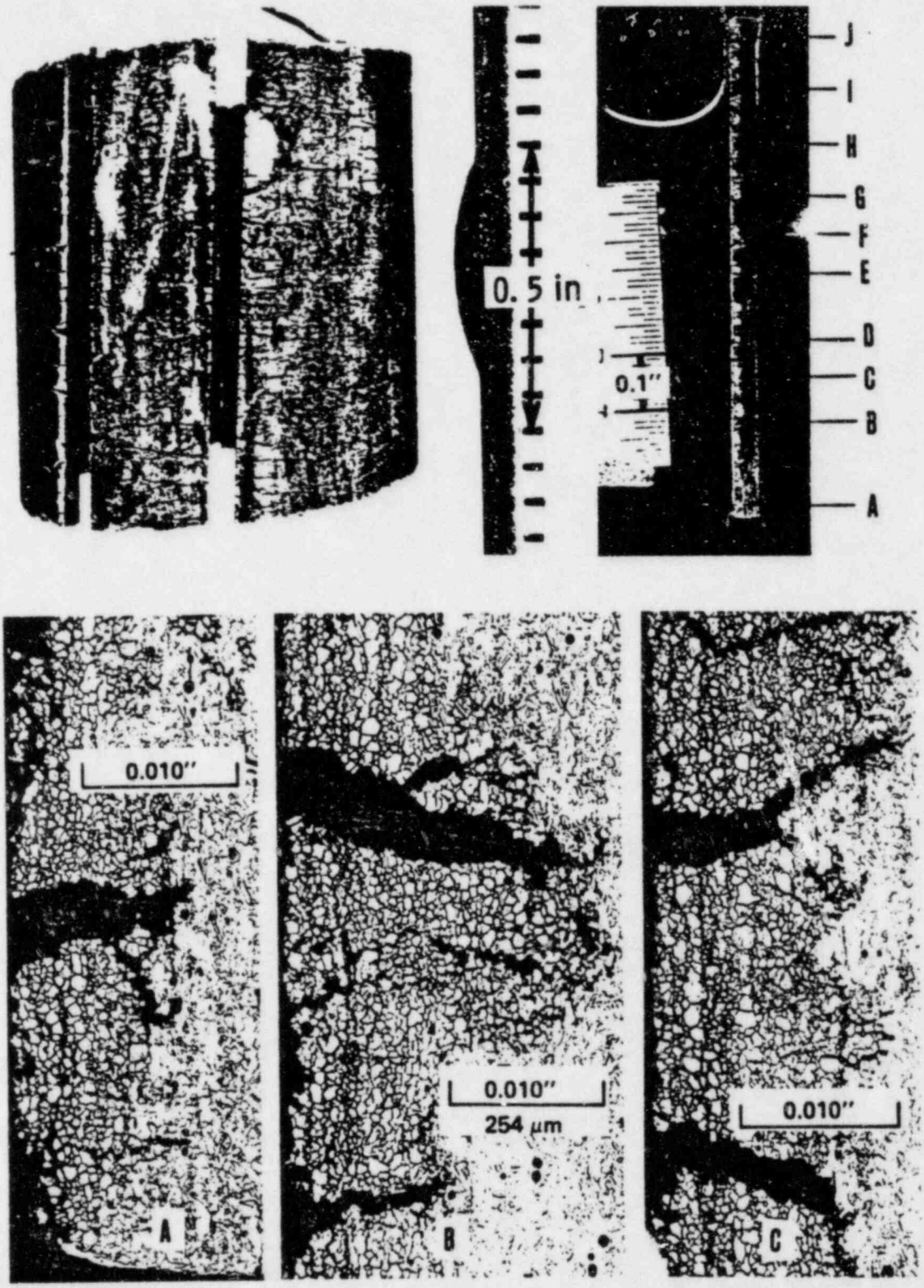

FIGURE 40. B(19-37), Longitudinal Cross Section from within the Tube Sheet. (Sample 3 of Figure 29.) Upper pair shows sectioning and resultant polished and etched sample. The series of photomicrographs at OD areas A - J was taken to determine the localized extent of tube stretching during removal by measurements of openings of the grains. The OD is at the left in the cross sections and the primary flow was upward.

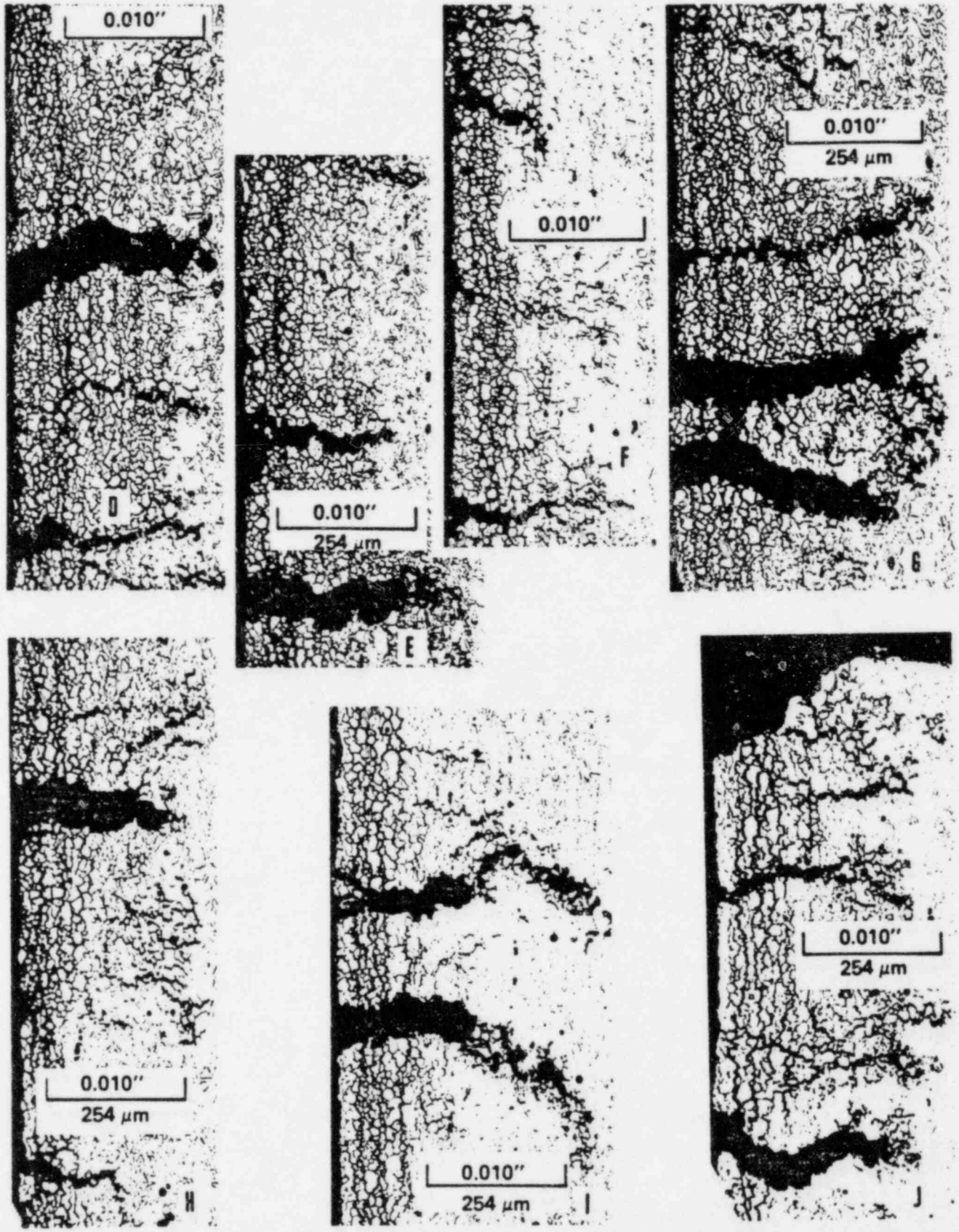

FIGURE 41. B(19-37), Longitudinal Section within Tube Sheet. Continuation of Figure 40; OD Areas D - J.

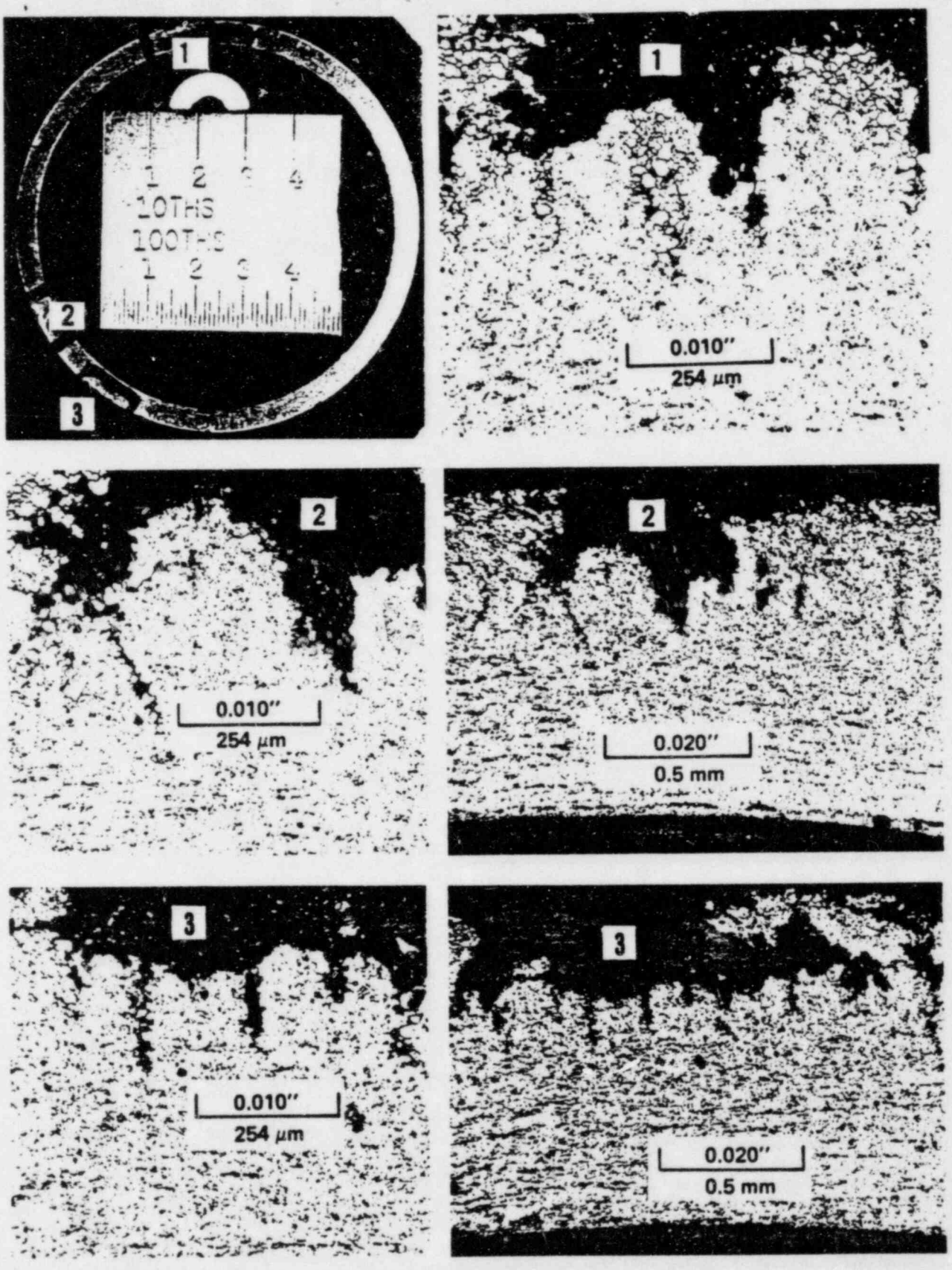

FIGURE 42. B(19-37), Transverse Cross Section from within the Tube Sheet. Sample 4 of Figure 29. The higher magnification pictures show OD edges.

ATTACHMENT 2

RE-EVALUATION OF EDDY CURRENT TAPES FOR TUBES R19C37, R30C41, R26C53, R30C44, R28C38, R32C42, R22C46, AND R30C57

The eddy current tapes from the various inspections of the tubes noted above have been re-evaluated for signature comparisons. Pictorial presentations are included as Figures 1 through 8 and a more detailed discussion of each tube is presented below.

Rough estimates of the volume (equivalent diameter) of each of the indications have been compiled in Table I. These calculations were made using the formula

$$D_I^2 = \frac{V_I D_S^2}{V_S}$$

where D_I = Equivalent diameter of the indication.

D_S = Diameter of the flat-bottom hole in the eddy current standard that has the depth-of-wall penetration closest to that of the indication.

V_I = Peak-to-peak voltage of the indication.

V_S = Peak-to-peak voltage displayed by the flat-bottom hole described by D_S.

Rough estimates of the lengths of the indications have been calculated from high speed strip charts. These are presented individually in Figures 9 through 16 and compiled in Table I.

Row 19 Column 37 (Figure 1)

This indication is small volume, 1/2" above the tube sheet, and was probably masked during previous on-site evaluations by probe motion (wobble) and the inability of being able to slow down the playback speed. Using slow playback speeds and low-pass filtering techniques, we have been able to track this indication back to March 1975. The phase angle and amplitude of the indication have remained approximately the same since that time which is indicative of no change. Equivalent hole diameter is 0.047 inches and the length <0.15 inches.

Row 30 Column 41 (Figure 2)

Another small volume indication, 1/2" below the top of the tube sheet, which has also been traced back to March 1975 has remained essentially the same. The equivalent hole diameter is 0.080 inches and the length <0.10 inches.

Row 26 Column 53 (Figure 3)

This tube indication has become apparent since December 1979 and is typical of tube cracking in the crevice. The equivalent hole diameter is 0.052 inches and the length is <0.58 inches.

Row 30 Column 44 (Figure 4)

This indication is located at the tube/tube sheet interface and has been masked by the tube sheet entry signal. Use of multiple frequency techniques make the indication quite visible. Progression of this indication cannot be traced other than to note distortion of the tube sheet signal back to December 1975. The equivalent hole diameter is 0.055 inches and the length is <0.68 inches.

Row 28 Column 38 (Figure 5)

The same as R30C44 above. The equivalent hole diameter is 0.108 inches and the length is <0.20 inches.

Row 32 Column 42 (Figure 6)

The same as R19C37 above with traceability to March 1975 and remaining essentially the same since then. The equivalent hole diameter is 0.061 inches and the length is <0.29 inches.

Row 22 Column 46 (Figure 7)

The same as R30C44 above. The equivalent hole diameter is 0.083 inches and the length is <0.29 inches.

Row 30 Column 57 (Figure 8)

The same as R30C44 above. The equivalent hole diameter is 0.058 inches and the length is <0.53 inches.

TABLE I

R-C	S/G	LOCATION	%DEPTH	VOLTS P - P	STD.VOLTS P - P	DIA. OF EQUIV. HOLE	LENGTH	READ FROM
19-37	B	1/2"↑TTS	58	0.72	3.82	0.047	< 0.15	400
30-41	B	1/2"↓TTS	47	0.60	3.26	0.080	< 0.10	400
26-53	B	In Tubesheet	86	1.63	3.68	0.052	< 0.58	400
30-44	B	TTS	83	1.61	3.29	0.055	< 0.68	MIX
28-38	B	TTS	45	0.94	2.85	0.108	< 0.20	MIX
32-42	B	1/2"↑TTS	61	1.91	2.94	0.061	< 0.29	400
22-46	A	TTS	55	1.70	2.94	0.083	< 0.29	MIX
30-57	A	TTS	80	1.60	2.94	0.058	< 0.53	MIX

WEP - POINT BEACH NO. 1
S/G B INLET
R19C37 - 1/2" ABOVE TOP OF TUBESHEET

3/75 - 400 kHz

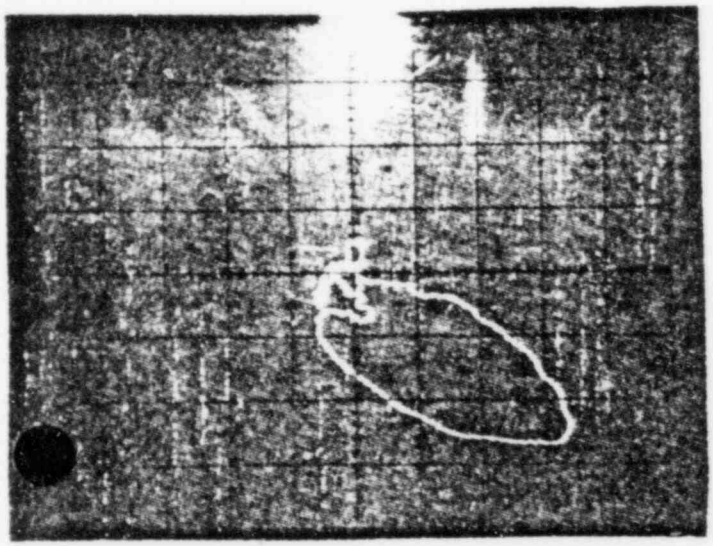

10/76 = 400 kHz

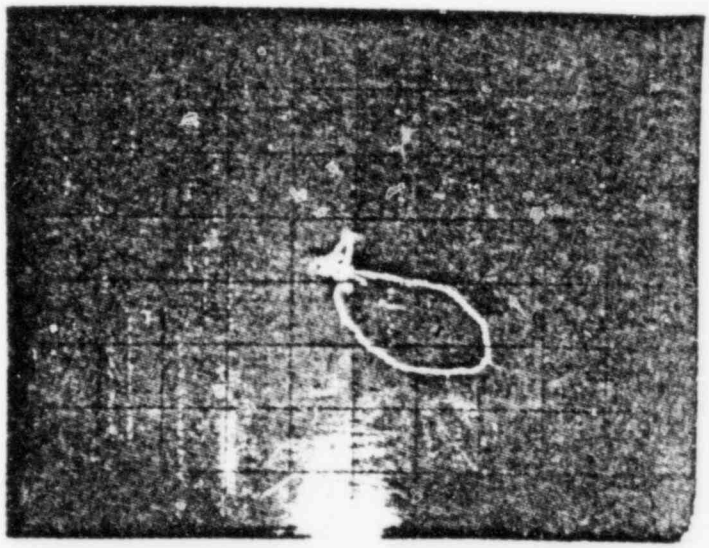

10/77 = 400 kHz

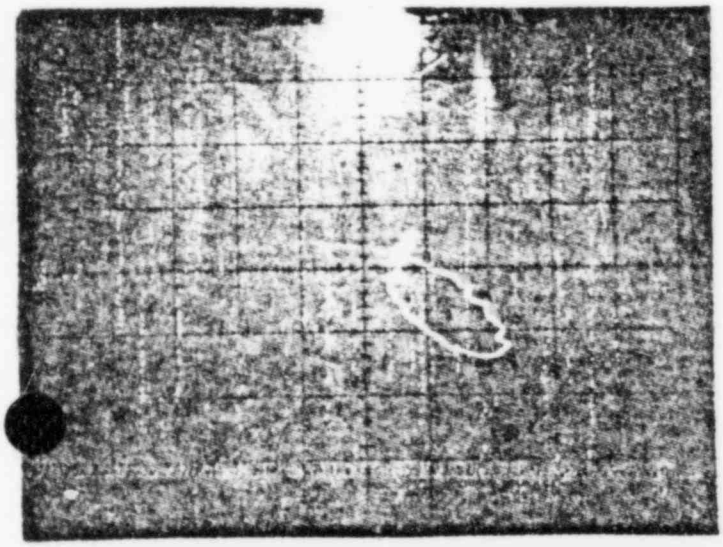

8/79 = 400 kHz

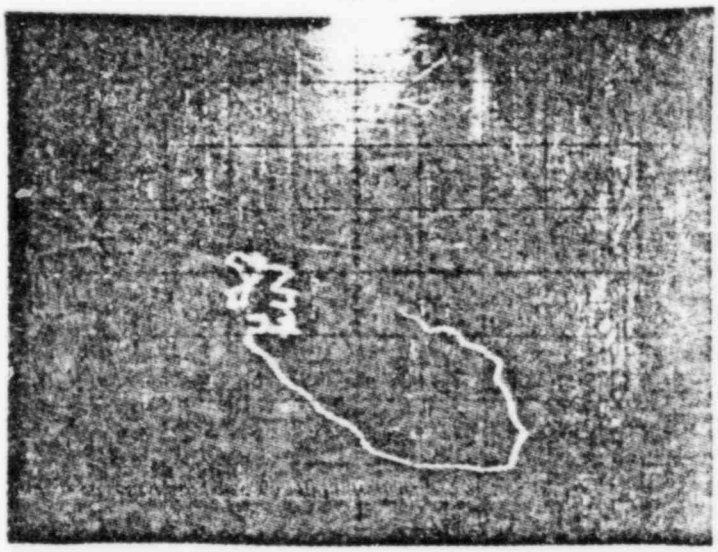

12/79 = 400 kHz

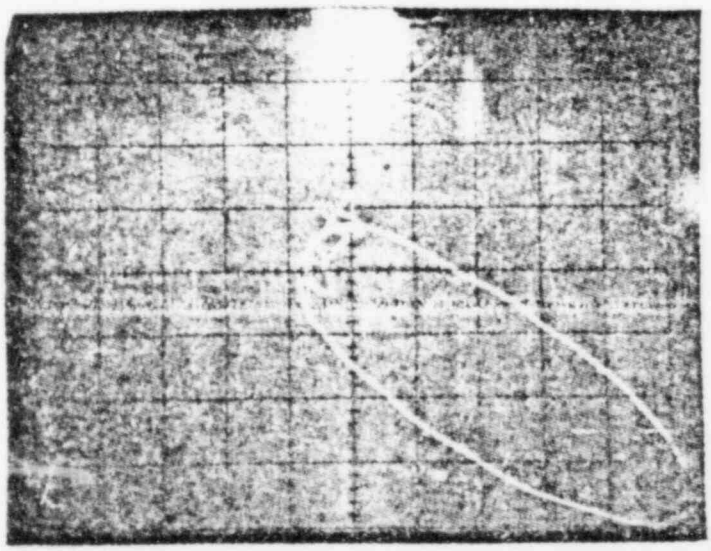

3/80 = 400 kHz

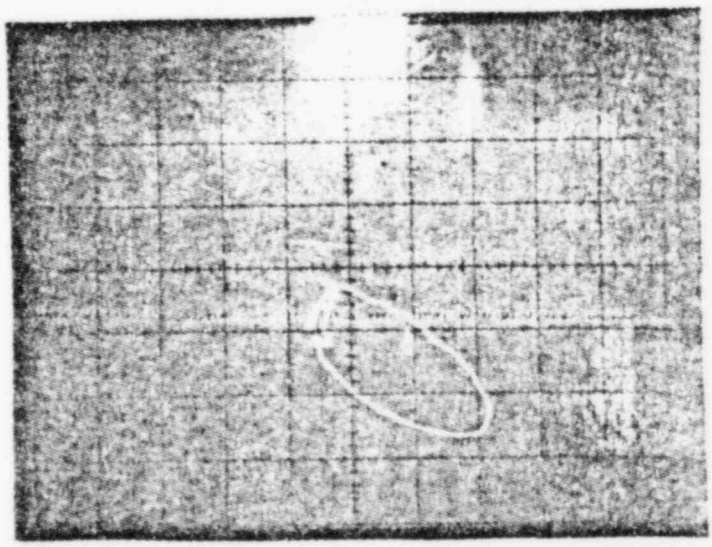

FIG. 1

WEP - POINT BEACH NO. 1
S/G B INLET
R30C41 - 1/2" BELOW TOP OF TUBESHEET

3/75 - 400 kHz

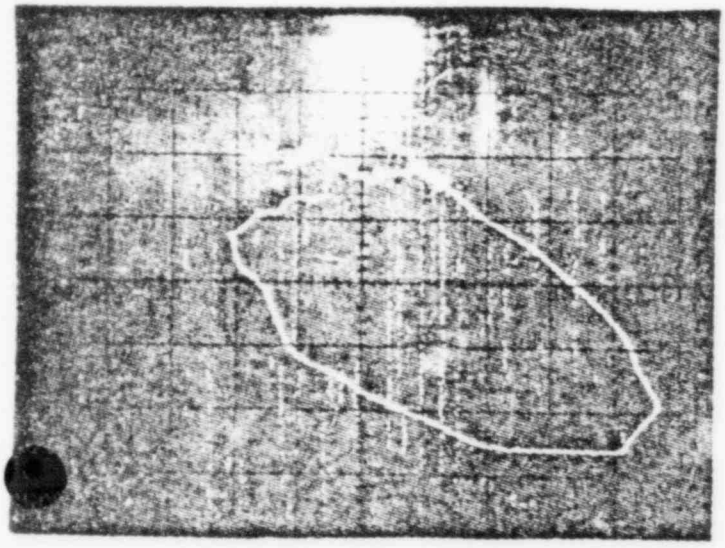

10/76 - 400 kHz

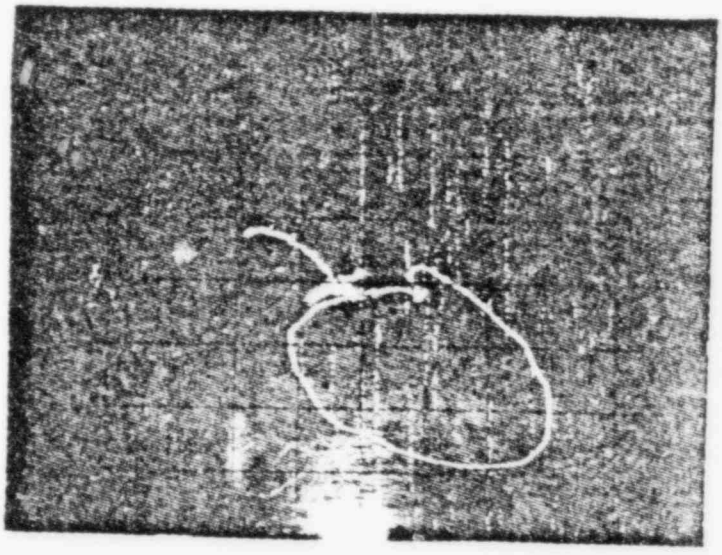

9/78 = 400 kHz

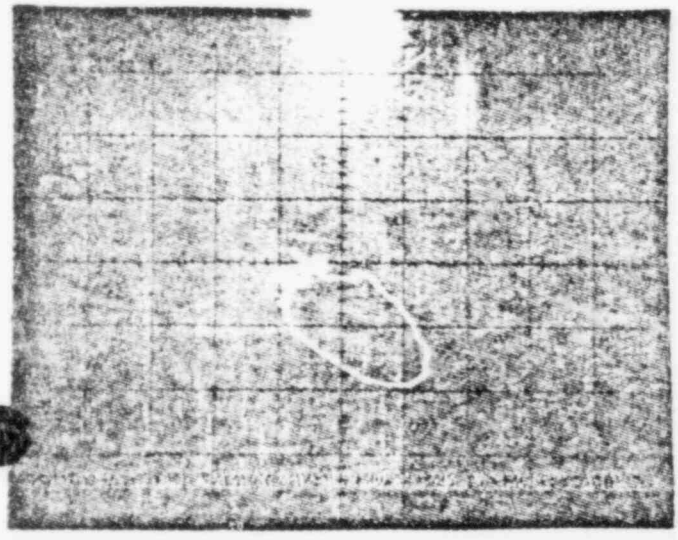

8/79 = 400 kHz

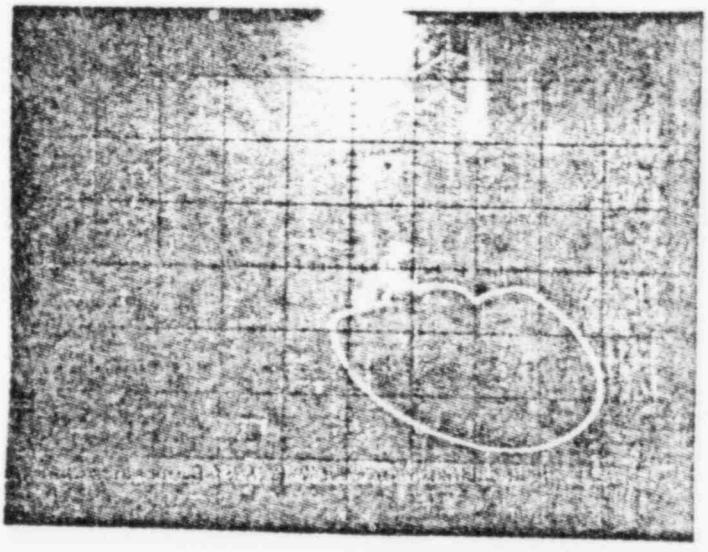

12/79 - 400 kHz

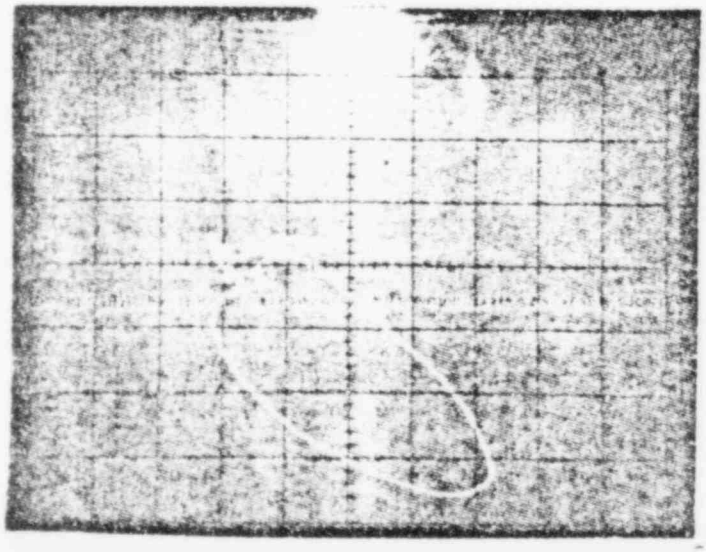

3/80 = 400 kHz

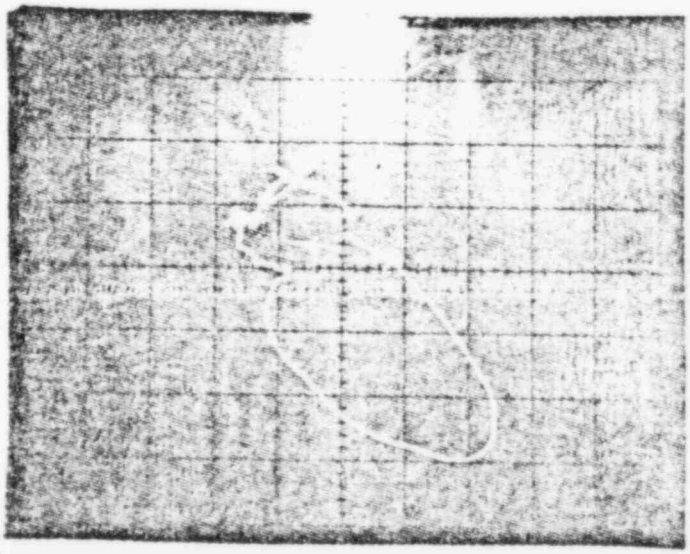

FIG. 2

WEP - POINT BEACH NO. 1

S/G B INLET

R26C53 - IN TUBESHEET

9/78 - 400 kHz

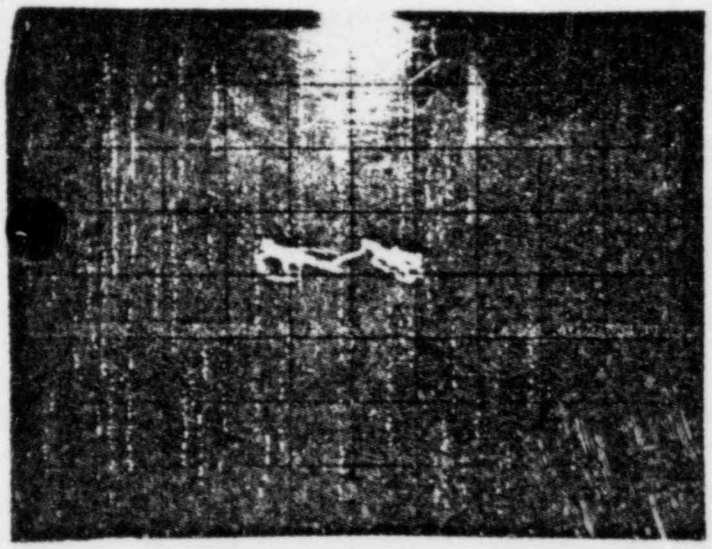

8/79 - 400 kHz

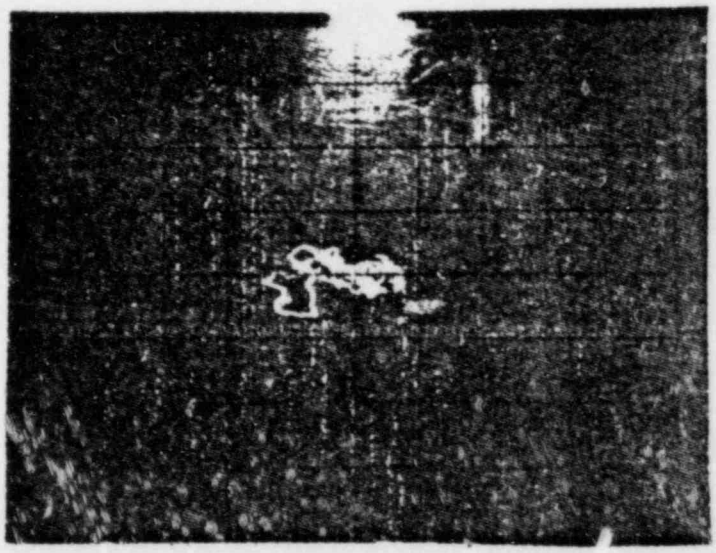

12/79 - 400 kHz

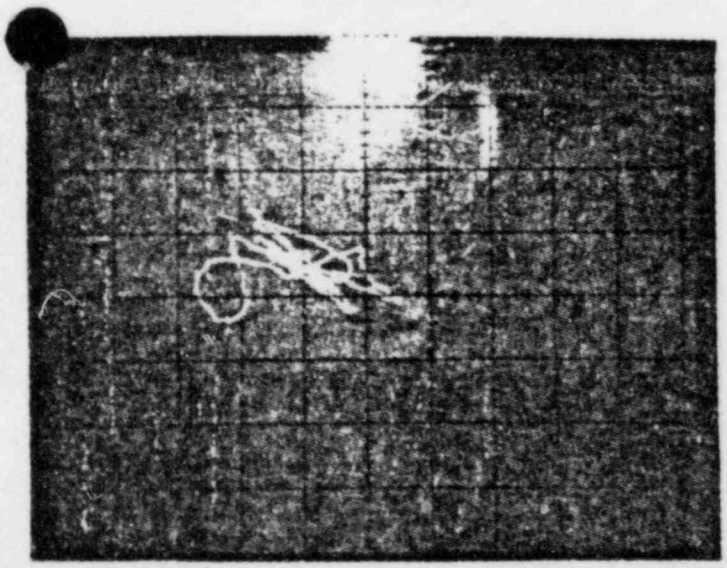

3/80 = 400 kHz

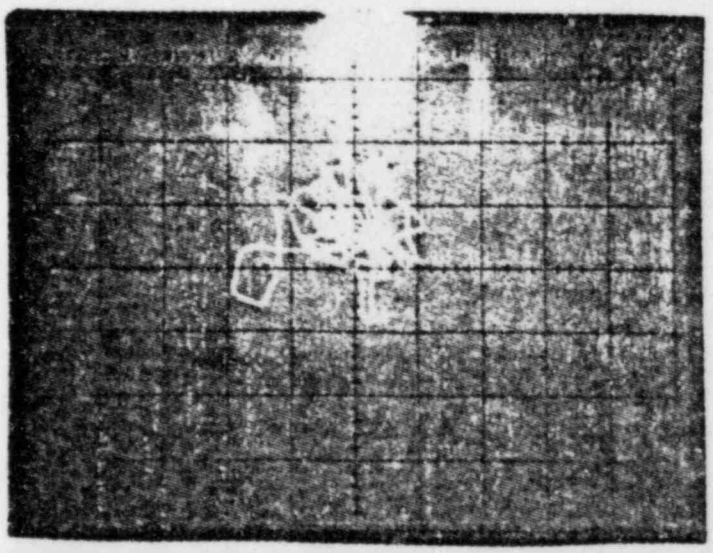

FIG. 3

WEP - POINT BEACH NO. 1
S/G B INLET
R30C44 = TUBESHEET

12/75 = 400 kHz

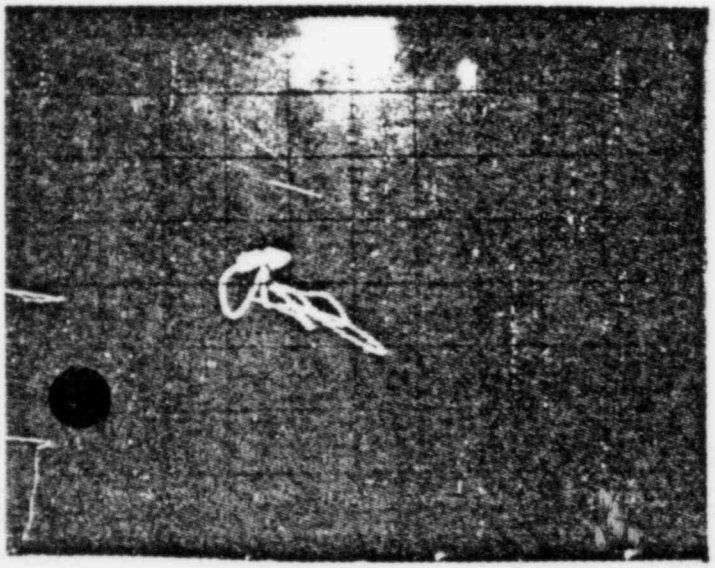

9/78 = 400 kHz

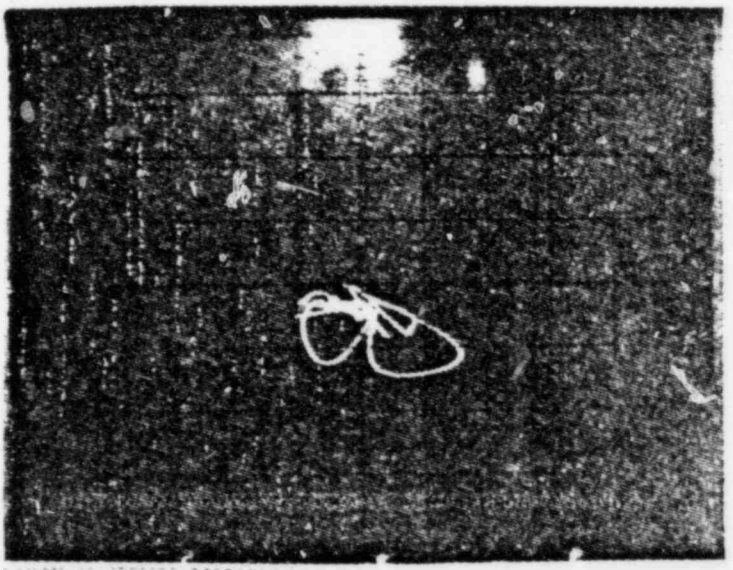

8/79 = 400 kHz

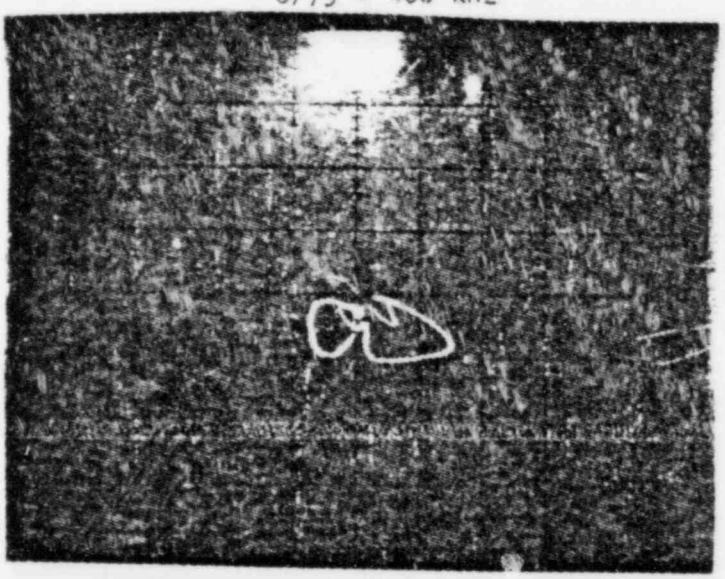

10/79

Top Left = 400 kHz

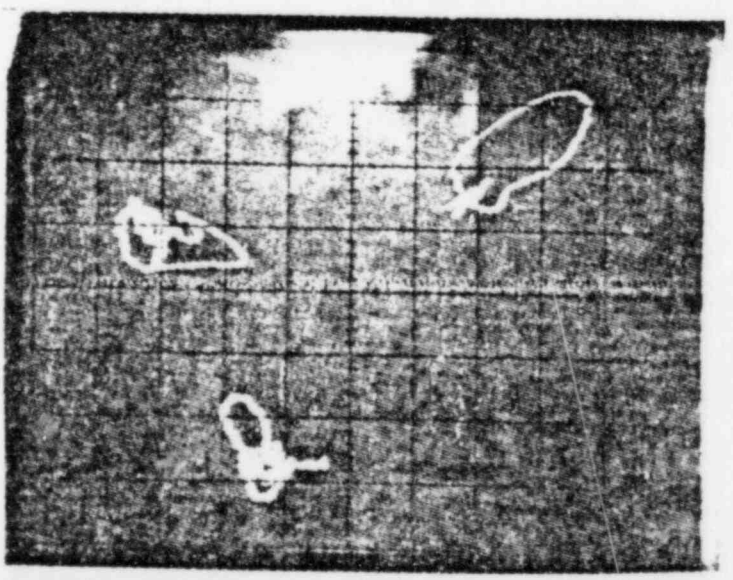

Top Right = 100 kHz

Bottom = Mix
83%
Top of Tubesheet

FIG. 4

WEP - POINT BEACH NO. 1
S/G B INLET
R28C38 = TUBESHEET

12/75 = 400 kHz

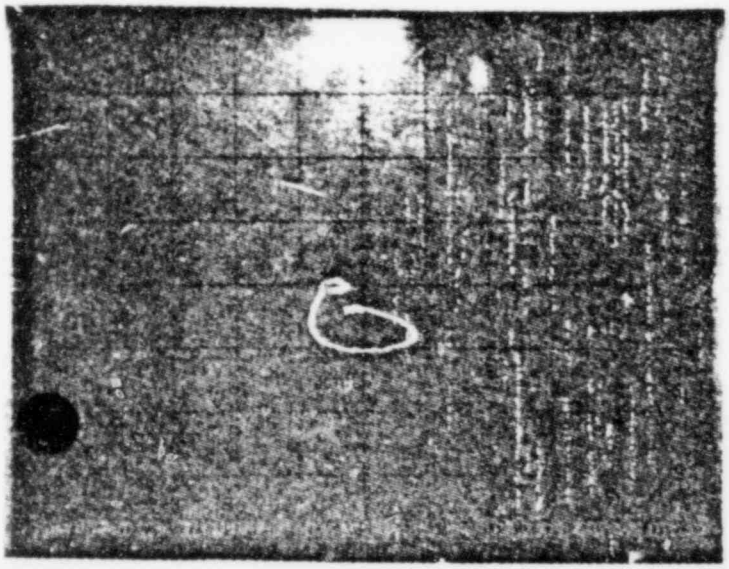

10/77 = 400 kHz

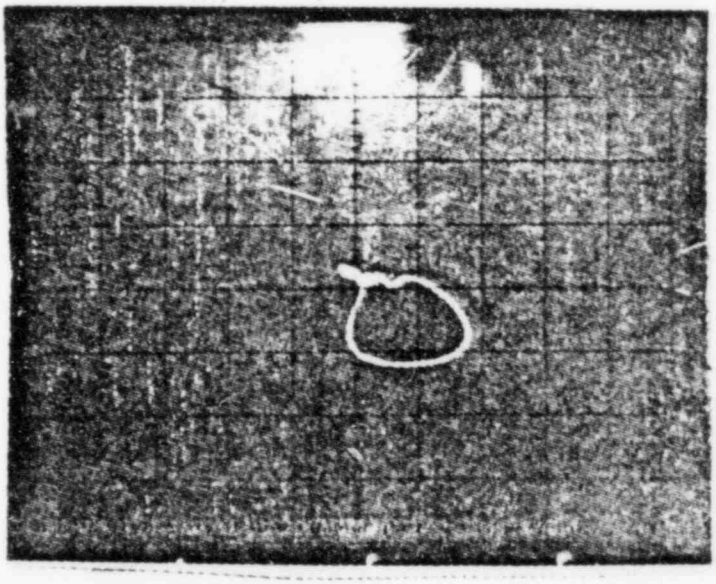

8/79 = 400 kHz

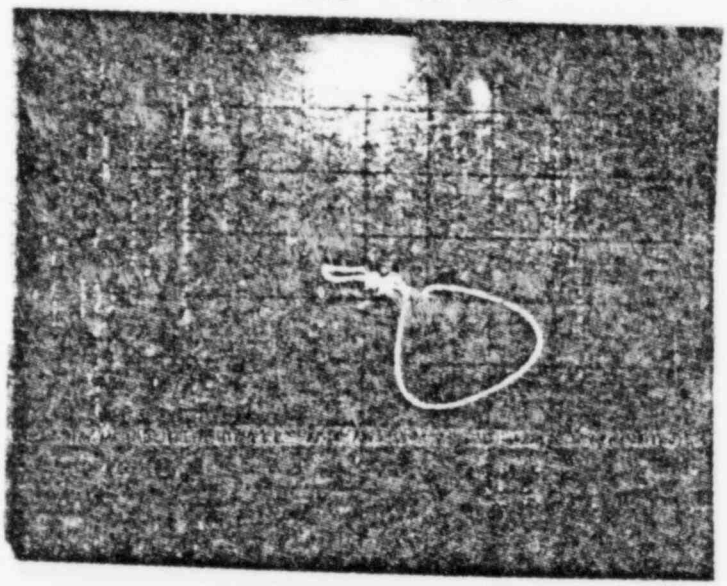

10/79

Top Left = 400 kHz

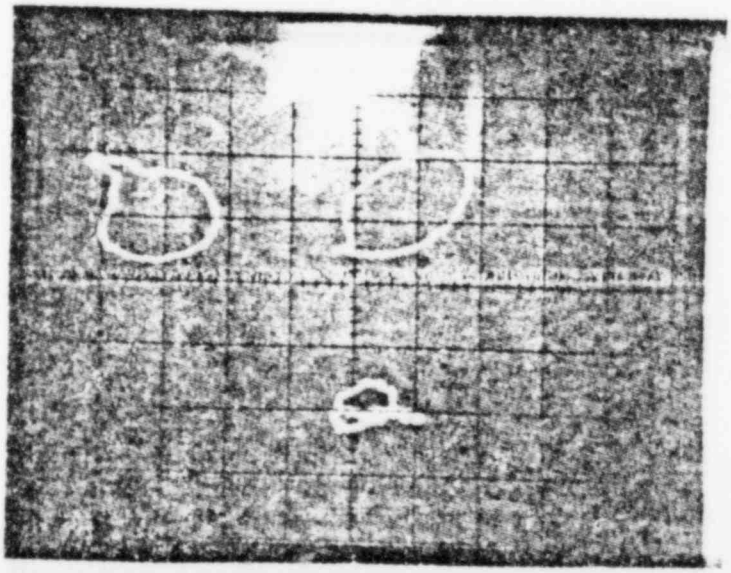

Top Right = 100 kHz

Bottom = Mix
45°
Top of Tubesheet

FIG. 6

WEP - POINT BEACH NO. 1
S/G B INLET
R32C42 - TUBESHEET

3/75 = 400 kHz

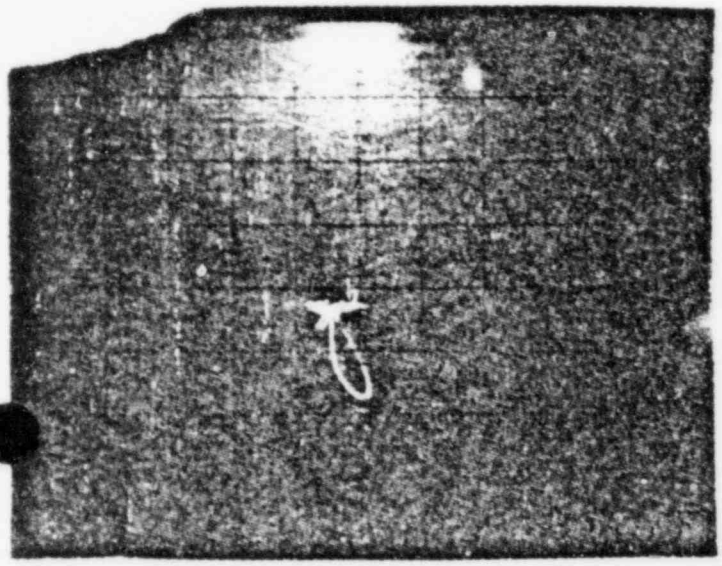

10/76 = 400 kHz

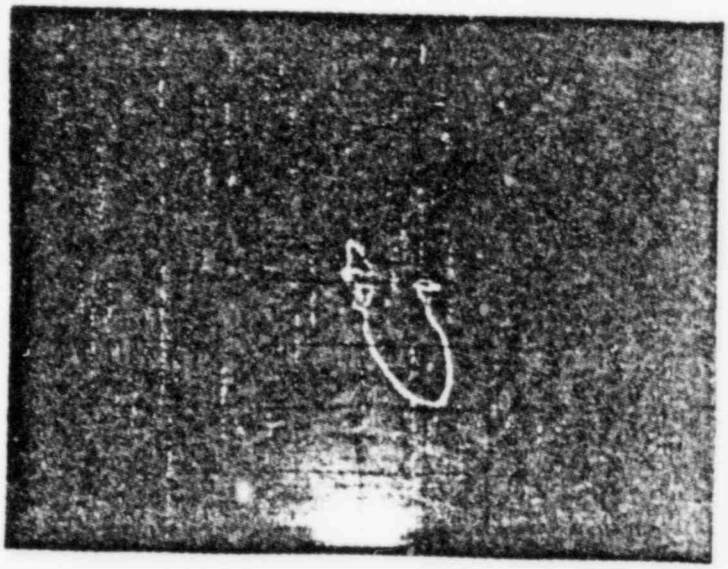

8/79 = 400 kHz

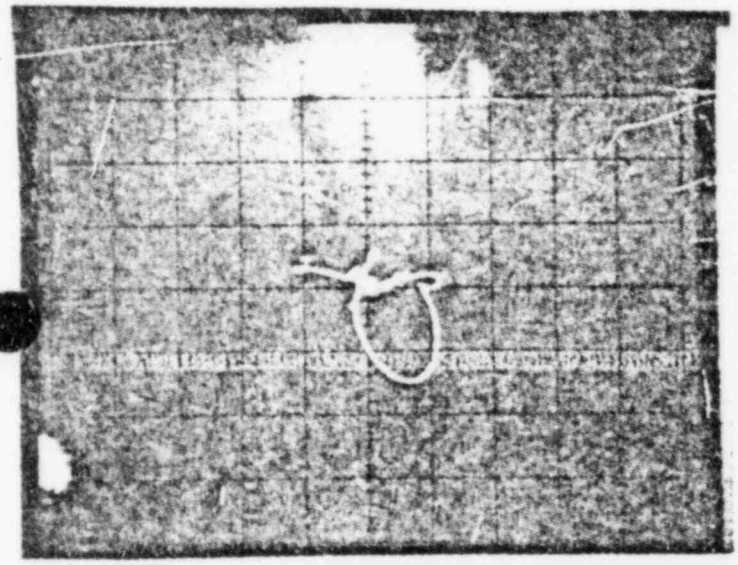

10/79 = 400 kHz

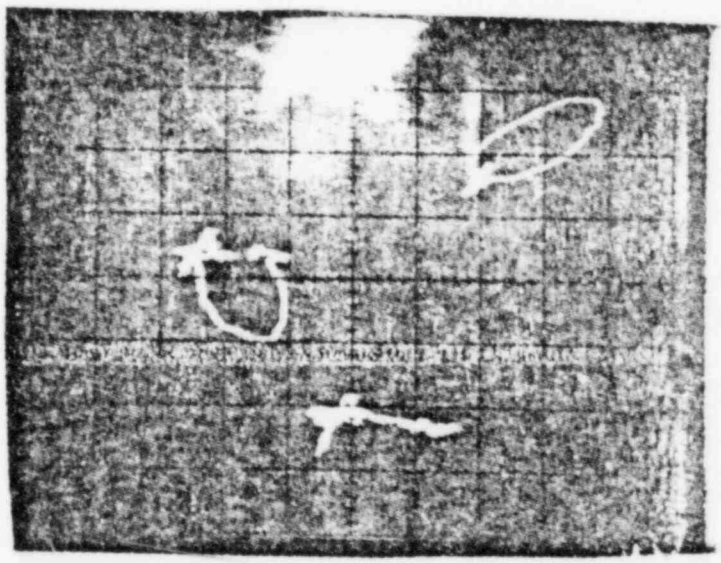

TOP LEFT - 400 kHz
TOP RIGHT - 100 kHz
BOTTOM - MIX
61%=1/2" ABOVE TUBESHEET

FIG. 6

WEP - POINT BEACH NO. 1

S/G A INLET

R22C46 = TUBESHEET

11/75 = 400 kHz

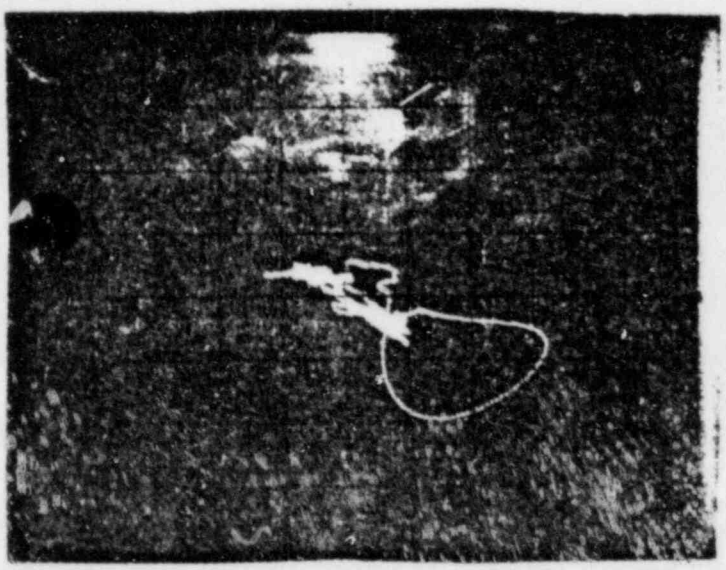

9/78 = 400 kHz

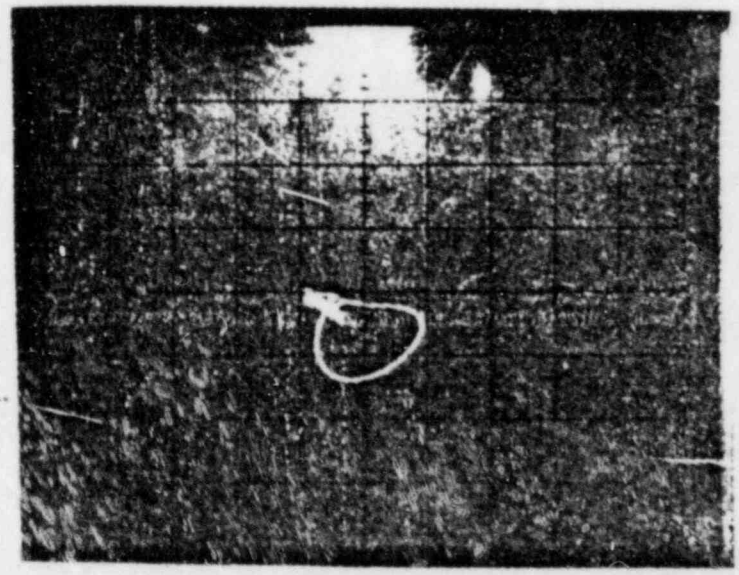

10/79

Top Left = 400 kHz

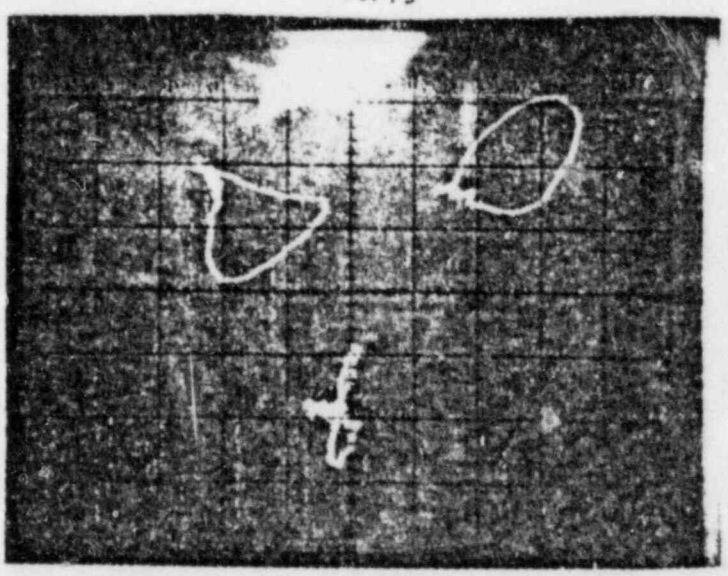

Top Right = 100 kHz

Bottom = Mix
55%
Top of Tubesheet

FIG. 7

WEP - POINT BEACH NO. 1
S/G A INLET
R30C57 = TUBESHEET

11/75 = 400 kHz

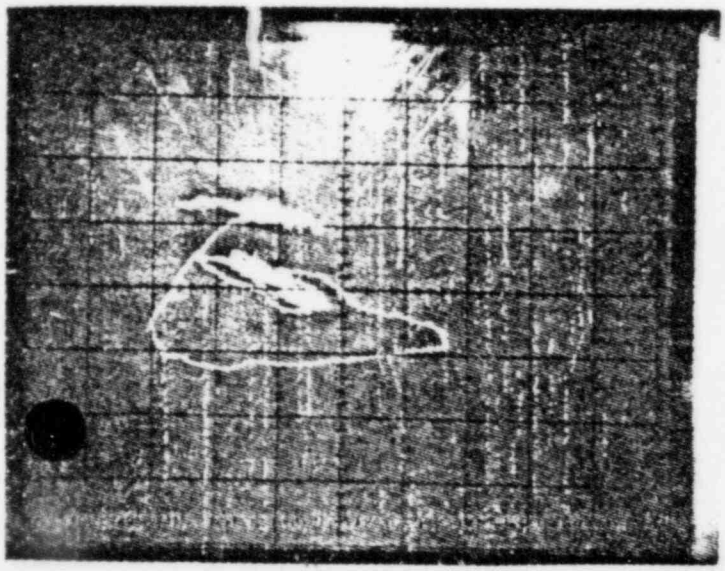

10/77 = 400 kHz

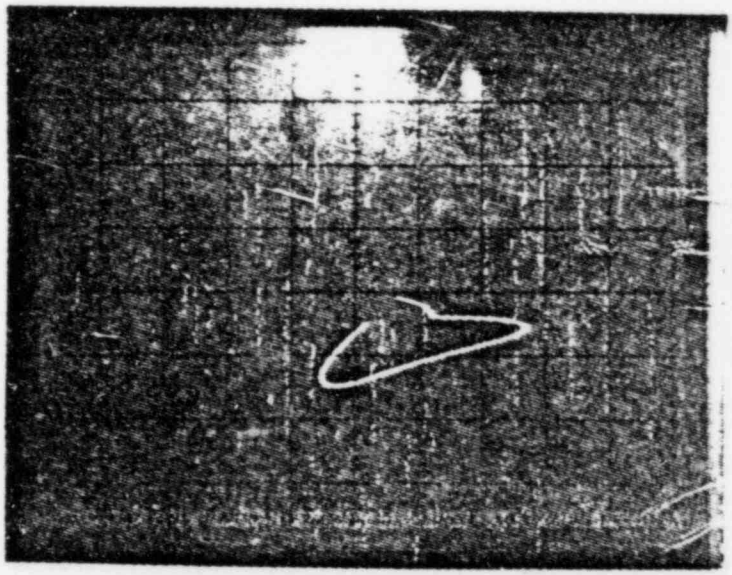

9/78 = 400 kHz

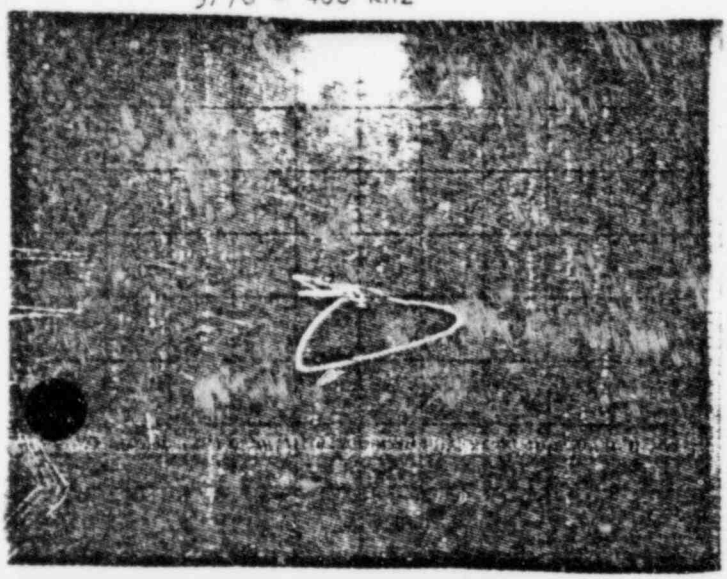

8/79 = 400 kHz

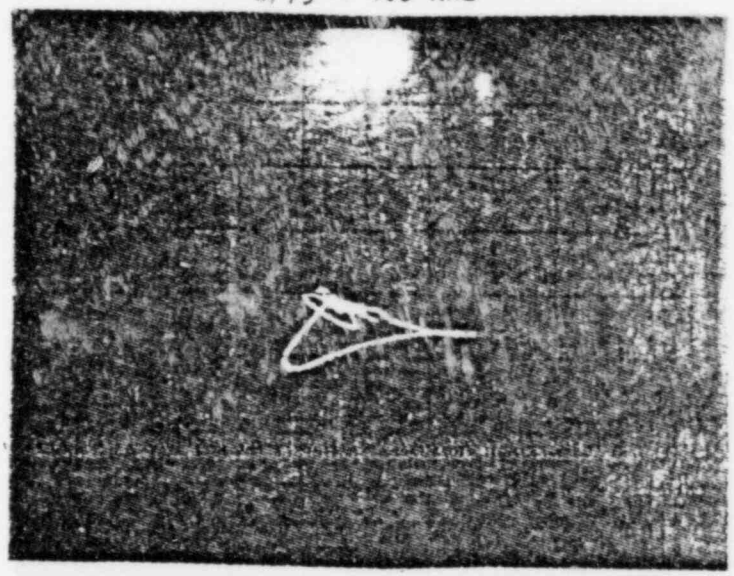

10/79

Top Left = 400 kHz

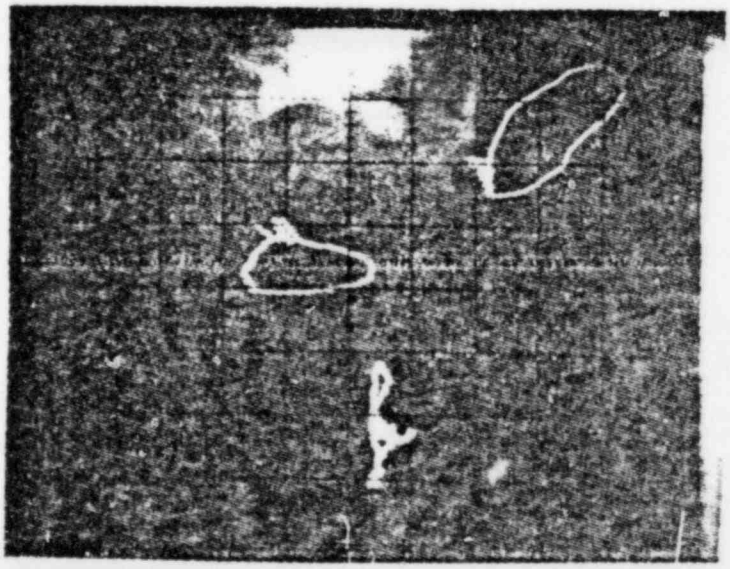

Top Right = 100 kHz

Bottom = Mix
80%
Top Of Tubesheet

FIG. 8